eman ta zabal zazu
Universidad del País Vasco
Euskal Herriko Unibertsitatea
FACULTY OF ENGINEERING BILBAO
UNIVERSITY OF THE BASQUE COUNTRY

MASTER'S DEGREE IN

TELECOMMUNICATION ENGINEERING

MASTER THESIS

DEVELOPMENT OF A PLATFORM TO MANIPULATE MULTIMODAL DATA TO EVALUATE THE HEMODYNAMIC STATE OF THE PATIENT DURING CARDIAC ARREST USING NONIVASIVE SENSORS

Student Zubia, Garea, Gorka
Director Irusta, Zarandona, Unai
Department Communications Engineering
Academic year 2020-2021

Barakaldo, 10th of June, 2021

Abstract

Out-of-hospital-cardiac-arrest (OHCA) is a sudden cardiovascular event that constitutes a major public health problem and is one of the leading causes of death in the world. The survival rate from OHCA decreases with time, therefore its early recognition and treatment is key. Defibrillation and cardiopulmonary resuscitation maneuver are the fundamental OHCA therapies. Electrocardiogram (EKG) is a low cost noninvasive technique used to monitor the electrical status of the heart. However, in many OHCA cases the EKG shows a close to normal electrical activity of the heart when actually the hemodynamic activity of the heart (blood flow and pressure) is not effective.

Consequently, a noninvasive, inexpensive and reliable technique that allows real-time monitoring of the hemodynamic status of the patient would be of great value. However, currently no such technique exists for out-of-hospital situations and it is only available in hospitals. Cardiac output (CO) and stroke volume index (SVI) are the main indicators of hemodynamic status.

The objective of this master thesis has been to develop and implement the tools to help establish correlations between CO and SVI values measured by well-established in-hospital technologies (invasive blood pressure and doppler echocardiography), and the measures taken from novel noninvasive signals such as ballistocardiography (BCG) sensors that could be easily used in OHCA.

The first step was to collect data from a cohort of healthy subjects with both types of technologies. In May 2021 started the collection of real OHCA cases. To accomplish the main objective several intermediate objectives have been defined and achieved; first, the creation of a multisource, standardized and common open format database using raw data from the different proprietary measurement devices. For this purpose, existing data converters have been applied and custom data converters have also been developed. The data have been preliminarily pseudo-synchronized with a custom-made algorithm based on the temporal annotations of the physicians.

Two graphical interfaces have been created, one for each site (out-of- and in-hospital) that have collected the measurements for the database. The graphical interfaces are user-friendly, flexible, and functional to enable visualization, annotation and time alignment fine tuning of the multisource standardized database. They also integrate algorithms to help the analysis of the data and find possible hidden correlations between signals. The creation of these two interfaces has led to two outcomes: on the one hand, the extraction of analysis windows together with the physicians of the Oslo University Hospital. On the other hand, the creation of a generalist graphical interface development method. Thanks to this method, a third graphical interface has been built to analyze the extracted windows. This also integrates a fifth algorithm for data processing.

In conclusion, a scalable platform has been created both in number of patients and mesurement devices, consisting of a multisource, standardized, common open format database and three graphical interfaces for its visualization, annotation and processing. This platform sets the framework to help the future identification of the correlation between the different technologies that will save lives thanks to real-time hemodynamic monitoring in emergency medical services-treated OHCA cases.

Key words: **biomedical signal processing**, **hemodynamics**, **cardiopulmonary resuscitation**, **emergency medicine**, **database management**.

Laburpena

Ospitalez kanpoko bihotz geldialdia (OKBG) ustekabeko gertakari kardiobaskular bat da, osasun publikoko arazo garrantzitsua dena, munduko heriotza-kausa nagusietako bat izanez. OKBGaren biziraupentasa murriztu egiten da denborarekin, eta, beraz, haren antzemate eta tratamendu goiztiarrak funtsezkoak dira. Bi dira OKBGaren oinarrizko terapiak: desfibrilazio eta bihotz-biriketako berpizte (BBB) goiztiarrak. Elektrokardiograma (EKG) kostu txikiko teknika ez-inbaditzailea da, bihotzaren egoera elektrikoa monitorizatzeko erabiltzen dena. Hala ere, OKBGko kasu askotan, EKGak bihotzaren jarduera elektriko sasinormala erakusten du, nahiz eta bihotzaren jarduera hemodinamikoa (odol-fluxua eta presioa) eraginkorra ez izan.

Beraz, oso baliagarria litzateke teknika ez-inbaditzailea, merkea eta fidagarria izatea pazientearen egoera hemodinamikoa denbora errealean monitorizatzeko. Zoritxarrez, gaur egun ez dago horrelako teknikarik ospitalez kanpoko egoeretarako eta ospitaleetan baino ezin da erabili. Egoera hemodinamikoaren adierazle nagusiak bi dira: bihotz-gastua (BG) eta bolumen sistolikoaren indizea (BSI).

Master amaierako lan honen helburua dagoeneko ondo ezarrita dauden ospitalez barruko teknologiek (odol-presio inbaditzailea eta doppler ekokardiografia), eta OKBGan erraz erabil daitezkeen diren seinale berri ez inbasiboak, hala nola, balistokardiografia (BCG) sentsoreak neurtutako BG eta BSI balioen arteko korrelazioak topatzen lagunduko duten tresnak garatzea eta inplementatzea izan da.

Lehenengo urratsa bi teknologia motekin datuak biltzea izan zen, subjektu osasuntsuen talde batetik abiatuta. 2021eko maiatzean hasi ziren benetako OKBG kasuetako datuak biltzen. Helburu nagusia lortzeko, tarteko helburu batzuk definitu eta lortu dira; lehenik eta behin, iturri anitzetako datu-base estandarizatua eta formatu ireki komunekoa sortu da. Horretarako, neurketa-ekipoek jasotako datu gordinak (formatu jabeduna zeukatenak) erabili dira. Hori lortzeko, dagoeneko existitzen ziren datu-bihurgailuak aplikatu dira, baita garatutako datu-bihurgailu propioak ere. Datuak aldez aurretik sinkronizatu dira algoritmo propio baten bidez. Algoritmo horrek medikuen denbora-oharrak hartzen ditu oinarritzat.

Bi interfaze grafiko sortu dira, datu-baserako neurketak hartu dituzten teknologien aplikazio-esparru bakoitzeko bat (ospitalez kanpoko eta barrukoa). Interfaze grafikoak erabiltzeko errazak dira, malguak eta funtzionalak. Haiei esker datu-basea bistaratzen, anotatzen eta denbora-lerrokatzea doitzen da. Interfazeek datuak aztertzen laguntzeko eta seinaleen arteko ezkutuko korrelazioak aurkitzeko algoritmoak ere badituzte. Bi interfaze horiek sortzeak bi emaitza ekarri ditu: batetik, analisi-leihoak atera dira Osloko Unibertsitate Ospitaleko medikuekin batera. Bestetik, interfaze grafikoak garatzeko metodo orokor bat sortu da. Metodo horri esker, hirugarren interfaze grafiko bat eraiki da ateratako leihoak aztertzeko. Interfaze honek bosgarren algoritmo bat ere integratzen du datuak prozesatzeko.

Ondorioz, plataforma eskalagarri bat sortu da, bai paziente zein neurketa-ekipoen kopuruari dagokienez. Plataforma hori osatzen dute iturri anitzetako datu-base estandarizatu eta formatu ireki komuneko bat, eta hiru interfaze grafiko, datuak ikusi, anotatu eta prozesatzeko.

Gako-hitzak: **seinale biomedikoen prozesaketa**, **hemodinamika**, **bihotz-biriketako berpiztea**, **larrialdi medikuntza**, **datu-baseen kudeaketa**.

Resumen

La parada cardiorespiratoria extrahospitalaria (PCREH) es un evento cardiovascular súbito que constituye un importante problema de salud pública y es una de las principales causas de muerte en el mundo. La tasa de supervivencia a una PCREH disminuye con el tiempo, por lo que su reconocimiento y tratamiento tempranos son clave. La desfibrilación y la maniobra de reanimación cardiopulmonar son las terapias fundamentales de la PCREH. El electrocardiograma (EKG) es una técnica no invasiva de bajo coste que se utiliza para monitorizar el estado eléctrico del corazón. Sin embargo, en muchos casos de PCREH el EKG muestra una actividad eléctrica del corazón relativamente normal cuando realmente la actividad hemodinámica del corazón (flujo y presión sanguínea) no es efectiva.

Por lo tanto, resultaría muy útil contar con una técnica no invasiva, barata y fiable que permitiera monitorizar en tiempo real el estado hemodinámico del paciente. Sin embargo, actualmente no existe ninguna técnica de este tipo para situaciones extrahospitalarias, tan sólo está disponible en los hospitales. El gasto cardíaco (GC) y el índice de volumen sistólico (IVS) son los principales indicadores del estado hemodinámico.

El objetivo de este trabajo de fin de máster ha sido desarrollar e implementar las herramientas que ayuden a establecer correlaciones entre los valores de GC y IVS medidos por tecnologías intrahospitalarias ya consolidadas (presión arterial invasiva y ecocardiografía doppler), y

las medidas tomadas a partir de novedosas señales no invasivas como los sensores de balistocardiografía (BCG) que podrían ser fácilmente utilizados en la PCREH.

El primer paso fue recopilar datos de una cohorte de sujetos sanos con ambos tipos de tecnologías. En mayo de 2021 se inició la recogida de casos reales de PCREH. Para lograr el objetivo principal se han definido y alcanzado varios objetivos intermedios; en primer lugar, la creación de una base de datos multifuente, estandarizada y con un formato abierto común, utilizando los datos sin procesar en formato propietario de los diferentes equipos de medida. Para ello, se han aplicado conversores de datos existentes y también se han desarrollado conversores de datos propios. Los datos se han sincronizado preliminarmente con un algoritmo propio que toma como base las anotaciones temporales de los médicos.

Se han creado dos interfaces gráficas, una por cada lugar de aplicación (extra e intrahospitalaria) de las tecnologías que han captado las medidas para la base de datos. Las interfaces gráficas son fáciles de usar, flexibles y funcionales para permitir la visualización, la anotación y el ajuste de la alineación temporal de la base de datos. También integran algoritmos para ayudar al análisis de los datos y encontrar posibles correlaciones ocultas entre las señales. La creación de estas dos interfaces ha dado lugar a dos resultados: por un lado, la extracción de ventanas de análisis junto con los médicos del Hospital Universitario de Oslo. Por otro, la creación de un método general de desarrollo de interfaces gráficas. Gracias a este método, se ha construido una tercera interfaz gráfica para analizar las ventanas extraídas. Ésta también integra un quinto algoritmo para el procesamiento de datos.

En conclusión, se ha creado una plataforma escalable tanto en número de pacientes como de dispositivos de medición, que consiste en una base de datos multifuente, estandarizada y de formato abierto común y tres interfaces gráficas para su visualización, anotación y procesamiento. Esta plataforma establece el marco para ayudar a la futura identificación de la correlación entre las diferentes tecnologías que salvarán vidas gracias a la monitorización hemodinámica en tiempo real en las PCREH tratados por los equipos médicos de emergencia.

Palabras clave: **procesamiento de señales biomédicas**, **hemodinámica**, **reanimación cardiopulmonar**, **medicina de urgencias**, **gestión de bases de datos**.

Contents

1 Introduction **1**

2 Background **3**
2.1 OHCA in figures 3
2.2 The heart. From mechanics to electrical signals 6
2.3 The EKG: a key tool for CVD diagnosis 7
2.4 OHCA 8
2.5 Chain of survival: key therapy for resuscitation 10
2.6 Monitoring blood flow 11
2.7 Ballistocardiograpy: mechanichs may be the answer 12
2.8 Clinical drill: trying to replicate EMS attended OHCA 15

3 Objectives and scope of the study **17**

4 Benefits of the study **19**
4.1 Technical benefits 20
4.2 Social benefits 20
4.3 Economic benefits 20

5 State of the Art **23**
5.1 Normal heartbeat in the EKG 23
5.2 well-established technologies hemodynamics measurement 25
5.2.1 Doppler echocardiography 25
5.2.2 Invasive blood pressure 31

5.2.3 Fick's direct method 32
5.2.4 Thermodilution 32
5.2.5 FloTrac® sensor 33
5.3 Possible new hemodynamics measurement methods 34
5.3.1 Ballistocardiography 34
5.3.2 Transthoracic impedance 35
5.3.3 Capnography 36
5.3.4 Pulse-oximetry 37
5.4 Automatic algorithms 38
5.4.1 Heartbeat detector 38
5.4.2 EKG delineator 39
5.4.3 Extraction of circulation component 39
5.4.4 Ventilation detector 41

6 Analysis of alternatives 45
6.1 Software suite 45
6.1.1 MATLAB 45
6.1.2 OCTAVE 46
6.1.3 C 46
6.1.4 Python 47
6.1.5 Software selection criteria 47
6.2 Heartbeat detector 49
6.2.1 Hamilton-Tompkins algorithm 49
6.2.2 Physionet algorithms 49
6.2.3 Methods based on the advanced signal processing 50
6.2.4 Heartbeat detection criteria 51
6.3 EKG delineation algorithm 52
6.3.1 Wavedec algorithm 52
6.3.2 Low-pass differentiation 52
6.3.3 Second order derivatives 52
6.3.4 EKG delineation algorithm selection criteria 52
6.4 Extraction of the TTI circulation component 54
6.4.1 RLS adaptive filtering based ICC extractor 54
6.4.2 LMS adaptive filtering based ICC extractor 54
6.4.3 TTI circulation component extractor selection criteria 54
6.5 TTI Ventilation detector 56
6.5.1 TTI Ventilation detector during mechanical CPR 56
6.5.2 Dynamic threshold TTI ventilation detector 56
6.5.3 Neural network TTI ventilation detector 57
6.5.4 TTI ventilation detector selection criteria 57
6.6 CO2 Ventilation detector 58
6.6.1 Adaptive threshold CO2 ventilation detector 58
6.6.2 Duration based decision CO2 ventilation detector 58
6.6.3 Primitive CO2 ventilation detector 59

6.6.4 CO2 ventilation detector selection criteria 59

7 Risks analisys 61
7.1 Risk of coding errors (A) 62
7.2 Risk of delays (B) 62
7.3 Risk of data loss (C) 62
7.4 Risk of staff leaving (D) 63
7.5 Risk of COVID-19 (E) 63
7.6 Knowledge risks (F) 63
7.7 Risk of excessive costs (G) 64
7.8 Summary of the risk analysis 64

8 Description of the solution 65
8.1 Phase 1: data management and completion of the time aligned dataset 67
8.1.1 Physio-Control LP® -15 69
8.1.2 BCG sensors 71
8.1.3 FloTrac® sensor 73
8.1.4 Doppler echocardiography 75
8.1.5 Time alignment 76
8.2 Phase 2: preliminary database visualization and annotation tool 77
8.2.1 GUI for Physio-Control LP® -15 and BCG sensors data 78
8.2.2 GUI for FloTrac® and doppler echocardiography data 85
8.3 Phase 3: hypoventilation windows visualization and annotation tool 88
8.4 Summary of results 91
8.5 Results of Phase 1 91
8.6 Results of phase 2 92
8.7 Results of Phase 3 96

9 Methodology 99
9.1 Working group 100
9.2 Work packages 100
9.3 Gantt diagram 106

10 Budget of the project 107
10.1 Human resources 107
10.2 Material resources 108
10.2.1 Depreciable material 108
10.2.2 Consumables 109
10.3 Summary of the budget of the project 109

11 Conclusions and future work 111

List of Figures

2.1 OHCA incidence and survival rate per 100,000 people in the Basque Country (BC), European Union (EU) and United States of America (USA). The global average incidence and survival are also displayed [Yan20]. 4

2.2 Physiological heartbeat sequence: (1) rest, (2) sinoatrial (SA) node starts the electric impulse, (3) atrial contraction or diastole, (4) atrial relaxation or systole, (5) ventricular systole and (6) ventricular diastole [Col13]. 6

2.3 Example of a 10 s interval of a normal/healthy EKG record. 7

2.4 Examples of the common types of equipment used for EKG acquisition: **a)** 12-lead electrocardiograph [God]; **b)** Holter [GRO]; **c)** Defibrillator. 7

2.5 Typical EKGs of the 5 main types of rhythms in OHCA; from top to bottom: ventricular tachycardia (VT) (ventricular rhythm with high and regular rate), ventricular fibrillation (VF), pulseless electrical activity (PEA) (electromechanical dissociation of the heart, there is pseudo-organized electrical activity but no efficient mechanical activity that does not generate a proper blood flow), pulsed rhythm (PR) (organized rhythm that generates a proper blood flow) and asystole (AS) (absence of electrical activity of the heart). Figure adapted from [Isa20]. 8

2.6 Example of cardiopulmonary resuscitation (CPR) therapy following the European Resuscitation Council (ERC) Image adapted from [Per15a]. 9

2.7 The Chain of Survival: (1) early recognition and call for help; (2) early CPR; (3) early defibrillation; (4) postresuscitation care. Extracted from [Nol06]. 10
2.8 Blood ejected from the ventricles into the aortich arch the end of the systolic phase. 12
2.9 The EKG signal of a subject (top panel) with the BCG signals of the sensors placed on the carothid artery (middle panel) and around torso (bottom panel). 13
2.10 Typical ballistocardiogram examples. In the top panel 10 s of BCG; in bottom panel, just 1 s. From top to bottom: normal BCG, BCG of a subject being transported to the ambulance and BCG of a subject with hypoventilation 14
2.11 Some of the control measures taken for each subject. From top to bottom: distance between jugulum and xiphoid sternum junction, circumflex distance of chest over the nipples and below jugulum, circumflex distance 5 cm below xiphoid sternum junction. 15
2.12 The 5 steps of the performed cannulation to the subjects, in the first step EMLA is administered (a local anesthetic used prior to the needle puncture) [Age21]. Figure extracted from [But13]. 15
2.13 Examples of the Trendelenburg positon: **a)** in-hospital scenario [Ebl20]; **b)** out-of-hospital scenario [Mis14]. 16

3.1 The Sustainable Development Goals (SDG) proposed by the United Nations (UN) [Nat19]. 18

5.1 Example of a 5 s normal EKG (up) and a labeled normal heartbeat (down). 24
5.2 Example of an echocardiography of the heart. On the left, the aortic arch; on the right, the velocity time integral of the blood flow through the aortic arch. Image extracted from [Rom11]. 25
5.3 Example of **a)** typical in-hospital echocardiograph (image extracted from [Son]), **b)** an echocardiograph intended for out-of-hospital situations [NV]. **c)** Example of use [Dip20]. 26
5.4 The Vscan Air device from GE. Healthcare. Image extracted from [Com21]. 28
5.5 Calculation of **a)** the area of the left ventricular outflow tract (LVOT) and **b)** the velocity time integral (VTI). **c)** 3D combination of Figure 5.5a and Figure 5.5b. Images extracted from [Edu]. 30

5.6 Examples of cardiac catheterization **a)** one phyisician inserting the catheter**b)** different forms the catheter can adopt for coronary artery probing. Images extracted from [Kar20] and [Sys], respectively. 31
5.7 **a)** FloTrack® sensor (image extracted from [Cor19]) which goes placed in the stand presented in Figure 5.8 and **b)** block diagram of the connections for hemodynamic measurements using the equipment from Edwards Lifesciences. 33
5.8 **a)** The HemoSphere® advanced monitoring platform displaying hemodynamic measures. **b)** The HemoSphere® advanced monitoring platform in top of its roll stand. 34
5.9 Placement of the BCG sensors for hemodynamics measurement. 34
5.10 The Physio-Control LIFEPAK® 15 monitor-defibrillator; **a)** the different devices that can be attached to a Physio-Control LIFEPAK® 15, from left to right: 12-lead EKG electrodes, pulse-oximetry sensor, paper to print the records, defibrillation pads and an airway adapter for capnography measurements [Phy20]. **b)** Carried by emergency medicine services (EMS) personnel [Phya]. **c)** The defibrillator pads correct position is indicated in their cover [Phyb]. 36
5.11 Example of **a)** capnography recording device [Cre] and **b)** the disposable airway attached to the device used to measure the exhalated air [Sol]. 36
5.12 Example of **a)** pulsi-oximeter probe attached to a monitor-defibrillator [Phy20] and **b)** the operating principle of the photoplethysmography (image extracted from [Hea]. 37
5.13 Common structure of the QRS detectors, adapted from [Koh02]. 38
5.14 Block diagram of an impedance circulation component (ICC) removal algorithm, based on [Rui13; Alo16]. 40
5.15 Example of **a)** LUCAS® mechanical chest compression system [AED12] and **b)** LUCAS in OHCA [Str]. 41
5.16 Scheme of a ventilations detector based on the transthoracic impedance (TTI) signal, adapted from [Jau20]. 42
5.17 Scheme of a ventilations detector based on the TTI signal, adapted from [Ara17]. 43
5.18 The four phases of the normal capnogram, adapted from [Ara17]. 43

6.1 Block diagram of the Hamilton-Tompkins (HT) heartbeat detector, adapted from [Ham86]. 49

6.2 Block diagram of the WQRS heartbeat detector algorithm, adapted from [Ham86]. 50
6.3 Block diagram of the ventilation detection based on the TTI signal of Alonso et al., adapted from [Alo15]. 56

7.1 Severity-probability matrix. Green: acceptable risk. Yellow: as low as reasonably practicable risk (ALARP). Red: unacceptable risk. Sheet extracted from [Ale17]. 64

8.1 Block diagram of the main phases of the project. 66
8.2 Block diagram of the Phase 1 of the project. 67
8.3 The recorded and used signals for each subject. 68
8.4 Block diagram of the Phase 2 of the project. 77
8.5 Graphical user interface (GUI) for Physio-Control LP® -15 and BCG sensors data. 78
8.6 Display area of the GUI for Physio-Control LP® -15 and BCG sensors data. Just the annotations checkbox is clicked, the rest of the options are unactive. 78
8.7 Segment of the EKG signal with **a)** the context menu,**b)** the patch resulting of adding a heartbeat, **c)** the action of deleting a heartbeat. 79
8.8 Context menu of the CO_2 signal panel. 79
8.9 EKG superimposed to the BCG signals. 79
8.10 **a)** *Visual* area of the GUI for Physio-Control LP® -15 and BCG sensors data. **b)** CASE and **c)** SPAN pop-up of the GUI for Physio-Control LP® -15 and BCG sensors data. 80
8.11 **a)** *Summary* area of the GUI for Physio-Control LP® -15 and BCG sensors data. The selected signal is the EKG. **b)** SPAN pop-up of the summary area. 81
8.12 *Summary* area of the GUI for Physio-Control LP® -15 and BCG sensors data. 82
8.13 Example of heartbeat detection. The blue dashed vertical line represents the time instant of the R-peak and the orange one the detection of the HT algorithm. The orange dot indicates the R-peak of the QRS complex. 83
8.14 Segment of the EKG signal with the QRS checkbox deactivated **a)** and activated **b)**. 83
8.15 Segment of the TTI signal with the VENT. WF checkbox deactivated **a)** and activated **b)**. 84
8.16 Segment of the TTI signal with the VENT. WF checkbox deactivated **a)** and activated **b)**. 84
8.17 GUI for FloTrac® and doppler echocardiography data. 85
8.18 Patches funcionality within the GUI for FloTrac® and doppler echocardiography data. 86

8.19 **a)** *Visual* area of the 2nd GUI. Pop-up menus with the values of the **b)** doppler echocardiograph **b)** HemoSphere connected to the FloTrac sensor. **c)** Possible new values of the span. 87
8.20 Block diagram of the Phase 3 of the project. 88
8.21 GUI for the hypoventilation windows of the Physio-Control LP® -15 and BCG sensors data. 89
8.22 New options of the BCG context menu in the GUI for the hypoventilation windows of the Physio-Control LP® -15 and BCG sensors data. 89
8.23 The new funcionalities added to the patches of the GUI for the hypoventilation windows of the Physio-Control LP® -15 and BCG sensors data. 90
8.24 Example of the updated *Show EKG* option of the GUI for the hypoventilation windows of the Physio-Control LP® -15 and BCG sensors data. 90
8.25 *Visual* area of the GUI for the hypoventilation windows of the Physio-Control LP® -15 and BCG sensors data. 90
8.26 Logical scheme of the database of the project at the end of Phase 1. 91
8.27 Logical scheme of the generalized database. 91
8.28 **a)** Opening, **b)** case changing and **c)** patch drag& drop navigation performance measure of the GUI for Physio-Control LP® -15 and BCG sensors data. 93
8.29 Opening performance measure of the GUI for Physio-Control LP® -15 and BCG sensors data. 94
8.30 Segment of the TTI and EKG signals **a)** not time aligned and **b)** fine tuning time aligned using the **annotation mode** (vertical red lines). 95
8.31 Segment of the BCG1 and BCG2 signals **a)** not proper centered for that time window, **b)** with zoom applied manually using the magnifiers from the top toolbar of the GUI. 97

9.1 The GANTT diagram followed through the project. 106

List of Tables

6.1 Breakdown of the software suite selection criteria. 48
6.2 Breakdown of the heartbeat detector selection criteria. 51
6.3 Breakdown of the EKG delineator selection criteria. 53
6.4 Breakdown of the ICC extractor selection criteria. 55
6.5 Breakdown of the TTI ventilation detector selection criteria. 57
6.6 Breakdown of the CO_2 ventilation detector selection criteria. 60

8.1 The signals used for this project. 68
8.2 Example of the file names from 4 subjects. The files came raw from the Physio-control LP® -15 monitor defibrillator. 69
8.3 Data structure created from the comma-separated values (CSV) files of Table 8.5 with the convertCodeStat data converter. 70
8.4 The information extracted from the _EvetLog files. 70
8.5 Example of the file names from 4 subjects. The files came raw from the Physio-control LP® -15 monitor defibrillator. 70
8.6 Data structure created from the CSV files of Table 8.5 with the convertCodeStat algorithm. 71
8.7 Example of the CSV raw files of the BCG sensors from 2 subjects. 71
8.8 Data types of the CSV files created by the BCG signals acquisition. 72

8.9 Data structure created from the CSV files of Table 8.7 with the written specific algorithm. The dd/mm/yyyy expression refers to day/month/year and hh:mm:ss.ms to hours:minutes:seconds.miliseconds. 73
8.10 Example of a 11 different subjects xls raw files of the FloTrac® sensor, collected by the HemoSphere® advanced hemodynamics monitor. 73
8.11 Data types of the xlsx files from the HemoSphere® advanced hemodynamics monitor with the FloTrac® sensor. 74
8.12 Data structure created from the xlsx files obtained from the xls files of Table 8.10, with the written specific data converter. 74
8.13 Data types of the xlsx file from the Doppler Echocardiograph. 75
8.14 Data structure created from the original doppler echocardiography results xlsx file with the written data converter. 76
8.15 Time alignment of 2 out of the 20 subjets of the study. 76
8.16 Structure created to store the hypoventilation windows of every subject. 88

9.1 Working group of the project. 100
9.2 The first work package. 100
9.3 The second work package. 101
9.4 The third work package. 101
9.5 The fourth work package. 102
9.6 The fifth work package. 104
9.7 The working time schedule of the project. 104
9.8 Project milestones. 105
9.9 Project deliverables. 105

10.1 Hourly wage of the working group (WG) members. 107
10.2 Cost of the human resources. 108
10.3 Total cost of the depreciable material. 108
10.4 Total cost of consumables. 109
10.5 Summary of the total costs and expenses. 109

Acronyms

AED	automated external defibrillation
AHA	American Heart Association
ALARP	as low as reasonably practicable risk
ARC	Australian Resuscitation Council
AS	asystole
AV	atrioventricular node
BC	Basque Country
BCG	ballistocardiography
BioRes	Bioengineering and Resuscitation
BLE	Bluetooth® Low Energy
BMDLab	Biomedical Data Analysis Laboratory
BSA	body surface area
BSICoS	Biomedical Signal Interpretation and Computational Simulation group
CA	cardiac arrest
CHD	coronary heart diseases
CI	cardiac input
CO	cardiac output
CPR	cardiopulmonary resuscitation
CPU	central processing unit
CSV	comma-separated values

DIAART arterial diastolic blood pressure

EDV end-diastolic volume

EKG electrocardiogram

EM emergency medicine

EMS emergency medicine services

ERC European Resuscitation Council

ESV end-systolic volume

EtCO2 end-tidal CO_2

EU European Union

FP false positive

GUI graphical user interface

HDD hard disk drive

HR heart rate

HSFC Heart and Stroke Foundation of Canada

HT Hamilton-Tompkins

IBP invasive blood pressure

ICC impedance circulation component

ICU intensive care unit

ILCOR Liaison Committee on Resuscitation

IoT internet of things

IQR interquartile range

ISM industrial, scientific, and medical

IV intravenous

LED light-emitting diode

LMS least mean squares

LVOT left ventricular outflow tract

MAP mean arterial pressure

MIT-BIH Massachusetts Institute of Technology-Beth Israel Hospital

NAKOS Norwegian National Advisory Unit on Prehospital Emergency Medicine

OHCA out-of-hospital-cardiac-arrest

OOB out-of-bag

PEA pulseless electrical activity

PPV positive predictive value

PPV pulse preassure variation

PR pulsed rhythm

RCA Resuscitation Council of Asia

RF random forest

RLS recursive least square

ROSC restoration of spontaneous circulation

RR respiration rate

SA sinoatrial

SCA sudden cardiac arrest

SDG Sustainable Development Goals

Se Sensibility

SIG Special Interest Group

SpO2 peripheral capillary oxygen saturation

SSD solid-state drive

StO2 tissue muscle oxigenation

SV stroke volume

SVI stroke volume index

SVV stroke volume variation

SYSART arterial systolic blood pressure

TPI tissue perfusion index

TTI transthoracic impedance

UN United Nations

UPV/EHU University of the Basque Country

USA United States of America

VA ventricular arrhythmia

VF ventricular fibrillation

VT ventricular tachycardia

VTI velocity time integral

WG working group

WP work package

1. CHAPTER

Introduction

This Master Thesis has been developed within the Bioengineering and Resuscitation (BioRes) research group of the University of the Basque Country (UPV/EHU) at the Faculty of Engineering in Bilbao, in collaboration with the Norwegian National Advisory Unit on Prehospital Emergency Medicine (NAKOS) from the Oslo University Hospital and the Biomedical Data Analysis Laboratory (BMDLab) at the University of Stavanger (Norway). The work of the BioRes research group is focused towards the application of Digital Signal Processing and Machine and Deep Learning techniques to biomedical signals recorded by monitors and defibrillators during cardiac arrest (CA). The goal is to apply engineering to preserve life.

Emergency medicine (EM) is a medical specialty based on the knowledge and skills necessary for the prevention, diagnosis and treatment of acute illnesses and injuries, covering a wide range of physical disorders [Bar11]. Time is critical in this specialty; thus, to save as many lives as possible, protocols for the care of the most chronodependent processes is an important clinical practice.

The most chronodependent pathology is out-of-hospital-cardiac-arrest (OHCA). The survival rate for OHCA decreases exponentially with time and survival rates are currently around 5-20%. OHCA is responsible for roughly 20% of all deaths in Europe [Han]. When an episode occurs, the patient loses the respiratory and cardiac funtions. The heart stops pumping blood efficiently, and consequently, blood pressure

and flow reach a minimum level, resulting in hypotension. If not treated immediately, hypotension can lead to multiorgan dysfunction, commencing in the brain.

Traditionally, the functionality of the heart is monitored with the electrocardiogram (EKG), a non-invasive, general purpose and low-cost powerful tool for the diagnosis of cardiac dysfunctions. Nonetheless, the EKG only reflects the electrical activity of the heart, so its major limitation is the lack of information about the actual pumping (mechanical activity/blood flow, pressure) of the heart. Often, during cardiopulmonary resuscitation (CPR) the EKG shows close to normal electrical activity, but it is impossible to palpate pulse. This is called pulseless electrical activity (PEA) [Kos10; Dea10], which can also be found in other situations such as haemorrhagic bleeding due to trauma. The objective of resucitation theraphy is indeed to restore the automatic pumping function of the heart, which is known as restoration of spontaneous circulation (ROSC). In such cases the patient is said to present a pulsed rhythm (PR). Discriminating PEA from PR is therefore of paramount importance: first, to recognize if a patient is in cardiac arrest; and second to decide when the arrest is terminated and post resucitation care and transport to the hospital can be undertaken. PEA/PR discrimination can be framed as pulse detection, once an almost normal EKG is found (other arrhythmia with abnormal EKGs are also present in OHCA).

In order to track the mechanical activity of the heart, ultrasound (echocardiography) and invasive blood pressure measurements (thermodilution) are used [Bra14]. These are the gold standard, but they are difficult to perform out-of-hospital [Sun08; Lu06; War99; Gee11], because require special skills and equipment that most of the emergency medicine services (EMS) crews do not have. However, in urgent medical care situations, waiting to get to the hospital is not an option.

Currently, looking for pulse in a pre-hospital setting is undertaken using pulse palpation, which is a vague and subjective. Hence, there is a need for more objective measures, which should be noninvasive, easily deployed, inexpensive and preferrably allowing the real-time monitoring of the patients hemodynamic state (or pulse).

The hypothesis driving this master thesis work is that such inexpensive technology may be available through ballistocardiography (BCG) piezoelectric sensors placed in proper locations of the body. To test this, data will be acquired in a setting simulating an EMS-treated OHCA protocol (prehospital care and transport to hospital) with a cohort of healthy patients. This work will concentrate on providing the neccesary infrastructure for the data conversion, signal time alignment, visualization and analysis of the data generated in the experimental setup.

2. CHAPTER

Background

This chapter is intended to set the background for this master thesis. First, EMS intervention statistics are given, with special emphasis on OHCA interventions. Subsequently, a simple description of the heart's functionality and the electrocardiogram will be given. Next, OHCA will be explained, as well as its treatment: the chain of survival. Through this, the importance of recovering both the mechanical and electrical activity of the heart will be shown, including the parameters that must be taken into account to ensure adequate recovery of its mechanical activity.

Next, we will present the well-established technologies that allow monitoring the mechanical activity of the heart, which are limited to in-hospital use. Then, we will introduce the new technology to monitor the heart activity analyzed in this master thesis: the ballistocardiography. Finally, the clinical drill followed to acquire the signals used for this research is explained.

2.1 OHCA in figures

EMS in Europe deal with about 100,274,000 incidents a year [Kra], 300,000 in the Basque Country (BC) [Bar11; San], which means that every year, approximately 1/7 people in Europe have to be treated by the EMS. As mentioned in the introduction, the most chronodependent and life threatening pathology treated by the EMS is OHCA. OHCA is re-

versible during the first few seconds by an effective and relatively simple maneuver, defibrillation. However, defibrillation loses its effectiveness by approximately 10% for each minute that elapses from OHCA onset to defibrillation. As a consequence, statistics reveal that only 40% of defibrillations are successful. This is why time is key in OHCA.

The accurate incidence of OHCA is challenging to know since its definition may differ among different medical agencies. That is why in 1990 the American Heart Association (AHA), European Resuscitation Council (ERC), Heart and Stroke Foundation of Canada (HSFC) and the Australian Resuscitation Council (ARC), among others, met at the ancient Utstein Abbey (Norway) to establish uniform terms and definitions for out-of-hospital resuscitation. The recommendations agreed upon that meeting are called the Utstein recommendations and are updated periodically [Cum91a; Per15b; Nol19] .

The Utstein consensus recommendations aim to uniformize the reporting of OHCA data and include: a glossary of terms, a template to report the data and definitions for time points and intervals. Utstein ensures comparability between data collected from different medical agencies spread all around the world. Thanks to Utstein global average incidence estimating studies can be done, which report an average incidence of 55 cases per 100,000 population. Figure 2.1 below shows the breakdown of OHCA incidence and survival in the United States of America (USA), the European Union (EU) and BC.

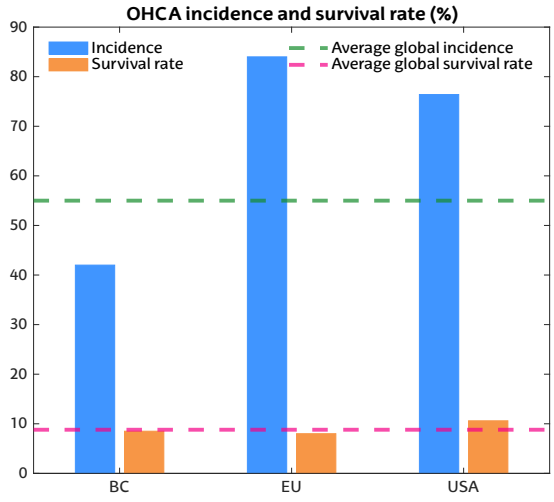

Figure 2.1: OHCA incidence and survival rate per 100,000 people in the BC, European Union (EU) and USA. The global average incidence and survival are also displayed [Yan20].

As we can see in the figure above, the incidence in the USA and the EU is similar and above the global average. According to the AHA, its *Heart Disease and Stroke Statistics - 2021 Update*, the incidence of OHCA in USA is around 76.4 cases per 100,000 inhabitants. In other words, approximately 251,000 people suffer OHCA annually in USA, of whom only 10.6% (26,610 people) survive [Vir21; Pan20].

In the EU, the ERC has carried out the EuReCa ONE (2016) and TWO (2020) studies to determine the incidence, process, and outcome for OHCA throughout the EU. These studies reveal that cardiac arrest is the main cause of death in Europe [Grä21]. They also report a slightly higher incidence figure than the USA, with 84 cases per 100,000 inhabitants, which translates into more than 431,000 people suffering OHCA and a survival rate of 8% (34,500 people) [Grä16; Grä20].

Lastly, in the BC the Basque health agency, Osakidetza, together with scientists from the UPV/EHU reported 826 EMS treated OHCA cases in 2016, [Iba15] which implies an incidence of 38 cases per 100,000 inhabitants, with a survival rate of 8.5% (just 70 survivors).These figures are in line with those of the EU, in which variation across countries and regions is large.Given the large indicidence and the low survival rates, measures to more efficiently treat OHCA would be of great value.

As we have seen OHCA is a sudden cardiovascular event that constitutes a major public health problem. The exact trigger of CA episodes is still uncertain, but studies suggest that about 80% are caused by coronary heart diseases (CHD) [Chu08], especially in older patients. CHD occur when the arteries that deliver blood to the heart muscle (myocardium) become hardened and narrowed by the accumulation of cholesterol and other materials in the artery walls. As a consequence, the heart muscle cannot receive the blood (and therefore the oxygen) it needs. It is also important to note that about two-thirds of sudden cardiac arrest (SCA) occur in adults considered to be a low-risk population [Soa21]. The remaining 20% corresponds to non-ischemic cardiomyopathies (mechanical or electrical dysfunctions of the heart exhibiting inappropriate ventricular hypertrophy or dilatation) [Chu08; Luu89; Kan17]. These cardiovascular diseases cause lethal ventricular arrhythmia, in particular ventricular tachycardia (ventricular tachycardia (VT)) which often preceeds ventricular fibrillation (ventricular fibrillation (VF)) [Cum91b; A B89; Kan17] .

For these reasons prompt treatment is key for survival.During treatment, it is fundamental to monitor the state of the heart (section 2.2), monitor its electrical activity through the electrocardigram (EKG) (section 2.3), and define possible methods to assess its mecanical activity in an out of hospital setting.

Finally, it is also important to mention that currently, the annual cost savings for the health systems per one-year survivor with favorable neurological outcome is more than **81,000 €** in 2018 euros. Hence, measures to more efficiently treat OHCA would be of great value. [Efe18; Sta18].

2.2 The heart. From mechanics to electrical signals

The heart is the muscle responsible to pump blood into the body. The heart produces electrical impulses at regular intervals that trigger a sequence of associated mechanical movements, as can be seen in Figure 2.2. These impulses originate in the sinoatrial (SA) node, the natural pacemaker of the heart, approximately once a second. They propagate through the atria (upper chambers) and ventricles (lower pumping chambers) originating blood flow. The electric impulses in the heart represent the different stages of a heartbeat: rest (1), stimulation (2,3,4) and recovery (5, 6). The generation and conduction of the electrical impulse of a heartbeat gives rich information on the state of the heart muscle, so the analysis of the electrical activity of the heart can be used to detect abnormal heart activity (arrhythmia, abnormal heatbeats, ...).

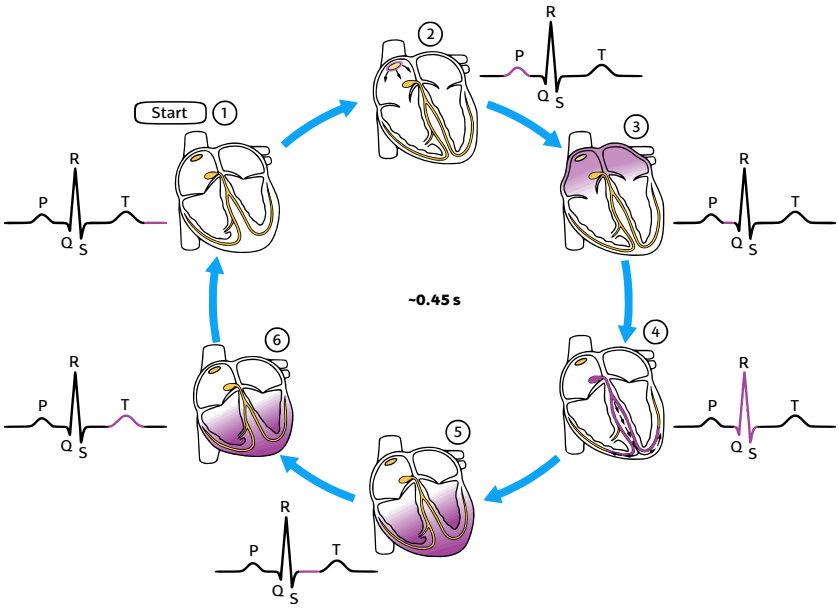

Figure 2.2: Physiological heartbeat sequence: (1) rest, (2) SA node starts the electric impulse, (3) atrial contraction or diastole, (4) atrial relaxation or systole, (5) ventricular systole and (6) ventricular diastole [Col13].

2.3 The EKG: a key tool for CVD diagnosis

The EKG provides useful information about the heart's function, and it is registered by placing two electrodes in the body of the subject. The EKG is the time evolution of the electric impulses that stimulate the heart and produce its contraction, but recorded on the body's surface. A typical example of 10 s of normal EKG activity is shown in Figure 2.3, where the sequence from Figure 2.2 repeats with a rate of 60 bpm.

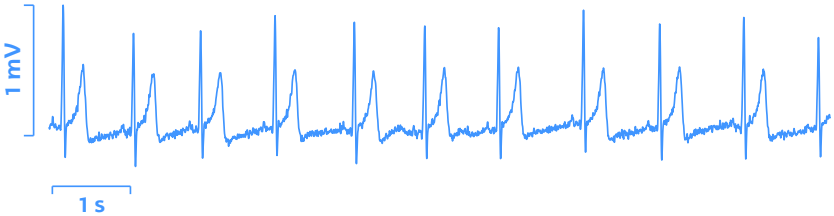

Figure 2.3: Example of a 10 s interval of a normal/healthy EKG record.

The EKG is a low-cost, non-invasive tool very well suited for either diagnosis or continuous monitoring of the patient. The waveform or signal shape of the EKG depends on where the electrodes are placed, and these different placements are called leads. Each lead picks up the same electrical activity of the heart, but from a different position. This permits to see the heart's electrical conduction system from many distinct angles. As shown in Figure 2.4, different equipment is used for EKG acquisition such as 12-lead electrocardiography (Figure 2.4a), Holters (Figure 2.4b) or defibrillators (Figure 2.4c). The Holter monitor is a small outpatient electronic device that records and stores the patient's electrocardiogram for at least 24 hours. It is often used in patients with suspected cardiac arrhythmia [Cor]. A defibrillator is a medical device designed to analyse the heart rhythm, identify deadly arrhythmia and administer an electric shock in order to restore a healthy heart rhythm [LAB13]. Holters are designed for the early detection of arrhythmia, while defibrillators are designed to prevent death in an emergency situation.

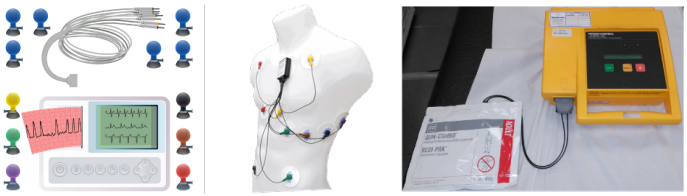

(a) **(b)** **(c)**

Figure 2.4: Examples of the common types of equipment used for EKG acquisition: **a)** 12-lead electrocardiograph [God]; **b)** Holter [GRO]; **c)** Defibrillator.

2.4 OHCA

The sudden, unexpected and potentially reversible cessation of the heart's mechanical activity is called SCA, which leads to loss of spontaneous circulation and breathing. The main cause of SCA is VT (see the top panel of Figure 2.5), which degenerates into VF (see the second panel from the top of Figure 2.5), which triggers 85% of cardiac arrests [Gir16; Rod07].

During VF the is no effective ventricular contraction and the ventricles fibrillate or quiver without order. In these cases, the only way to restore the mechanical and electrical activity of the heart is by defibrillation. Besides ventricular arrhythmia there are three other predominant rhythms/states of the heart during OHCA. These rhythms are defined in the ERC guidelines for resuscitation [Per15a; Soa15], and examples are shown in the following figure:

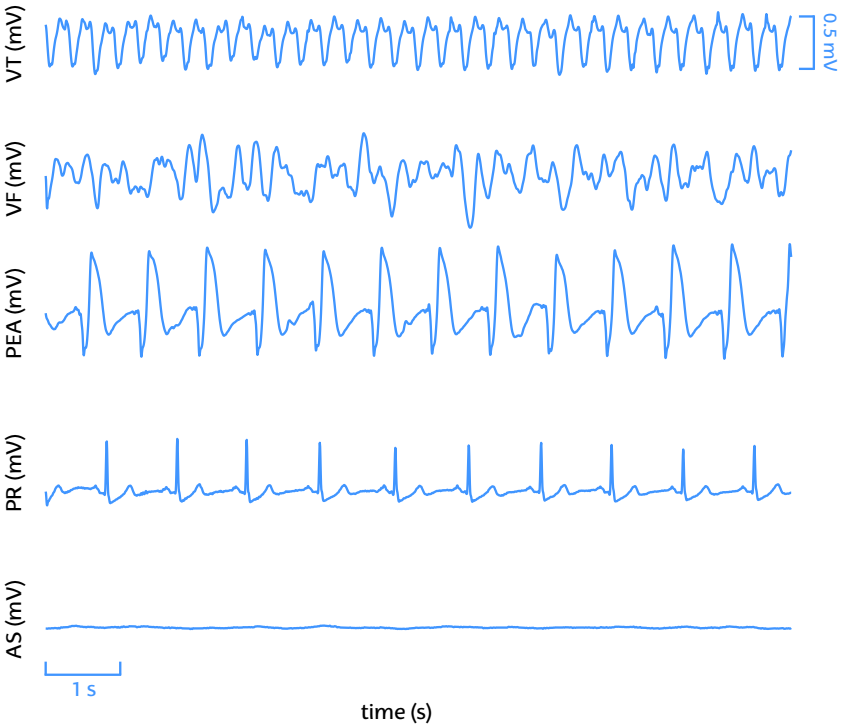

Figure 2.5: Typical EKGs of the 5 main types of rhythms in OHCA; from top to bottom: VT (ventricular rhythm with high and regular rate), VF, PEA (electromechanical dissociation of the heart, there is pseudo-organized electrical activity but no efficient mechanical activity that does not generate a proper blood flow), PR (organized rhythm that generates a proper blood flow) and asystole (AS) (absence of electrical activity of the heart). Figure adapted from [Isa20].

Ventricular arrhythmia (VT/pulseless VT) can be reverted through electrical defibrillation. If the electrical shock is successful a PR is restored, and the patient achives ROSC. Pulsed rhythms generate effective blood flow through organized electrical and mechanical cardiac activity [Zol52]. However, if VF is not defibrillated early, or the defibrillation is not successful, the VF degenerates into asystole (AS) [Wei02] or pulseless electrical activity (PEA). In both cases, there is no effective mechanical activity of the heart, so there is no proper blood flow. CPR can then be used to mantain a minimal artifical flow of oxigenated blood to the vital organs [Kra07; Kou60]. CPR consists in chest compressions and ventilations, as shown in Figure 2.6.

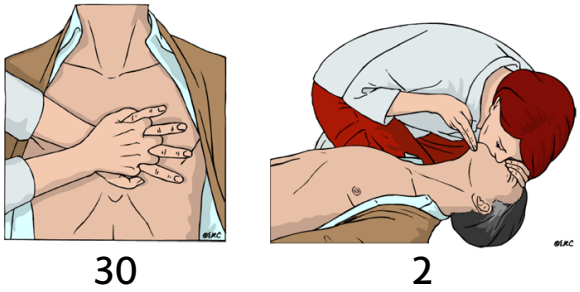

Figure 2.6: Example of CPR therapy following the ERC Image adapted from [Per15a].

Acording to the ERC, after recognizing SCA, CPR should start immediately with a 30:2 ratio, 30 chest compressions and 2 rescue ventilations. The frequency of the chest compressions should be between 100 and 120 compressions per minute with a compression depth of at least 5 cm but not more than 6 cm [Ola21].

PEA and PR present similar (almost normal) EKGs, but during PR the patient has spontaneous pulse and during PEA there is no effective blood flow. A patient in PR (or ROSC) should be transported to hospital and placed in post-resuscitation care. CPR should be continued in patients in PEA. So it is important to differentiate whether the OHCA patient has pulse. This is a very frequent situations, since in approximately 55% of EMS treated OHCA the rhythm found when the rescue team arrives is PEA [Bal16].

However, CPR alone is not always sufficient to treat a patient in PEA. For example, adrenaline, if available, should be used as soon as possible when the OHCA rhythm is non-shockable, or after 3 defibrillation attempts for a shockable OHCA rhythm [Soa21]. Therefore, in most cases not only CPR is necessary, but also defibrillation, tracheal intubation and drug administration (adrenaline/epinephrine) [Soa21]. Hence it is necessary to have a unified protocol to treat OHCA.

2.5 Chain of survival: key therapy for resuscitation

The major resuscitation organisations, such as the AHA, ERC or the Resuscitation Council of Asia (RCA), cooperate within the International Liaison Committee on Resuscitation (ILCOR) to define the resuscitation guidelines. These guidelines reflect the consensus on science and treatment for OHCA and are updated every 5 years. One of the fruits of their work is the chain of survival, presented in Figure 2.7, a protocol generally composed of 4 links indicating specific treatment protocol from the time OHCA is witnessed until the patient is put into hospital [Per15a]. The witness and EMS crews will always try to optimize all critical steps required to improve outcomes.

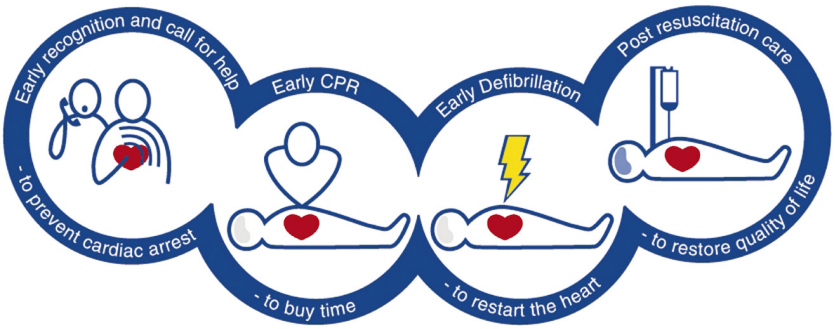

Figure 2.7: The Chain of Survival: (1) early recognition and call for help; (2) early CPR; (3) early defibrillation; (4) postresuscitation care. Extracted from [Nol06].

The four links of the chain of survival are:

- **Early recognition and call for help:** be aware of having witnessed an OHCA and as quickly as possible activate the EMS system by calling the local emergency number (112 in Europe). These actions are directly related to a higher survival rate [Sas10].
- **Early CPR:** initiate CPR to slow the deterioration rate of the brain and heart by sustaining a sufficient perfusion until the EMS crew arrives. If the bystander is not trained to perform CPR, the ERC guidelines recommend performing only compressions.
- **Early defibrillation:** in many cases OHCA is caused by VF or pulseless VT [Pan20] so early defibrillation using an automated external defibrillation (AED) is critical to recover a perfusing rhythm, and therefore to survival; furthermore, defibrillation is most successful when administered as soon as possible after onset of VT/VF. If defibrillation is necessary and delivered within the first

5 minutes of OHCA, it can increase the probability of survival by 50%-70% [Per15a]. Survival rates decreases about a 10% for every minute defibrillation is delayed [Cha08; Val97].

- **Postresuscitation care:** these are the actions taken by the medical team when they arrive at the scene of the event. As mentioned above, sometimes early CPR and defibrillation is not sufficient, and the attending EMS crew may require for the patient drug dispensation, intubation or transportation to the hospital [Sun07].

A key element during treatment is monitoring the hemodynamic state of the patient, in particular the recovery of spontaneous pulse. In a healthy subject two important quantitative measures of the hemodinamic state can be defined: cardiac output (CO) and stroke volume index (SVI).

2.6 Monitoring blood flow

Cardiac output is the amount of blood pumped by the heart to the rest of the body through the aorta every minute, has a value that under normal conditions ranges between [4.5, 8.5] l/min and is calculated by the following equation [Hal16; Bar13b; Sil19]:

$$CO(L/min) = SV(L/beat) \times HR(beat/min). \tag{2.1}$$

where stroke volume (SV) is the stroke volume and heart rate (HR) the heartrate. Stroke volume is the volume of blood ejected by the heart at each systole (each beat), it usually has values in the range of [70, 100] ml and is defined as follows [Hal16; Bar13b; Sil19]:

$$SV(mL/beat) = EDV(mL/beat) - ESV(mL/beat) \tag{2.2}$$

where end-diastolic volume (EDV) is the end-diastolic volume and end-systolic volume (ESV) the end systolic volume. The ESV is approximately 40-50 ml, or one third of the EDV [Hal16; Bar13b; Sil19].

However, not all patients are of the same size, so this calls for a parameter that allows direct comparison between large and small subjects: the SVI. SVI is the volume of blood pumped by every heartbeat divided by the body surface area (BSA)[Du 16],

$$SVI(mL/m^2/beat) = SV(mL/beat)/BSA(m^2) \tag{2.3}$$

Normal SVI is about [33, 47] mL/m2/beat. BSA is an anthropometric variable obtained by applying formulas based on weight (W) and height (H) [Ane],

$$BSA(m^2) = 0.007184 \times W(kg)^{0.425} \times H(cm)^{0.725} \tag{2.4}$$

Currently both CO and SVI can only be measured in-hospital, because the most common and reliable measurement techniques are ultrasound (doppler echocardiography) and invasive blood pressure measures (thermodilution). These techniques require stable and clean clinical settings different from those found in prehospital emergencies, and specialized skills that most EMS crews don't have. Therefore, it would be interesting to have a novel way to measure CO and SVI out-of-hospital in real-time through non-invasive, simple to use and portable sensors.

2.7 Ballistocardiograpy: mechanichs may be the answer

A potential solution to the stated problem is ballistocardiography, a methodology for measuring ultra-low frequency mechanical signals, which are recorded in a ballistocardiogram. The ballistocardiogram is the recording of the recoil of the body in reaction to the ejection of blood from the ventricles into the aorta [Gor77; Par18; Kim16]. More precisely, the ballistocardiogram records the reactionary forces experienced by the body as a result of the impact of the blood on the aortic arch in each cardiac cyle (see Figure 2.8).

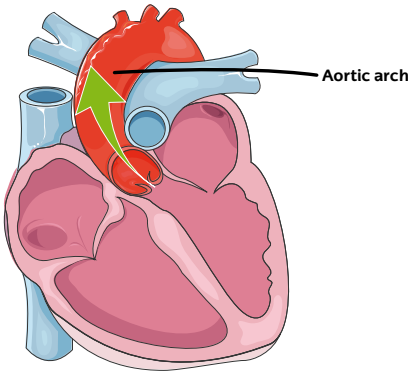

Figure 2.8: Blood ejected from the ventricles into the aortich arch the end of the systolic phase.

In the systolic phase of every heartbeat, the volume of blood is ejected into the aorta, and it moves the center of mass of the body towards head. As the volume of blood is turning crossing the aortic arch and spreads along the body, center of mass moves accordingly towards the feet.

So depending on how much the body moves in one direction or another, one may extrapolate what the CO and SVI are using a BCG

sensor. The BCG is a low frequency signal (1-20Hz) that provides an indirect assessment of heart performance. For instance, the activity recorded by a BCG sensor placed in the carotid together with the EKG signal is shown in Figure 2.9, where the variations associated to each heartbeat are clear.

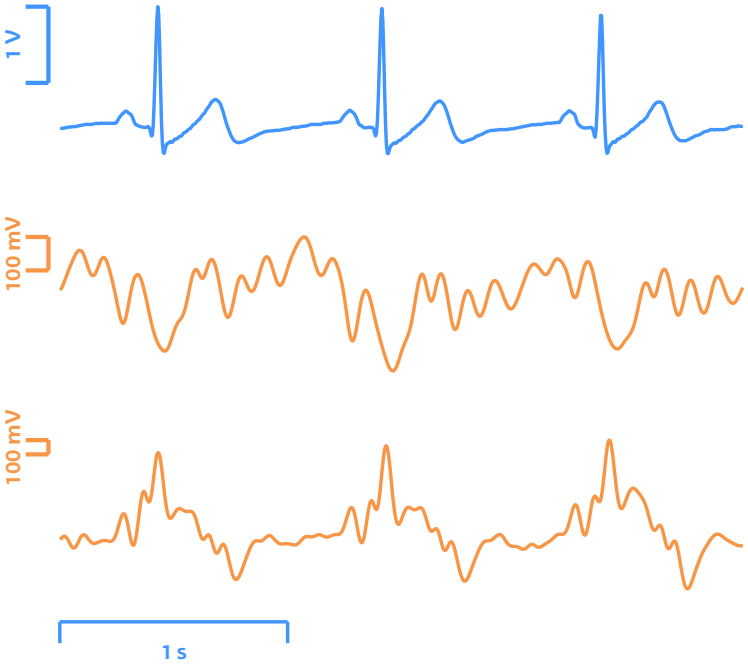

Figure 2.9: The EKG signal of a subject (top panel) with the BCG signals of the sensors placed on the carothid artery (middle panel) and around torso (bottom panel).

Recently, Svensoy et al demonstrated the use of BCG sensor to measure hemodinamic variables in a study submitted to the Norvegian Regional Comittee for Medical Health and Research Ethics. They monitored in-hospital patients with both BCG biosensors and well-established technologies, and proved that the measurements reported by BCG technology in these cases were safe, easy to use, and reliable. Now, the same should be tested for out-of-hospital situations, where the situation is not controlled and the conditions are not as ideal as in the hospital: there is additional noise from the transport of the patient from the floor to the stretcher, the entrance to the ambulance, the movement of the ambulance, the transport from the ambulance to the intensive care unit (ICU)..... These situations alter the BCG waveform considerably, as shown in Figure 2.10 for three different situations.

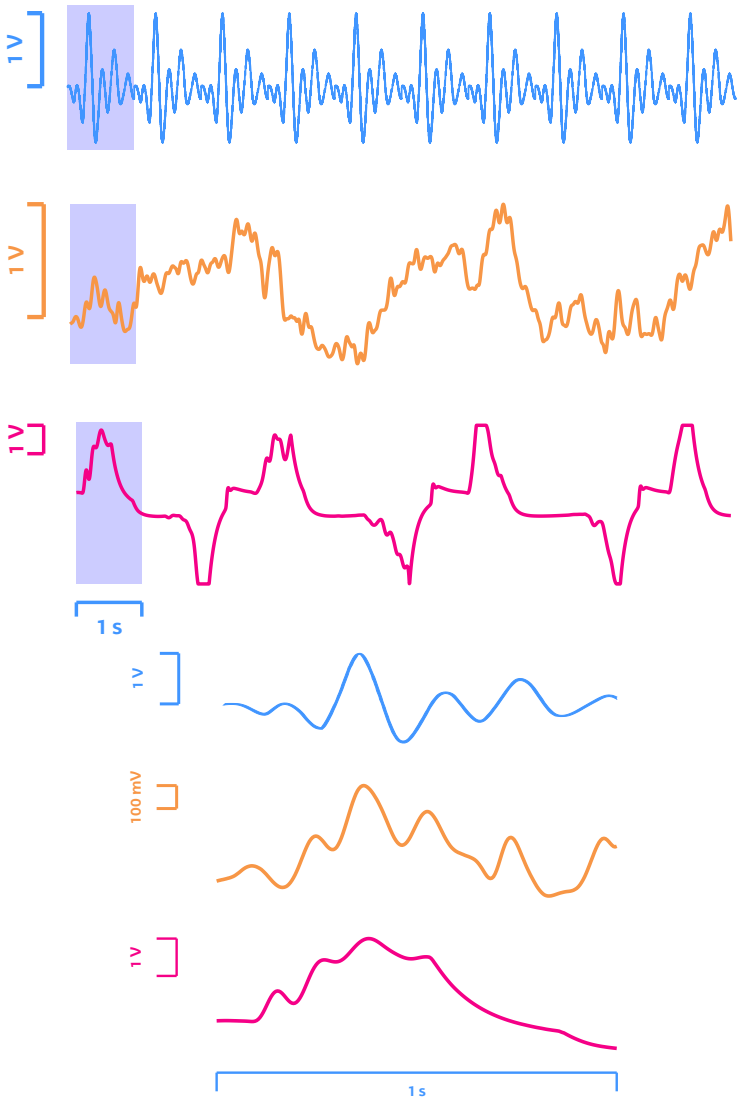

Figure 2.10: Typical ballistocardiogram examples. In the top panel 10 s of BCG; in bottom panel, just 1 s. From top to bottom: normal BCG, BCG of a subject being transported to the ambulance and BCG of a subject with hypoventilation

Figure 2.10 shows the typical BCG signal corresponding to a heartbeat under ideal in-hospital conditions (see Figure 2.10 top), with patient movement (see Figure 2.10 center) and with the patient hypoventilating (insufficient respiration, see Figure 2.10 bottom). As can be seen, the BCG signal varies considerably from one situation to another.

2.8 Clinical drill: trying to replicate EMS attended OHCA

When each of the 20 subjects arrive to the hospital are control measured as shown in Figure 2.11: weight, height, circumflex distance of chest over the nipples and below jugulum and circumflex distance 5 cm below xiphoid sternum junction.

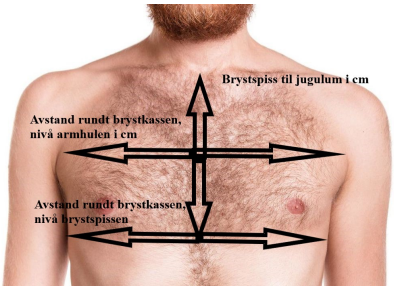

Figure 2.11: Some of the control measures taken for each subject. From top to bottom: distance between jugulum and xiphoid sternum junction, circumflex distance of chest over the nipples and below jugulum, circumflex distance 5 cm below xiphoid sternum junction.

Thereafter, the subject is cannulated with intra-arterial blood pressure lines (see Figure 2.12), defibrillation pads are attached, pulse oximetry probe placed on the finger, cerebral oximetry electrodes placed on forehead, capnography inserted, and BCG biosensors placed, which are connected to the computer through Bluetooth.

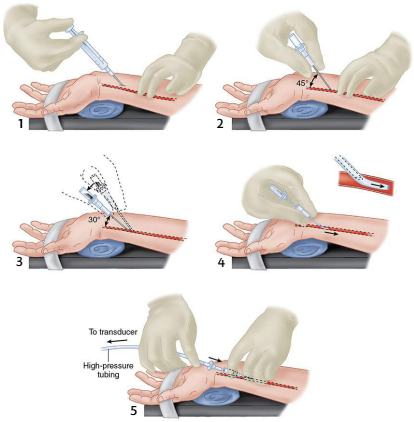

Figure 2.12: The 5 steps of the performed cannulation to the subjects, in the first step EMLA is administered (a local anesthetic used prior to the needle puncture) [Age21]. Figure extracted from [But13].

Also, a GoPro camera is attached to the stretcher for audio, event, time interval documentation, and start and stop of scenarios. The physician operating the doppler echography device identifies the best spot on the chest for measurement and marks it on the skin.

Once the prior procedure has been completed, the protocol continues as follows:

1. The subject lays down on the stretcher. When all equipment is connected to the subject and the doppler echography probe is put on the marked spot the measuremets start. This start is marked with an annotation for each measuring device.

2. During the first 10 minutes of measures the subject is asked to normo-, hypo-, and hyperventilate for 8.5, 1.0 and 0.5 minutes, respectively.

3. Then, the subject will then be put into a 30º Trendelenburg position (see Figure 2.13) and all measures are done for 5 minutes in this position.

(a) **(b)**

Figure 2.13: Examples of the Trendelenburg positon: **a)** in-hospital scenario [Ebl20]; **b)** out-of-hospital scenario [Mis14].

4. After scenario 3 is finished, the stretcher is deployed in an ambulance for a 10 minute ride while all the measures are done (except for the doppler echography)

5. When the ambulance arrives from the ride, the subject on the stretcher is moved to the place where he/she started and receives a 500 ml infusion of Ringer Acetat (a fluid administered to adult subjects in the resuscitation phase with hypotension) as fast as possible. Simultaneously, the measures performed in scenario 1 are done for 3 minutes.

6. End of protocol: saving and download all the data.

3. CHAPTER

Objectives and scope of the study

The main objective of this master thesis is to create **the tools to help establish correlations between cardiac output (CO) and stroke volume index (SVI) values measured by well-established technologies, and the measures taken from novel noninvasive signals such as BCG sensors that could be easily used in OHCA.** This should allow continuous real-time hemodynamic monitoring during EMS treated OHCA episodes.

To ensure the success of a project, it has to be clear what the aim of the project is. To ensure that, a series of secondary objectives must be defined, which must be specific, reachable and measurable. In other words, the secondary objectives must be clear, achievable and set out in such a way that their fulfillment can be verified.

1. **Data management.** Obtain the data from the different equipment used in the clinical trial. These data will make up the database, but each device uses a different proprietary format. Hence, the second step will be to standardize the database by converting the data from a raw proprietary file format to an open MATLAB format. Since each device is turned on at a different time, and also each device has a different clock, the final step in this objective will be the time alignment of the data.

2. **Preliminary database visualization and annotation tool for EMS crew equipment.** This will allow the integration of the different signals recorded for each patient with the equipment used in out-of-hospital situations. The graphical user interface (GUI) will integrate different algorithms for signal processing, which will allow QRS detection, automatic detection of ventilations...
3. **Custom-made visualization and annotation tool for the data acquired from the well-established technologies** (doppler echocardiography and thermodilution). Both this GUI and the previous one will allow fine tuning the time alignment of the signals so that they are perfectly aligned.
4. The fourth objective would be to **identify and extract the time intervals of interest**. A more specific GUI will be created to analyze correlations between measures in specific time intervals.
5. The final objective would be to **filter the BCG signals to eliminate the unwanted components,** such as the noise, which is quite disturbing in out-of-hospital situations. At this point the already built scenario will allow us, together with physicians to try to identify the correlation between the different technologies.

The project would also contribute to meet two of the Sustainable Development Goals (SDG) set by the United Nations (UN) five years ago:

- **Goal 3: Ensure healthy lives and promote well-being for all at all ages.** As mentioned above, the tool resulting from this project may help to improve the OHCA survival rates.
- **Goal 17: Revitalize the Global Partnership for Sustainable Development.**To carry out this project, a multidisciplinary collaboration (mostly engineers and physicians) between 3 research groups from two EU countries has been created.

Figure 3.1: The SDG proposed by the UN [Nat19].

4. CHAPTER

Benefits of the study

The main outcome of this project will be the framework that allows correlating hemodynamic measurements from BCG sensors with those from well-established technologies. And a secondary, but also important, deliverable will be a revised and annotated open format database. This will be rich in biomedical signals (more than 15) from 20 healthy patients. This will be used to try to infer additional parameters from the BCG signals together with those from EKG, thermodilution, doppler echocardiography etc.

- The proposed framework (GUIs plus algorithms for different signal filtering) is a major step towards the correlation between the hemodynamic measures, namely CO and SVI, from BCG sensors and well-established technologies. Its potential lies in that it will set the scenario for analyzing measurements from future researches. Currently there is an ongoing clinical study parallel to this master thesis which is collecting the same signals that have been taken for the cohort of 20 healthy patients, but for cases of real EMS attended OHCA interventions. This framework will be extremely helpful analyze that new data.

- The creation of an open common format database and the necessary algorithms for that will ease the integration of new collected data; this will help to build up an over time larger and larger database. With more data, more statistically sound results will be

obtained.

4.1 Technical benefits

The completion of the objectives of the project will produce several technical benefits related to the research conducted by BioRes.

First, it will consolidate the use of algorithms created by BioRes for the extraction of data from different medical devices and their conversion to a common open format. Having these algorithms already prepared will facilitate similar work in the future. Second, working with BCG signals has required prior study of this area of knowledge, which benefits the research group itself. Third, the graphical interface of the final GUI of this project is more advanced than the previous ones created by BioRes, so its a leap in the ability to make GUIs in the group.

Fourth, this project has helped to consolidate the different algorithms already worked on by BioRes, such as the detection of beats in the EKG signal, the elimination of the ventilation component of the impedance signal... and has also helped to test algorithms that had another purpose but have been used for filtering BCG signals. Fifth, the existing alliance with researchers at Oslo University Hospital has been strengthened and the groundwork has been settled for further data and measurements share with BioRes for joint analysis.

4.2 Social benefits

As shown in section section 2.1, OHCA is the major cause of mortality in developed countries. The developments of low cost, non-invasive and general-purpose tools to monitor the patients hemodynamic state (blood flow and preassure) and the quality of the applied CPR in OHCA would yield important benefits for the population. The whole research within this master thesis is developed may contribute to treat potentially lethal complications derived from untreated or unmonitored PEA and heart dysfunctions.

4.3 Economic benefits

As mentioned in section 2.1, the costs associated to OHCA are considerable for the health care system. With the outcome of the major research associated to this master thesis it will be possible to monitor the hemodynamic state of the patient in out-of-hospital situations, thereby preliminary measures could be taken to prevent deterioration of the patient's state, which would result in higher costs for the health care system: increased use of drugs, personnel, instrumentation, etc.

Moreover, since the hypothesized solution works with BCG signals, it would be a very cheap solution when compared to more advanced and costly techniques like cardiac imaging based on doppler echocardiography, for instance.

In addition, the development of user-friendly tools like the BCG visualisation and annotation GUI will speed up the time needed to construct annotated datasets in the future. These datasets can be used to improve these types of solutions, since the algorithms improve as more data are available, to infer the statistical patterns to differentiate the targeted conditions (cardiac output and stroke volum index in hypoventilation stages). Also, thanks to the BCG filtering algorithms, diagnostic errors will be avoided in noisy BCG scenarios (transport to the ambulance, the ambulance to hospital transportation,...). Both reducing errors and shortening analysis times will result in improved productivity.

5. CHAPTER

State of the Art

This section contains a summary of the most important topics relevant for the development of this research. It starts by reviewing the typical EKG morphology of a heartbeat. Then, the well-established technologies for hemodynamics monitoring are presented. After that, the signals that might be helpful to measure the hemodynamic state of the patient during OHCA. Finally we review the main signal processing algorithms that allow analizing the signals proposed in the previous section, with the objective of achiveing a platform to help establish correlations between the CO and SVI values measured by piezoelectric BCG sensors and those acquired by well-established technologies.

5.1 Normal heartbeat in the EKG

Each normal heartbeat is reflected as a new cycle on the patient's EKG signal. One typical cycle and its constituent waves and intervals is shown in Figure 5.1. The cycle represents the succession of two different processes: the atrial depolarisation/repolarisation and the posterior ventricular depolarisation/repolarisation.

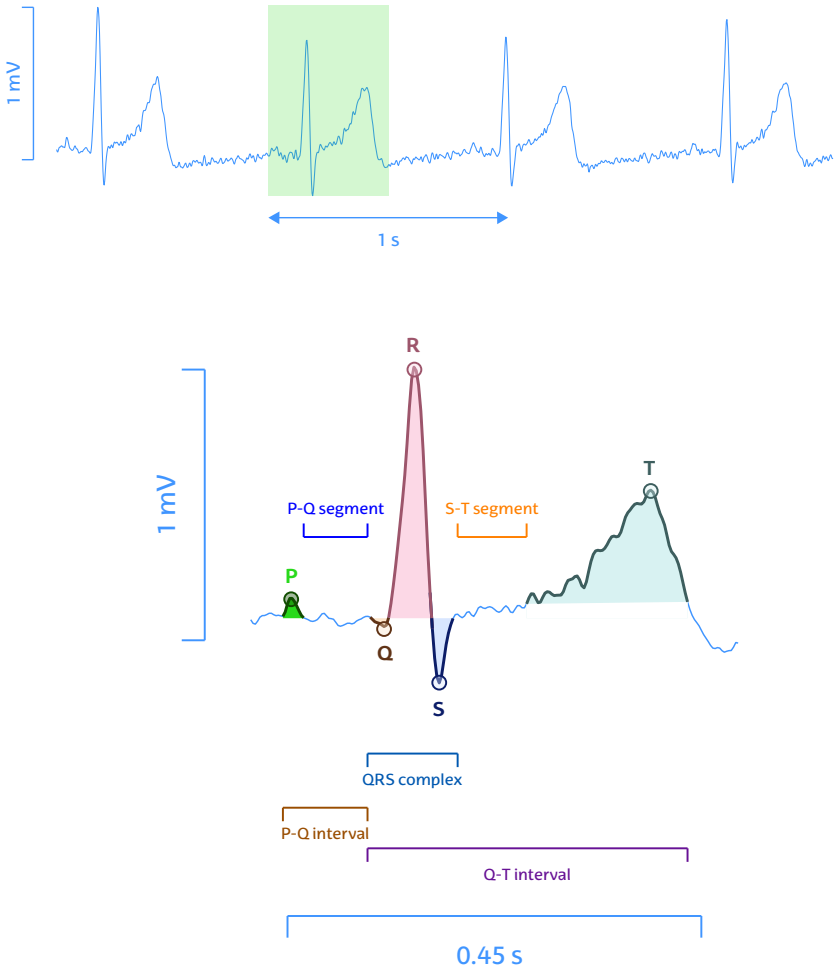

Figure 5.1: Example of a 5 s normal EKG (up) and a labeled normal heartbeat (down).

Therefore, the EKG of a normal heartbeat has the following characteristics [Ein95; Dub07]:

- **P-wave:** represents the depolarisation and contraction of the atria.
- **PQ segment:** 0.1 s pause in the atrioventricular node (AV) node to let the blood flow from the atria to the ventricles.
- **PQ interval:** time interval for the depolarisation/repolarisation of the atria. Atrial repolarisation is not visible as is masked by ventricular depolarisation.

- **QRS complex:** ventricular depolarisation, formed by three waves:
  - *Q-wave.* The beginning of the QRS complex and its first inferior deflection.
  - *R-wave.* First superior deflection, which is larger than the P-wave because ventricular activity is predominant over atrial activity.
  - *S-wave.* The inferior deflection during ventricular depolarisation.
- **ST segment:** the pause after the QRS complex. There is no mechanical activity here.
- **T-wave:** the repolarisation of the ventricles so they can be stimulated in the following heartbeat.
- **QT interval:** refers to the time interval for the depolarisation/repolarisation of the ventricles. This happens simultaneously for both ventricles.

5.2 well-established technologies hemodynamics measurement

5.2.1 Doppler echocardiography

Echocardiography is a medical imaging technique to picture the heart using ultrasound waves (mechanical wave). Echocardiography generates 2D and 3D images of the heart, which allow to calculate the shape and size of the heart, as well as to assess its function in real time [Hal16; CAR20; Jam18]. An example is shown in the following Figure 5.2,

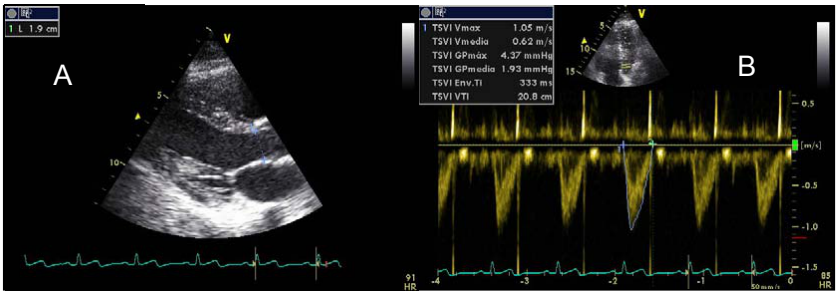

Figure 5.2: Example of an echocardiography of the heart. On the left, the aortic arch; on the right, the velocity time integral of the blood flow through the aortic arch. Image extracted from [Rom11].

The echocardiographs fall into two main categories according their site of use: in-hospital and out-of-hospital. Intrahosptial echocardiographs are complex machines such as those shown in Figure 5.3a, which are extremely reliable, accurate and allow all types of cardiological examinations.

Technological progress in recent years has allowed miniaturization of the technology and there are now solutions for out-of-hospital echocardiography as the one presented in Figure 5.3b,). Historically, echocardiographs consisted of 5 elements: transducer probe, CPU, display, keyboard and control knobs and a printer.

The echocardiography must be performed with the subject in lateral decubitus position (see Figure 5.3c to bring the heart closer to the chest wall[CAR20], with the trunk elevated about 30º (see Figure 2.13).

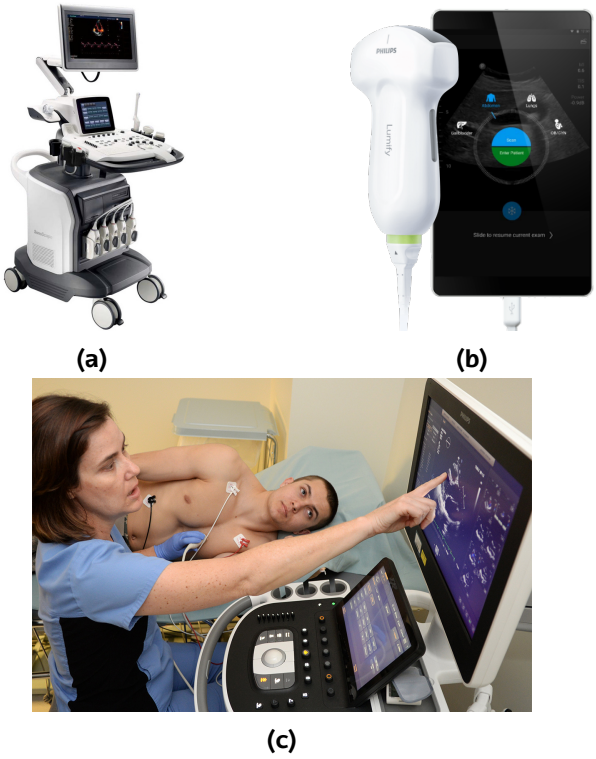

Figure 5.3: Example of **a)** typical in-hospital echocardiograph (image extracted from [Son]), **b)** an echocardiograph intended for out-of-hospital situations [NV]. **c)** Example of use [Dip20].

The 5 most common elements of an echocardiograph are [JGu19]:

- **Transducer probe**: the frequency of the emitted ultrasound waves is in the range of [1,10] MHz. The waves are emitted from piezoelectric crystals that are placed in a transducer (see device in the physician's hand in Figure 5.3c). Piezoelectric crystals (e.g., quartz or Seignette salt) have the ability to convert electromagnetic waves (e.g. electrical potential) into pressure (acoustic) waves of the same frequency, and vice versa; thus, the transducer acts as both an emitter and a receiver of ultrasound. The waves emitted by the transducer penetrate the human body and when interacting with different tissues (e.g., blood, muscle, fat, air,... each one has a different refractive index) they refract and reflect and are received by the transducer (ultrasound waves follow the laws of optics in terms of transmission, reflection and refraction) [Sco21]. The propagation velocity (v) of sound in tissue is ≈ 1540 m/s. Since the imaging resolution equals approximately half the wavelength (λ) of the emission frequency (f_{emission}), the higher the emission frequency, the higher the spatial resolution [Moh10].

$$\lambda = \frac{v}{f} \tag{5.1}$$

$$f_{\text{emission}} \uparrow \Rightarrow \text{spatial resolution} \uparrow$$

  For example, if the emission frequency of the transductor probe is 10 MHz, then solving Equation 5.1 gives $\lambda = 154\ \mu m$, so the imaging resolution $\approx 77\ \mu m$ However, the higher the frequency ($f_{\text{emission}} \uparrow$), the shorter the emitted wavelength ($\lambda \downarrow$) and therefore the lower the penetration depth of the emitted wave. This is why the emission frequency is a compromise value between image resolution and target tissue depth. Most machines operate across frequencies of 2.5 to 5 MHz. After the transducer probe receives the waves, the front end processor combines and amplifies them and the resultant signal is sent to the *central processing unit (CPU)*.

- **Central Processing Unit (CPU)**: is the brain of the machine. On the one hand, it tells the transducer probe what and how to do based on the settings adjusted by the technician using the *keyboard and control knobs*. On the other hand, it takes care of the image generation from the reflected waves captured by the transducer probe. The generated image is shown on the *display*.

- **Display**: is the interface that facilitates the interaction between the technician and the machine. It shows both the machine settings and the test result (image and data).

- **Keyboard and control knobs**: the keyboard is used to register information into the *CPU*.Tthe control knobs are used by the technician to adjust the resolution of the image depending on the application being searched.
- **Printer**: the printer allows the technician to make a hard copy of the ultrasound image.

Today, thanks to solutions such as Lumify (Philips, Amsterdam, Netherlands) any smartphone can be converted into an out-of-hospital echocardiograph. In this context, the smartphone takes the place of the *CPU*, *display* and *keyboard and control knobs* historically used in echocardiographs. This is achieved by installing an app on the smartphone and connecting the mobile probe (transducer) included in the solution (see Figure 5.3b) and is connected to the smartphone with a USB-C cable. The mobile probes in this kind of devices are waterproof, drop-resistant and small (fit in the palm of a hand). Another example is the Vscan Air (GE Healthcare, Boston, USA) showed in Figure 5.4, a battery-operated general-purpose diagnostic ultrasound imaging system which connects to the smartphone via Bluetooth BLE 4.

Figure 5.4: The Vscan Air device from GE. Healthcare. Image extracted from [Com21].

When combined with doppler techniques, echocardiography can be used to measure the velocity of fluids like blood. Knowing that the doppler shift (Δf)is defined as,

$$\Delta f = \frac{f_{emission} \times v_{bf}}{v} \tag{5.2}$$

where v_{bf} is the velocity of blood flow to be measured. For doppler echocardiograpy, it is necessary to multiplicate it by a factor of 2. To complete the above equation, it must be also taken into account that

the doppler pulses must be parallel to the blood flow direction. When this is not satisfied, it must be corrected with a $\cos\theta$ factor, where (θ) is the insonation angle (the angle between the path of the doppler pulses and the direction of flow). The Equation 5.2, would be rewritten as,

$$\Delta f = \frac{2 \times f_{emission} \times \cos\theta v_{bf}}{v} \tag{5.3}$$

Thus, the velocity of blood flow can be defined as,

$$v_{bf} = \frac{\Delta f \times v}{2 \times \cos\theta \times f_{emission}} \tag{5.4}$$

Then, CO can be estimated from the size of the cardiac chambers as well as the velocity of blood flow during the time period (inverse of $f_{emission}$) from the left ventricular outflow tract (LVOT) [Bar13a]. Some examples of the recorded blood velocity curve are shown in Figure 5.5a and Figure 5.5b. The area under that curve is the velocity time integral (VTI), which measures how far blood travels during the time period. So, the SV is calculated as,

$$SV = \text{area}_{LVOT} \times VTI_{LVOT} \tag{5.5}$$

Knowing that area_{LVOT} can be calculated as,

$$\text{area}_{LVOT} = \pi \times r^2 \tag{5.6}$$

where r is the radius of the LVOT (estimated from the ecocardiography image in a first approximation, assuming it is circular). Now the CO and SVI can be calculated using Equation 2.1, Equation 2.3 and Equation 2.4.

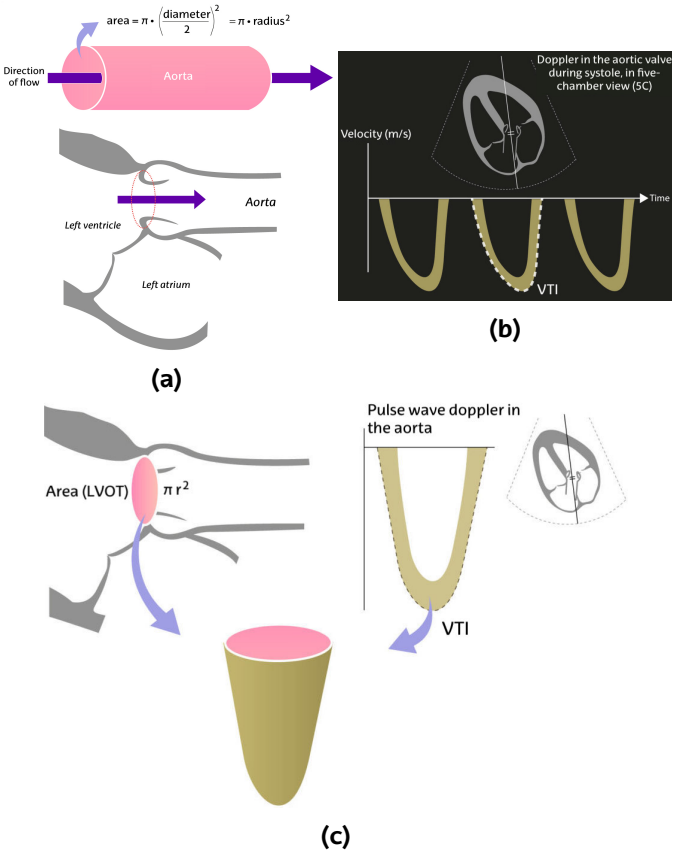

Figure 5.5: Calculation of **a)** the area of the LVOT and **b)** the VTI. **c)** 3D combination of Figure 5.5a and Figure 5.5b. Images extracted from [Edu].

Its safety, together with its noninvasiveness, has made doppler ultrasound one of the most widely used methods for hemodynamics assesment. Its limitations derive from the poor transmission of ultrasound through air, which makes it difficult to obtain good image quality in certain cases, for example with morbidly obese patients. This limitation has been overcome with two invasive techniques [CAR20].

- **Transducers** that are introduced into the esophagus through the oral cavity.
- **Contrast substances** intravenously introduced.

It is important to point out that this hemodynamics assessment method is technician-dependent and that the quality of the test is subject to the skill and experience of the clinician.

5.2.2 Invasive blood pressure

Invasive blood pressure (IBP) is measured with cardiac catheterization, an invasive procedure which consists of the insertion of catheters into the cardiac artheries and chambers to register and analyze the hemodynamics, study the anatomy of the coronary arteries, evaluate ventricular and cardiac valve performance, and screen the presence of congenital heart diseases [M S20]. A catheter is a tube-like device (see Figure 5.6b) which is approximately 2 mm diameter and 30 cm long [Tog13]. Catether sizes are regulated by the ISO 10555-5 standard [Nor14].Cardiac catheterization is the gold standard in the assessment of the anatomy and physiology of the heart [Leo18]; cardiac catheterization is widely spread, for example, in the USA is done 1.5 million times every year and is the second most common surgery [Leo18].

(a) (b)

Figure 5.6: Examples of cardiac catheterization **a)** one phyisician inserting the catheter**b)** different forms the catheter can adopt for coronary artery probing. Images extracted from [Kar20] and [Sys], respectively.

The cardiac catheterization procedure is performed in a hemodynamic room, under aseptic conditions and preparing a sterile field over the patient. The necessary material for this type of surgery is the following:

1. Sterile clothing.
2. Gauze and compresses.
3. Sterile basins.
4. Intramuscular or subcutaneous needle for anesthesia.
5. Scalpel.
6. 10 ml syringe.
7. Connections for mechanical contrast injection device.

8. Percutaneous puncture needle (0.908 mm for radial).

9. Introducer: for the insertion and change of catheters without bleeding of the vessels.

10. Guide: to introduce the catheters up to the LVOT. The guidewire should always be advanced ahead of the catheter to avoid trauma to the vascular wall. The standard guidewire has a curved or "J" end, with a thickness of 0.889 mm and 260 cm length.

11. Catheters: They are classified by their shape, length, diameter and composition. The choice of catheter depends on the anatomical characteristics, the procedure to be performed, the approach route and other factors.

12. Saline solution.

Fick's direct method and thermodilution are the two of the most used methods to calculate CO are based on Fick's principle: *the amount of a substance released by an organ is the product of the blood flow in that organ by the difference between the concentrations of that substance in the inflow (arterial) and outflow (venous) circulation.*

$$CO(L/min) = \frac{substance \text{ consumption [mL/min]}}{\text{arterial } substance - \text{venous } substance \text{ [mL/L]}} \tag{5.7}$$

5.2.3 Fick's direct method

In this method, the substance is oxygen, and the Equation 5.7 can be reformulated as:

$$CO(L/min) = \frac{O_2 \text{ consumption [mL/min]}}{\text{arterial } O_2 - \text{venous } O_2 \text{ [mL/L]}} \tag{5.8}$$

where the O_2 consumption is the oxygen uptake in the lungs and is measured with a spirometer. Nowadays there are also new minimally based methods [Mat12] like the FloTrac® sensor, explained later.

5.2.4 Thermodilution

In this second and less laborious method, the used substance is 10 mL of saline solution at room temperature. The saline solution is injected into a thermistor-tipped catheter (also called Swan-Ganz catheter) which measures the resulting thermal changes in the pulmonary artery. A small computer is used to provide a digital readout of the calculation.

5.2.5 FloTrac® sensor

FloTrac® sensor (Edwards Lifesciences, Nyon, Switzerland) calculates the SV knowing that it is proportional to the pulse pressure, which is difference between systolic and diastolic pressure. Then CO and SVI fundamental hemodynamic parameters are directly calculated with Equation 2.1 and Equation 2.3.

In order to display the measures, the arterial pressure waveform is analyzed and averaged over a period of 20 s.The main advantage from FloTrac® sensor over the contrast methods is that it is atteched directly to the start of a normal radial/cubital arterial catheter as show in Figure 5.7 for hemodynamic parameter calculation.

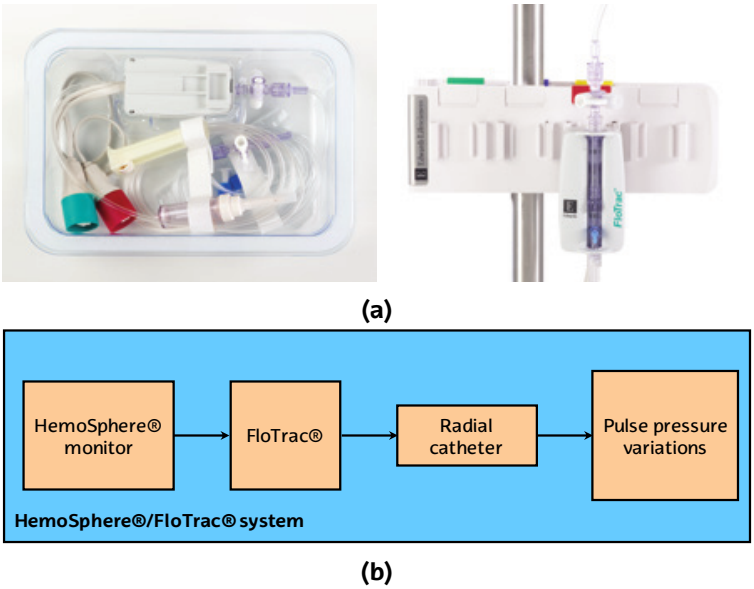

Figure 5.7: a) FloTrack® sensor (image extracted from [Cor19]) which goes placed in the stand presented in Figure 5.8 and **b)** block diagram of the connections for hemodynamic measurements using the equipment from Edwards Lifesciences.

The HemoSphere® advanced monitoring platform (Edwards Lifesciences, Nyon, Switzerland) pictured in Figure 5.8 is used to display in real time the measurements taken by any of the different methods presented.

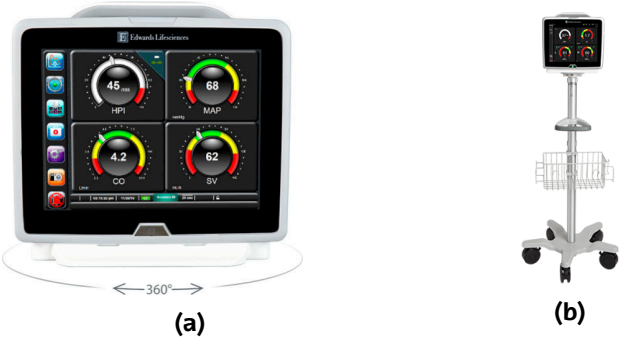

Figure 5.8: a) The HemoSphere® advanced monitoring platform displaying hemodynamic measures. **b)** The HemoSphere® advanced monitoring platform in top of its roll stand.

5.3 Possible new hemodynamics measurement methods

5.3.1 Ballistocardiography

The BCG sensor is a piezoelectric-effect sensor which measures the time and strength of every heartbeat. As shown in Figure 5.9, two BCG sensors are used for this kind of measurements. Once per second it records the HR, respiration rate (RR) and the SV.

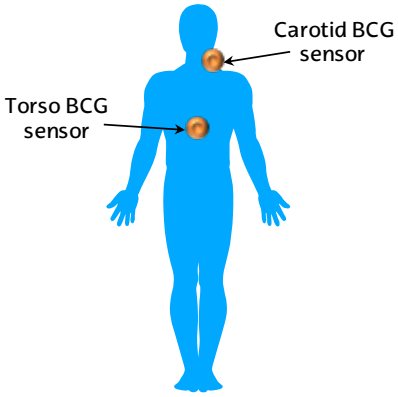

Figure 5.9: Placement of the BCG sensors for hemodynamics measurement.

This technology has been assessed in controlled in-hospital situations, but not it is unknown how will perform during OHCA, hypotension or transportation of intensive care patients.

Data transmission from BCG sensors to the data processing

servers is done via Bluetooth® Low Energy (BLE) protocol. The Bluetooth® Special Interest Group (SIG) currently develops and manages the Bluetooth standard, which follows the client/server model. This standard, also known as classic Bluetooth, offers a higher data rate and scope than other technologies such as ZigBee. However, it consumes more than an order of magnitude of energy than ZigBee. Like other wireless data transmission technologies like Wi-Fi or ZigBee, it operates within the industrial, scientific, and medical (ISM) 2.4 GHz frequency band.

The classical Bluetooth® can offer a typical data rate of 2.1 Mbps in an radius of 100 m [Blu]. In recent years, due to the rise of internet of things (IoT) the BLE has been developed, an appropriate Bluetooth® standard for IoT applications. As the name suggests, the BLE standard is a low-power version, offering a data rate (about 230 kbps) and a restricted coverage ([1.5-2.5] m) [Tos17].

5.3.2 Transthoracic impedance

transthoracic impedance (TTI) is the resistance to the transmission of electrical current flow represented by the thorax (skin, fat, muscle and lung tissues) of a subject. It can be measured by exciting the tissues of the thorax high frequency alternating current and analyzing the induced voltage drop [Gon18]. AEDs record the TTI to assess correct placement of the electrodes (defibrillation pads) to the chest of the subject and adjust defibrillation energy (see Figure 5.10c).

TTI values in adult humans vary considerably as TTI depends, among other things, on chest size, distance between the electrodes and electrode size. In addition, TTI also varies within same subjects due to respiration, composed by ventilations and exhalations (increase and decrease of air volume in the lungs, respectively). With each ventilation the TTI signal rises and it reduces with exhalations.Therefore, although typical values range from 70 Ω to 80 Ω, the range of acceptable TTI values may be [15, 150] Ω [Ker81; Ker84]. The following Figure 5.10 shows the Physio-Control LIFEPAK®-15, a common monitor-defibrillator used by the physicians of the EMS teams.

Since blood is a good electrical conductor, TTI is reduced when the aorta fills and rises when aorta empties. From that variation SV may be inferred. This is why the pulse generated by blood flow causes changes in the TTI signal, proof of which is that it has been used to verify ROSC in clinical trials[Wik05] with a sensitivity (the percentage of subjects with ROSC who have a positive result [Mar11]) of 94% [Alo16].

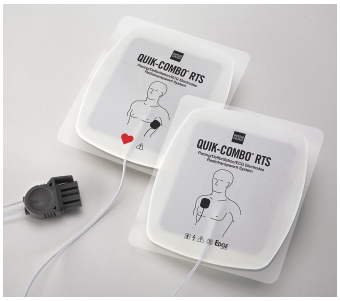

Figure 5.10: The Physio-Control LIFEPAK® 15 monitor-defibrillator; **a)** the different devices that can be attached to a Physio-Control LIFEPAK® 15, from left to right: 12-lead EKG electrodes, pulse-oximetry sensor, paper to print the records, defibrillation pads and an airway adapter for capnography measurements [Phy20]. **b)** Carried by EMS personnel [Phya]. **c)** The defibrillator pads correct position is indicated in their cover [Phyb].

5.3.3 Capnography

Capnography is the continuous noninvasive monitoring of the partial pressure of carbon dioxide (CO_2) exhaled by the subject over time [Die09]. Each exhalation is preceded by a ventilation. Capnopgrahy is measured with a device like the one showed in Figure 5.11.

Figure 5.11: Example of **a)** capnography recording device [Cre] and **b)** the disposable airway attached to the device used to measure the exhalated air [Sol].

Maximum concentration of CO_2 occurs at the end of each exhalation, which is known as end-tidal CO_2 (EtCO2). When the ventilation is stable and controlled a decrease of EtCO2 indicates lower blood flow. However, in OHCA ventilation is not stable and may therefore influence wrongly the interpretation of the EtCO2 value. Thus, EtCO2 is circulation-dependent and is used as an indicator of CO [Fal88; Gud88].With normal physiology, EtCO2 values are [35, 45] mmHg.

5.3.4 Pulse-oximetry

It is a noninvasive technology used to measure oxygen saturation. Oxygen saturation is the ratio of oxigenated hemoglobin to total hemoglobin [Haf21]. Blood oxygen saturation is measured using photoplethysmography, by transmission of light of two different wavelengths into the tissue, which usually is the fingernail bed (see Figure 5.12b).

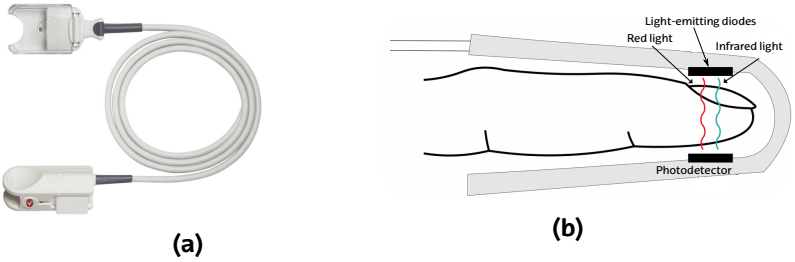

Figure 5.12: Example of **a)** pulsi-oximeter probe attached to a monitor-defibrillator [Phy20] and **b)** the operating principle of the photoplethysmography (image extracted from [Hea].

The measurement is made using a pulse oximeter (a clamp-like sensor) such as the one included in the Physio-Control LIFEPAK® 15 AED and shown in Figure 5.10a and Figure 5.12a. The blood oxygen saturation measured by that device may help in SV estimation for CO calculation.

When measured as presented in the figure above, it is known as peripheral capillary oxygen saturation (SpO2). SpO2 provides information on the adequacy of respiratory function [Nit14].

Hemoglobin is a red-colored protein molecule in red blood cells that transports O_2 from the respiratory organs to the tissues, and CO_2 from the tissues to the lungs which remove it. When hemoglobin transports oxygen, it is called oxyhemoglobin and absorbs red light (wavelengths on the order of 660 nm); however, when hemoglobin loses that oxygen, it is called deoxygenated hemoglobin, which has the

dark red color of venous blood and absorbs light around 920 nm.

As seen in Figure 5.12b, two light-emitting diodes (LED) emit light at the wavelengths described, the proportion of the light of each wavelength that passes through the finger is received by the photodector placed at the other end.

5.4 Automatic algorithms

5.4.1 Heartbeat detector

The automatic detection of heartbeats in the EKG is known as QRS detection, since the QRS complex is the fundamental waveform in the heartbeat. Therefore, the QRS complex is the easiest wave to detect (see Figure 5.1). QRS detection is the first step towards the HR calculation, which is necessary parameter for CO calculation (remember Equation 2.1).

In the literature one can find many signal processing algorithms for QRS detection, Kohler et al [Koh02] provide an excellent review and introduction to the topic. Some of those approaches include the derivative of the signal (QRS is the EKG interval with largest slopes), wavelet-based algorithms, adaptive filters or methods based on the Hilbert transform. However, all of them follow a common structure, which is shown in Figure 5.13.

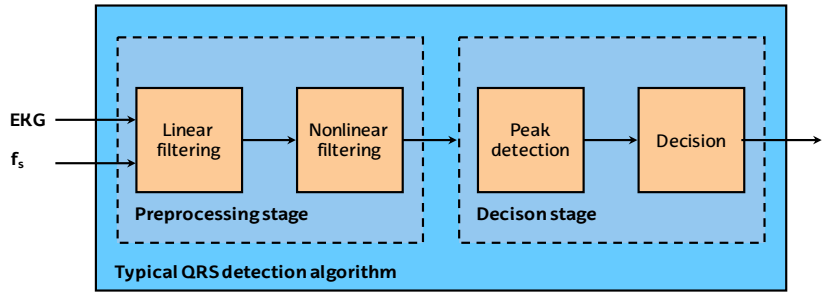

Figure 5.13: Common structure of the QRS detectors, adapted from [Koh02].

Among the various QRS detectors in the literatute, one of the most widespread is the Hamilton-Tompkins (HT). This algorithm takes into account the EKG slope, which it squares and averages with an integrator. Another attractive feature of this algorithm is that it has adaptive amplitude and noise thresholds. More about the HT QRS detector is written in subsection 6.2.1.

5.4.2 EKG delineator

Once the fiducial points of the R-waves are detected, to estimate the position of the remaining Q and S-waves, an EKG delineation algorithm is needed. This will determine the amplitudes and time intervals of the Q,R, and S-waves. One popular approach is the Wavedec algorithm, developed by Biomedical Signal Interpretation and Computational Simulation group (BSICoS) research group from the University of Zaragoza [Gro15]. This algorithm is based on the wavelet transform. A comparison between 3 of the most typical algorithms for EKG delineation is presented in section 6.3

The wavelet transform is a mathematical tool developed in the mid 1980's to overcome the limitations of the Fourier transform. Wavelet transform is efficient for the local analysis of non-stationary, rapidly changing or discontinuous signals [Add05]. This transform makes a multiresolution analysis based on filters.

5.4.3 Extraction of circulation component

The TTI signal is made up of different components. In OHCA, three are distinguished:

- ICC
- Compressions
- Respirations/ventilations

Depending on what we want to measure or detect, one or another component will be of interest. For example, to measure patient hemodynamics (CO, SVI parameters) from the TTI signal, the impedance circulation component (ICC) is used (see subsection 5.3.2). Thus, it is necessary to extract the ICC circulation from the TTI signal.

However, if the objective is to detect the subject's ventilations from the TTI signal (see subsection 5.3.3), it is important to remove the ICC component from the TTI signal. Therefore, both for measuring the subject's hemodynamics and detecting ventilations from the TTI signal, it is essential to have extracted/filtered the ICC component.

One can find many approaches in the literature towards ICC extraction [Cro08; Cro10], but for this explanation the approach of Alonso et al. [Alo16] is used. That approach is shown in Figure 5.14 and improves the one of Ruiz et al. [Rui13] approach).

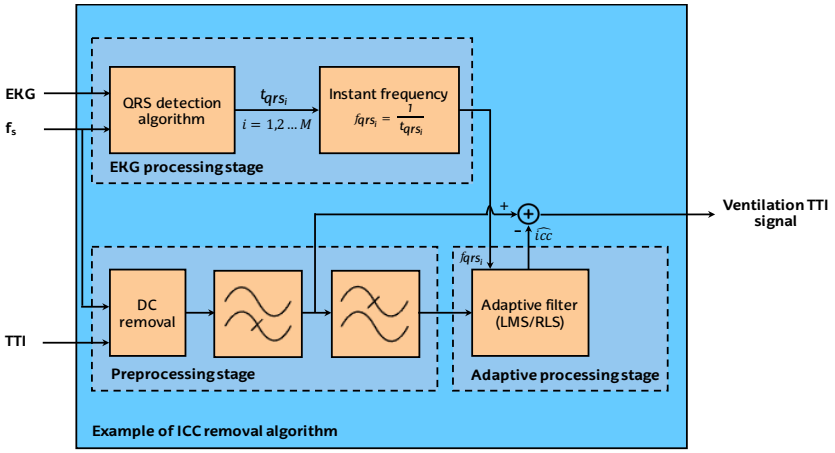

Figure 5.14: Block diagram of an ICC removal algorithm, based on [Rui13; Alo16].

The approach consists of three main stages.First cames the EKG processing, where a heartbeat detector gets the instants of the QRS complexes (t_qrs_i)for the M complexes of the EKG signal. The instantaneous frequency f_qrs_i, is the frequency between two consecutive QRS complexes. This will be used for the adapative filtering stage.

Secondly, the TTI signal is preprocessed by removing its DC component by subtracting the mean value. After that, the high-frequency noise is suppressed using a low-pass filter and low-frequency components below the fundamental frequency of the circulation component are suppressed with a the high-pass filter.

On the third stage, the adaptive filter fed by the instantaneous frequency calculated in the first stage will remove additional noisy components and the estimated ICC signal will be extracted.

Finally, the ventilation signal is extracted by substracting the estimated ICC signal to the low-pass and DC-removed TTI signal.

5.4.4 Ventilation detector

Identifying the ventilations of a subject in OHCA is essential to assess the quality of the CPR and improve OHCA survival. In this research it is particularly important since, together with capnography (see subsection 5.3.3) and/or pulse oximetry (see subsection 5.3.4), it can help to measure the hemodynamic situation (CO and SVI levels) of the patient in OHCA.

5.4.4.1 Ventilation detector in the TTI signal

In the literature there are different algorithms for the detection of ventilations in the TTI signal [Ris07; Ede08; Alo15] although possibly the most novel and accurate is the one proposed by Jaureguibeitia et al [Jau20] last year, which allows the detection of ventilations in cases of OHCA during concurrent mechanical CPR (instead of conventinal manual CPR), which ensure high-quality chest compressions and have become widespread in OHCA treatment.

Mechanical chest compressions are provided from a chest compression system like the one showed in Figure 5.15. Mechanical chest compressions are stable in rate (30:2 standard, see Figure 2.6) and depth ([5,6] cm see section 2.4).

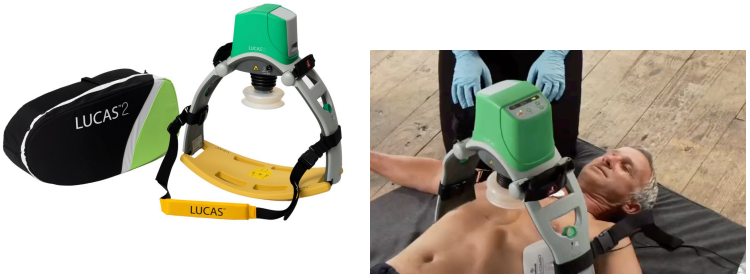

(a) **(b)**

Figure 5.15: Example of **a)** LUCAS® mechanical chest compression system [AED12] and **b)** LUCAS in OHCA [Str].

The typical structure of a impedance-based ventilation detector algorithm is composed by 3 stages: preprocessing, peak detection and characterization and a decision stage. The following Figure 5.16 depicts the proposed algorithm by Jaureguibeitia et al. [Jau20]:

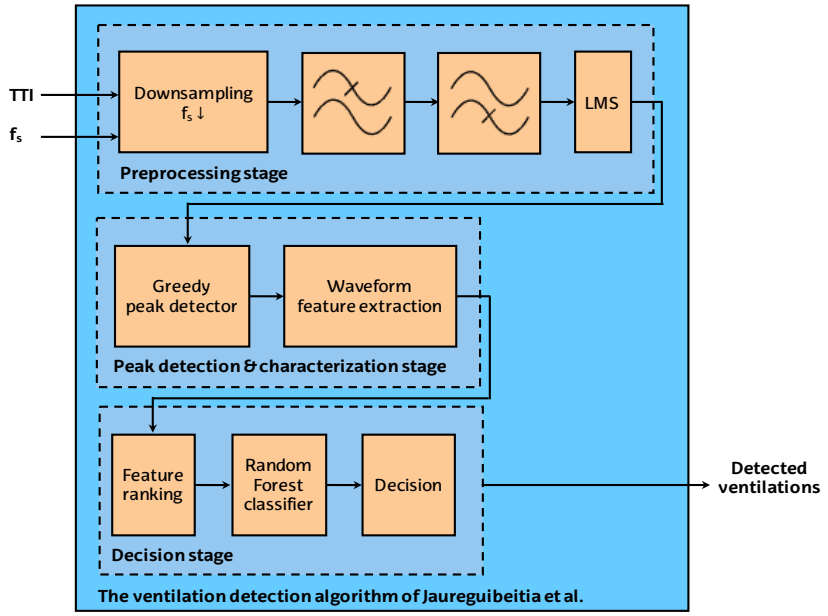

Figure 5.16: Scheme of a ventilations detector based on the TTI signal, adapted from [Jau20].

As can be seen in the figure above, first the raw TTI signal is adaptively filtered to obtain the ventilation waveform. For this purpose, the algorithm downsamples the TTI signal to facilitate the design of the filters and reduce the computational load.

Then, the TTI signal is high-pass filtered to remove the DC component, low-pass filtered to remove high frequency residuals and finally, filtered with a least mean squares (LMS) filter to remove chest compression components.

Once the ventilation waveform has been obtained from the raw impedance signal, the local maxima are detected with a greedy peak detector and to characterize the ventilation waveform for each detected peak several features are extracted.

Finally, to identify true ventilations (the greedy peak detector may has also detected some noise artifacts) a random forest (RF)-based classifier with the best feature subset (features where ranked using the permuted out-of-bag (OOB) error).

5.4.4.2 Ventilation detector in the CO2 signal

Alonso et al. [Alo15] demonstrated that CPR compression artifacts affect the detection of the ventilations in TTI signal. In the study they analyzed 63 in-hospital and OHCA episodes with a mean duration of 11 mins. They found that in some episodes the error rate (defined as ›2 vent/min) was up to 68 %. The mean of the study was 28 %. In addition, the false negative rate (the percentage of ventilations that were not detected over the real total of ventilations) was around 20 %. The algorithm can be represented by the following block diagram:

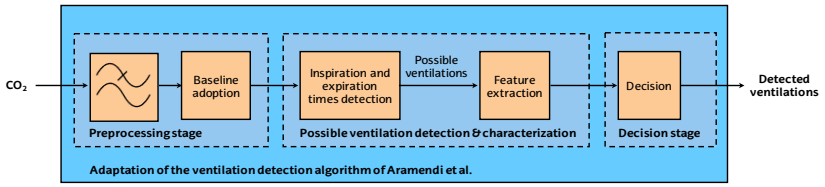

Figure 5.17: Scheme of a ventilations detector based on the TTI signal, adapted from [Ara17].

Therefore, it was demonstrated that ventilation detection algorithms, especially in long resuscitation episodes, presented unacceptably large errors in terms of ventilation detection. For this reason, no system for monitoring the ventilation rate using the TTI signal is currently commercially available.

One possible solution is the detection of ventilations from the CO_2 signal (capnogram). However, few algorithms have been developed for this purpose [Ara14]. Aramendi et al. [Ara17] developed in 2016 an accurate algorithm detect ventilations and give accurate feedback on ventilation rate using only the CO_2 signal. The algorithm is based on the 4 phases of a normal capnogram ventilation (see Figure 5.18):

- Inspiration baseline.
- Expiration upstroke.
- Expiratory plateau.
- Expiration downstroke.

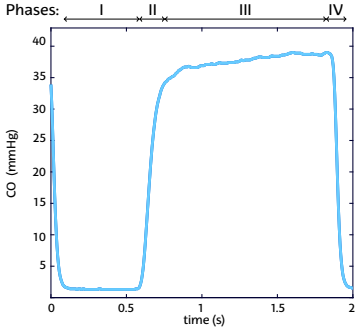

Figure 5.18: The four phases of the normal capnogram, adapted from [Ara17].

6. CHAPTER

Analysis of alternatives

In order to achieve the objectives mentioned in chapter 3 in the most efficient way, this chapter examines the different alternatives that have been considered in the development of the project.

First, the most suitable software suite was chosen for programming the algorithms and developing the visualization and annotation tools for hemodynamic signals. Secondly, the existing alternatives for the automatic haertbeat detection were analyzed. Thirdly, we reviewed the different EKG delineators. Then, circulation extraction methods were studied. Finally, the alternatives for the ventilation detector based on TTI and CO_2 were analyzed.

6.1 Software suite

For the software suite, four possible options for the development of the project were considered: MATLAB, Octave, Python and C. The characteristics and distinctions of each will be explained below.

6.1.1 MATLAB

The MATLAB software suite is a mathematical software tool with an integrated development environment (IDE). MATLAB has its own programming language (M language).

As an interpreted language, it offers a wide range of facilities

to the user, even if the user is not an expert. However, this also affects execution speed, because execution times are slower for interpreted languages than for compiled languages.

MATLAB offers very useful tools for the user, such as toolboxes, in which the developed applications and functions can be found for tools ranging from signal processing to machine learning. It also has a comprehensive help guide [Matb] and a technical support website [Mata]. Another advantage of the MATLAB software suite is its high-quality graphics. In addition, the development of GUIs will play an important role in this project. MATLAB offers an advanced and efficient environment for developing GUIs, called GUIDE.

The major disadvantage of MATLAB is its price. The license price for a single user is about 700 € and the price of each toolbox is 200 € [Matc]. Bearing in mind that it is necessary to use of at least three toolboxes, the total price for the user of the MATLAB platform could reach 1300 €. However, since 2019 the UPV/EHU has adquired a corporate license for MATLAB and now its **cost-free**.

6.1.2 OCTAVE

GNU Octave is a high-level language, similar to MATLAB and compatible with it but also independent. Despite the many similarities, there are many differences that should be considered [WIK21]. The main advantage of this software suite is that is free open source [Eat].

Besides the differences in programming language, there are also disparities in the available resources, i.e. the essential tools needed for the development of GUIs are quite limited in Octave.

Also, the help guide is not as specific and easy to use and the technical support is not as comprehensive, so that problem solving can be made more difficult.

6.1.3 C

The C programming language is aimed to the implementation of operating systems and is widely used to create applications and software systems. The main advantage of C is its fast runtime. Compared to the interpreted languages it is more effective. However, it does not offer facilities for handling matrixes and consequently, it's not as easy to work with large signal databases as in MATLAB or Octave.

6.1.4 Python

Python is the language of choice in machine learning projects, with many available libraries. In addition, it is free, easier than C programming language and allows the creation of GUIs with packages like tkinter, Python's default interface for GUI development [Fun21].

Although Python is very extended and provides all the tools necessary for the development of the project, one of its main disadvantages is the learning curve for the development of the project. In fact, Python is not in the bachelors nor in the masters degree of the UPV/EHU in telecommunications engineering.

6.1.5 Software selection criteria

6.1.5.1 Ease of use and expertise

The complexity of the software is identified as an important feature, thus, so already mastering the software to be chosen and not having to invest time in learning it is essential.

6.1.5.2 Algorithm development time

It is important to develop and implement algorithms in an easy and effective way, so that the development of the algorithms does not delay the project.

6.1.5.3 Organization and data visualization

This project will work with different kinds of signals. Consequently, the programming language must allow and easy and flexible management of large sets of data, and the possibility to easily and dynamically visualise the data.

6.1.5.4 Learning curve

This project is a Master Thesis. In consequence, the hours available for learning new tools as programming languages are very limited.

6.1.5.5 Computation time

The runtime of the algorithms is important in real-time applications; however, the objective of this project is to propose working solutions that can be implemented in efficient programming languages in the future.

6.1.5.6 Price

The price of the software suite is another factor to consider.

6.1.5.7 Final decision

From a weighted assessment of the above parameters, we concluded that the software suite that best fitted our needs was MATLAB. A detailed disaggregation of the weights is presented in Table 6.1:

Table 6.1: Breakdown of the software suite selection criteria.

Criteria	Weight	MATLAB	GNU Octave	C	Python
Ease of use	*0.2*	0.2	0.2	0.05	0.2
Algorithm development time	*0.2*	0.2	0.15	0.05	0.2
Organization and data visualization	*0.2*	0.2	0.15	0.05	0.2
Learning curve	*0.2*	0.2	0.1	0.15	0.05
Computation time	*0.1*	0.05	0.05	0.1	0.075
Price	*0.1*	0.1	0.1	0.1	0.1
Total	*1*	**0.95**	0.75	0.5	0.925

6.2 Heartbeat detector

There are several heartbeat detector algorithms types: combined methods (HT), open algorithms available from the Physionet platform (SQRS, WQRS), and methods based on advanced signal processing.

6.2.1 Hamilton-Tompkins algorithm

The HT algorithm it is a widely used heartbeat detection algorithm which we already presented in subsection 5.3.2. HT is a combined method based on the EKG slope (first derivative), squared and averaged by an integrator, with adaptive amplitude and noise thresholds. Figure 6.1 shows the block diagram of the HT heartbeat detector.

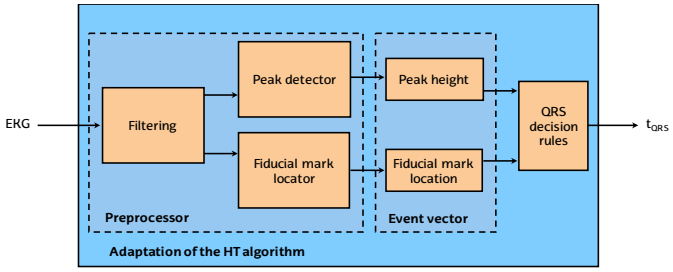

Figure 6.1: Block diagram of the HT heartbeat detector, adapted from [Ham86].

Hamilton and Tompkins applied their heartbeat detector to the most spread database for EKG signal analysis, the Massachusetts Institute of Technology-Beth Israel Hospital (MIT-BIH) database. The Sensibility (Se) and positive predictive value (PPV) of the algorithm were 99.69% and 99.77%, respectively [Ham86].

The sensitivity measures the proportion of heartbeats which are correctly identified as so [Mar11], while the PPV measures how confident we can be on the detection done by the algorithm [Ive11]. Hence, higher Se and PPV will mean a better heartbeat detection algorithm.

6.2.2 Physionet algorithms

The PhysioToolkit suite contains numerous tools and algorithms for physiological signal processing, including two free heartbeat detectors: SQRS and WQRS.The SQRS method uses the characteristic steep slope of the QRS complex for its detection.

First,the EKG signal is resampled at at 250 Hz, then low-pass filtered and finally its derivative is calculated. After this, using the slope

of that signal, the QRS complex is detected. On the other hand, the WQRS method (based on the length of the signal) is divided into three different parts, as can be seen in Figure 6.2.

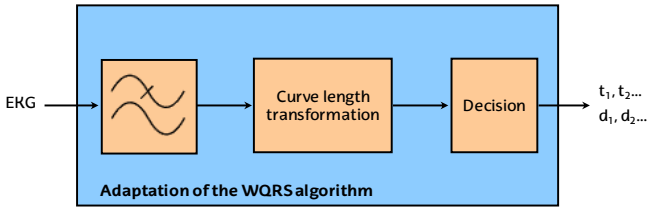

Figure 6.2: Block diagram of the WQRS heartbeat detector algorithm, adapted from [Ham86].

The WQRS algorithm has been applied to the EKG signals of the MIT-BIH database, achieving a Se and PPV values of 99.65 % and 99.77 %, respectively [Zon03]. This means that this algorithm has a very high accuracy. In addition, it is a widely tested algorithm. The main disadvantage of the WQRS algorithm is that, as it is developed in Java and the code is not open, wrappers must be used to make calls to the algorithm from MATLAB, which makes it difficult to use the algorithm. There are currently no versions of WQRS in MATLAB.

6.2.3 Methods based on the advanced signal processing

There are also methods based on advanced signal processing, for example wavelets and rules for determining QRS. Köhler et al. [Koh02] provides a detailed review of heartbeat detectors.

In this subsection, a robust heartbeat detector is analyzed against noise [Ber03]. This is a technique for the detection of heartbeats in EKG that are is based on a characteristic obtained by counting the number of zero crosses per segment. Zero crossing methods are robust against noise and are particularly useful for finite precision arithmetic.

This detection method includes this robustness and provides a high accuracy even in cases of signals of very noisy EKG. In addition, due to the simplicity of detecting and counting zero crosses, it provides a computationally efficient solution to the problem of heartbeat detection.

The excellent performance of the algorithm is confirmed by a Se of 99.70 % and a PPV of 99.57 % against the MIT-BIH database.

6.2.4 Heartbeat detection criteria

6.2.4.1 Accuracy

The accuracy of the algorithm is an important criteria to be taken into account for further analysis of the data.

6.2.4.2 Development time

The time stamps returned by the algorithms do not occur at the peak of the R-wave, but a little after. However, for this project we are interested in marking the precise instant of the R-wave. Hence, we will have to develop patches to correct the marks.

6.2.4.3 Accesibility

It is also very important to have MATLAB versions of the algorithm, to reduce the time needed to implement it in the tools developed in this project.

6.2.4.4 Final decision

From a weighted assessment of the above parameters, we concluded that the heartbeat detector which best suited our needs was the HT heartbeat detector. A detailed disaggregation of the weights is presented in Table 6.2:

Table 6.2: Breakdown of the heartbeat detector selection criteria.

Criteria	Weight	HT	Physionet	Advanced signal processing
Accuracy	*0.4*	0.38	0.37	0.36
Development time	*0.3*	0.3	0.1	0.1
Accesibility	*0.3*	0.3	0.1	0.1
Total	*1*	**0.98**	0.57	0.56

6.3 EKG delineation algorithm

6.3.1 Wavedec algorithm

Martinez et al. [Mar04] introduced the Wavedec algorithm in 2004. Wavedec is an EKG delineator based on the wavelet decomposition of the EKG. The wavelet decomposition analyses the signal in time and frequency by decomposing the signal in non-overlapping frequency sub-bands. The characteristic waves of the EKG occupy different frequency bands, and this property is used by wavelet-based algorithms to identify the waves and its characteristic time-points.

6.3.2 Low-pass differentiation

Low-pass differentiation (LPD) algorithms are widely used for noisy EKG signals segmentation, such as the ones recorded by the Holters. The EKGs obtained by Holters generally present a low signal-to-noise ratio (SNR), related to muscular activity and variations in the electrode to skin contact.

This kind of algorithms is used to obtain just the Q-T interval [Mei95] so their functionality is limited when compared to the Wavedec algorithm.

6.3.3 Second order derivatives

These kind of algorithms are often used to map ventricular arrhythmias (VA). VAs usually consist of just abnormal QRS complexes. These algorithms obtain the points where the QRS begins (onset) and ends (offset).

6.3.4 EKG delineation algorithm selection criteria

6.3.4.1 Accesibility

One important point is to be able to get the algorithm easily so that it can be implemented as soon as possible.

6.3.4.2 Accuracy

It is important to accurately measure the characteristic points of the EKG signal.

6.3.4.3 Computation time

A fast operation time of the algorithm would be ideal. However, as this project is not conceived to develop a real time application, this is not the most determining factor.

6.3.4.4 Final decision

From a weighted assessment of the above parameters, we concluded that the EKG delineator which best suited our needs was Wavedec. A detailed disaggregation of the weights is presented in Table 6.3:

Table 6.3: Breakdown of the EKG delineator selection criteria.

Criteria	Weight	Wavedec	LP2	2nd derivatives
Accesibility	*0.4*	0.4	0.2	0.2
Accuracy	*0.4*	0.3	0.1	0.1
Computation time	*0.2*	0.1	0.2	0.2
Total	*1*	**0.8**	0.5	0.5

6.4 Extraction of the TTI circulation component

6.4.1 RLS adaptive filtering based ICC extractor

Alonso et al. [Alo16] presented in 2016 a method to extract the ICC using the EKG and TTI signals. The proposed method first removes the noise from the EKG and TTI signal. Then detects the QRS complexes in the EKG signal and filters the *clean* TTI signal with an adaptive filter based on a recursive least square (RLS) algorithm.

6.4.2 LMS adaptive filtering based ICC extractor

This detector was developed by Ruiz et al. [Rui13] in 2013. An adapted block diagram representation of the detector is showed in Figure 5.14. This is the previous version of the RLS-filter-based method.

The key difference between the two methods is that Alonso et al. [Alo16] used a RLS algorithm instead of a LMS one to extract the ICC signal from the filtered TTI signal. The RLS algorithm is a more efficient estimator of the ICC component because it has a shorter transient interval. This means that the RLS algorithm has a quicker adaptation to the changes of the TTI signal than the LMS algorithm proposed by Ruiz et al. [Rui13].

6.4.3 TTI circulation component extractor selection criteria

6.4.3.1 Accesibility

One important point is to be able to get the algorithm easily so that it can be implemented as soon as possible.

6.4.3.2 Accuracy

It is important to extract the ICC from the TTI signal to permit detection of PRs during the analysis intervals of an a AED when a non-shockable rhythm with QRS complexes is detected.

6.4.3.3 Computation time

A fast operation time of the algorithm would be ideal. However, as this project is not conceived to develop a real time application, this is not the most determining factor.

6.4.3.4 Final decision

From a weighted assessment of the above parameters, we concluded that the ICC extractor which best suited our needs was the

one from Alonso et al. [Alo16], the adaptive threshold ICC extractor. A detailed disaggregation of the weights is presented in Table 6.4:

Table 6.4: Breakdown of the ICC extractor selection criteria.

Criteria	Weight	Alonso et al.	Ruiz et al.
Accesibility	*0.4*	0.4	0.3
Accuracy	*0.4*	0.3	0.25
Computation time	*0.2*	0.1	0.05
Total	*1*	**0.8**	0.6

6.5 TTI Ventilation detector

6.5.1 TTI Ventilation detector during mechanical CPR

Jaureguibeitia et al. [Jau20] introduced the first method for accurate ventilation detection using the impedance while chest compressions are concurrently delivered by a mechanical CPR device (like LUKAS®, see Figure 5.15).

This detector uses adaptive adaptive signal processing to obtain the impedance ventilation waveform. Then, it extracts 14 features which are fed to a RF classifier. The classifier does not use the same features for all the data, but the best features for each subset were selected with a feature ranking. The RF classifier is used to differenciate real ventilations from false positive (FP) (data detected by the detector as ventilations but which was not a real ventilation). More about this ventilation detector is explained in subsubsection 5.4.4.1.

The results of the performance of this detector are expressed in median interquartile range (IQR) range. The performance was evaluated in terms of Se and PPV, which were 99.2 (96-100) % and 98.3 (95.4-100) % respectively.

6.5.2 Dynamic threshold TTI ventilation detector

This detector was developed by Alonso et al. [Alo15] in 2014.The block diagram representation of the detector is shown in Figure 6.3. The key of this detector are the extracted features used for the classification:

1. Inflation time (from possible ventilation onset to maximum value of the possible ventilation), which was evaluated against a static threshold.
2. Inflation amplitude, which was evaluated against a dynamic threshold.

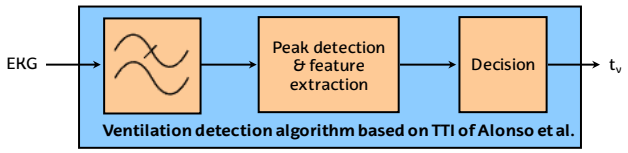

Figure 6.3: Block diagram of the ventilation detection based on the TTI signal of Alonso et al., adapted from [Alo15].

The performance of this detector reported a Se of 92.2 (87.4–95.8) % and a PPV of 81.0 (67.2–90.5) %.

6.5.3 Neural network TTI ventilation detector

Risdal et al. proposed in 2007 a method to detect ventilations in the TTI signal using Neural Networks. This methods includes the multichannel robust adaptive matching pursuit algorithm, which is used to remove the chest compressions artifacts from the TTI channel. Then the TTI is filtered using an infinite impulse response (IIR) filter and the direct current (DC) is removed.

After that, the possible ventilations are detected with a pattern recognition framework. The possible ventilations are then classified by a neural network. Risdal et al. reported a median Se of 90.6 % and a PPV of 97.8 %.

6.5.4 TTI ventilation detector selection criteria

6.5.4.1 Accesibility

One important point is to be able to get the algorithm easily so that it can be implemented as soon as possible.

6.5.4.2 Accuracy

In order to provide feedback on ventilation rates during OHCA treatment, it is important to accurately measure the ventilations on the TTI signal.

6.5.4.3 Computation time

A fast operation time of the algorithm would be ideal. However, as this project is not conceived to develop a real time application, this is not the most determining factor.

6.5.4.4 Final decision

From a weighted assessment of the above parameters, we concluded that the TTI ventilation detector which best suited our needs was the one from Jaureguibeitia et al. [Jau20], the TTI ventilation detector during mechanical CPR. A detailed disaggregation of the weights is presented in Table 6.5:

Table 6.5: Breakdown of the TTI ventilation detector selection criteria.

Criteria	Weight	Jaureguibeitia et al.	Alonso et al.	Risdal et al.
Accesibility	*0.4*	0.4	0.4	0.3
Accuracy	*0.4*	0.4	0.25	0.3
Computation time	*0.2*	0.1	0.1	0.05
Total	*1*	**1**	0.75	0.65

6.6 CO2 Ventilation detector

6.6.1 Adaptive threshold CO2 ventilation detector

Aramendi et al. [Ara17] introduced the adaptive thresholding based CO_2 ventilation detector algorithm in 2016. This detector is based on an adaptive thresholding to classify possible/candidate ventilations detected in the slope of the CO_2 signal. A simplified flowchart of the algorithm is shown below:

1. Detect possible ventilations in the slope of the CO_2 signal.
2. Calculate 5 features for each possible ventilation:
   (a) Duration of the inspiration baseline (phase 1 of a normal capnogram).
   (b) Mean CO_2 value of the inspiration baseline (phase 1 of a normal capnogram).
   (c) Mean CO_2 value of the expiratory plateau (phase 3 of a normal capnogram).
   (d) Area of the first second of the expiratory plateau (phases 2 and 3 of a normal capnogram).
   (e) Relative CO_2 increase (phases 1 and 3 of a normal capnogram). This is calculated by substracting the 3^{rd} feature to the 2^{nd} one and dividing the result by the 3^{rd} one again.
   (f) Inspiration baseline.
3. Compare the 1^{st} feature with a 0.3 s threshold, and the minimum distance between ventilations with 0.5 s.
4. Compare the 3^{rd}, 4^{th} and 5^{th} features with adaptive thresholds based on the last p ventilations.

Just like the heartbeat detector, the performance of this detector is evaluated in terms of Se and PPV, which were 99.0 (95.7-100) % and 97.6 (94.8-100) % respectively (median, IQR). Five features are calculated for every potential ventilation.

6.6.2 Duration based decision CO2 ventilation detector

Leturiondo et al. created a simple detector which follows a similar structure to the one proposed by Aramendi et al. The steps that follows are 3 [Let17]:

1. Possible ventilation detection.

2. Calculate 2 features for each possible ventilation
   (a) Duration of the expiratory phase of a ventilation (phases 2, 3 and 4 of a normal capnogram).
   (b) Duration of the inspiratory phase of the next ventilation (phase 1 of a normal capnogram).
3. Compare the 1st and 2nd parameters with certain static thresholds.

The performance of this detector was reported with 95% cardiac input (CI) instead of the median IQR range. The achieved Se was 99.7 (99.5-99.9) % and the PPV was 99.0 (98.7-99.3) %. These results are better than the ones reported by Aramendi et al. However, the detector thresholds were optimized for a clean training set (no CPR artifacts) to maximize Se and PPV. Thus, we do not know how good does this classifier perform in real OHCA situations, but we do for the robust one of Aramendi et al.

6.6.3 Primitive CO2 ventilation detector

This was presented in 2010 and was the first algorithm to automatically detect ventilations in the capnogram during CPR [Ede10]. This algorithm is a primitive version of the one from Aramendi et al. and the duration based decision CO_2 ventilation detector. The algorithm first detects possible ventilations in the first derivative. Then, the algorithm requires to the possible ventilation to meet three static thresholds before a ventilation is detected:

1. Duration of the expiratory phase between 0.3 and 5 s.
2. More than 0.4 s since last inspiratory phase.
3. CO_2 value less than 2 mmHg

Edelson et al. reported a Se 82 (75-93) % and a PPV of 91 (85-95) % for this CO_2 ventilation detector.

6.6.4 CO2 ventilation detector selection criteria

6.6.4.1 Accesibility

One important point is to be able to get the algorithm easily so that it can be implemented as soon as possible.

6.6.4.2 Accuracy

It is important to accurately measure the ventilations on the CO_2 signal.

6.6.4.3 Computation time

A fast operation time of the algorithm would be ideal. However, as this project is not conceived to develop a real time application, this is not the most determining factor.

6.6.4.4 Final decision

From a weighted assessment of the above parameters, we concluded that the CO_2 ventilation detector which best suited our needs was the one from Aramendi et al., the adaptive threshold CO_2 ventilation detector. A detailed disaggregation of the weights is presented in Table 6.6:

Table 6.6: Breakdown of the CO_2 ventilation detector selection criteria.

Criteria	Weight	Adapt. threshold	Duration based	Primitive
Accesibility	*0.4*	0.4	0.3	0.2
Accuracy	*0.4*	0.35	0.3	0.25
Computation time	*0.2*	0.1	0.15	0.1
Total	*1*	**0.85**	0.75	0.55

7. CHAPTER

Risks analisys

The objective of this section is to identify the possible risks throughout the development of the project and develop a contingency plan to minimize their possible impact. Since the project is already completed, we can say that all the risks that could impede the normal development of the project have been avoided. However, this was not a coincidence, but the result of anticipating the risks that could have occurred and the assessment of the risks they would pose on this project.

Two concepts have been considered to carry out this risk analysis. On the one hand, the probability of the risks to occur. On the other hand, the impact that these risks may have on the project. Therefore, the risk analysis will take into account the probability of occurrence and its possible incidence. These two parameters have been measured as follows:

- **Probability**: low, medium or high.
- **Impact**: low, medium or high.

The possible foreseen risks and their related contingency measures to face them are listed below.

7.1 Risk of coding errors (A)

When developing an algorithm or a GUI, it is very common to produce coding errors that result in a failed program execution, which hinders the normal progress of work. Coding errors are frequent (high probability), and can have a medium impact on the project as it can leave the project on standby for days.

Also, in the worst case, it may involve rewriting the code we have worked on. To reduce the effect of this risk, we use the debug tool of MATLAB to locate the bugs in the code. Besides, it is recommended to run the program with every change to make sure everything is correct. If the root of the problem is not found, members of the BioRes research group can be consulted.

7.2 Risk of delays (B)

It is very common to have delays in the different stages of the project, which can lead to not fulfilling the deadlines established at the beginning. This is very likely, but it has a low impact because the working group (WG) is very small and the working time is easily recoverable. To minimise this risk, a prior planning of the work is done, well-structured and in which the tasks have some margin for completion.

7.3 Risk of data loss (C)

This risk includes any loss of information that may occur during the project, whether in the documentation of the work, the latest versions of the code for the various algorithms and software tools, and the databases and annotations created. This event has a low probability of occurrence, but in case the impact would be high.

To avoid this risk, several systems are used to backup and store the data, like hard disk drive (HDD), solid-state drive (SSD) or the *cloud*. In addition, we periodically save the files while working on them, so that, in case the software fails, a recent version of them is available. To prevent this risk it is very convenient to use the Time Machine functionality offered by the Apple computers we have used. Once the external-drive (HDD or SSD) is connected, the computer itself performs a backup of the system automatically every hour or whenever important changes occur. Thanks to this, one can access backups with the desired date and time, so the loss of information, if any, is minimal.

7.4 Risk of staff leaving (D)

It is also necessary to consider the possible departures (for medical or personal reasons) of the different members of the working group. This is a rare fact (low probability), and the impact can be considered medium although it can vary depending on the responsibility that the individual has in the project and the duration of his absence.

In this case, there is no action that can be taken. In the event of termination, the project manager will decide whether it is necessary to postpone completion of the project or reassign responsibilities.

7.5 Risk of COVID-19 (E)

Since last year the whole world is suffering from the COVID-19 pandemic and the SARS-CoV-2 virus has already infected since March 2020 more than 198,980 people in the Basque Country (28,687 in Araba, 101,663 in Bizkaia, 68,630 in Gipuzkoa) [sal20].

Given that this master thesis began on November 11, 2020, it is reasonable to consider the possibility of becoming infected with SARS-CoV-2. The impact that would have if the director or student of this master thesis were infected with COVID-19 would be high, since he would have to be confined within a room in his house and would also have episodes of fever, respiratory distress and general malaise, making it very difficult to work under these conditions. In addition, once the COVID-19 disease is overcome, he would need a few days to recover.

To try to minimize this risk, the meetings between director and student are held in via Skype, or in case they are held in the director's office, with the mask on and with the office window open to allow continuous air circulation.

7.6 Knowledge risks (F)

The knowledge of the medical terminology, methods and theory for the development of this project is essential. In addition, having hardware/software problems or having problems in the integration of the developed interfaces or scripts, are examples of risks that can appear within this project.

Nevertheless, measures have been taken to avoid these risks. Since it was it was the first time G2 worked with hemodynamic-related signals like CO, SVI, or BCG, a lot of time has been invested in studying the state of the art of those signals before the project began. In addition, a proper use and maintenance of the equipment

was ensured. Therefore, in view of the above, it may be possible to have knowledge bugs, but thanks to the contingence measures they would be marginally influential.

7.7 Risk of excessive costs (G)

Exceeding the planned development costs is a concept that is included in the cost risks. This would would occur if not taken into account would appear, such as the need for more material, changes in prices, or flights to Oslo (Norway) to help with new measurements. Therefore, we added a 5% margin to the budget at the start of the project to cope with eventualities.

However, in order to develop our project, not much material has been purchased (for example, the MATLAB license was provided for free by the UPV/EHU). Thus, the probability of this risk is very low, and its impact on the project would also be small.

7.8 Summary of the risk analysis

Below in Figure 7.1 is a matrix showing the probability relationship of the different mentioned risks.

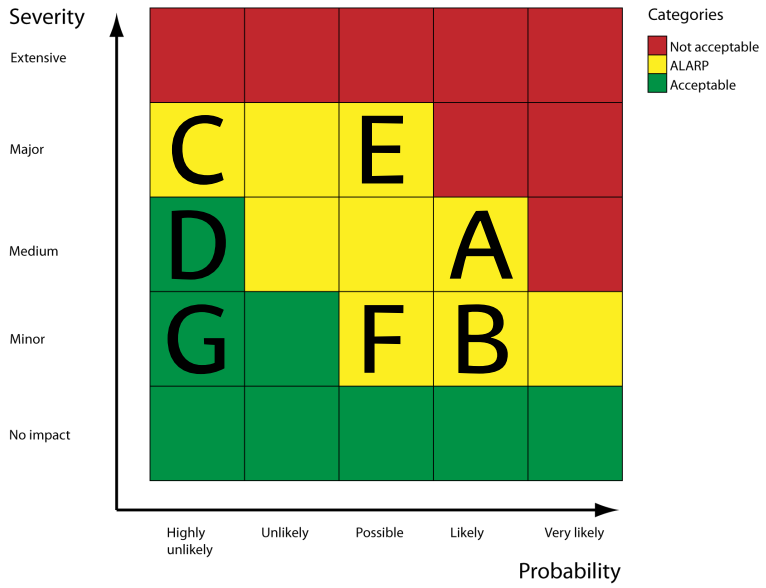

Figure 7.1: Severity-probability matrix. Green: acceptable risk. Yellow: as low as reasonably practicable risk (ALARP). Red: unacceptable risk. Sheet extracted from [Ale17].

8. CHAPTER

Description of the solution

Towards effectively carrying out and managing this project, its development has been divided in three phases. First, we converted the raw data from 4 different data sources to a common open MATLAB format. Since data were in propietary format, data converters had to be developed.

Second, we created two preliminary GUIs to visualize, annotate and analyze the generated database. We implemented the 4 algorithms selected in chapter 6 to detect and delineate the heartbeats in the EKG, extract the ICC component from the TTI signal and detect the ventilations in the TTI and CO_2 signals.

Third and last, the analysis windows were defined together with the physicians from NAKOS and we extracted them with a custom-made algorithm. We also made a third GUI to visualize the extracted analysis windows and annotate what could be special interest time segments.

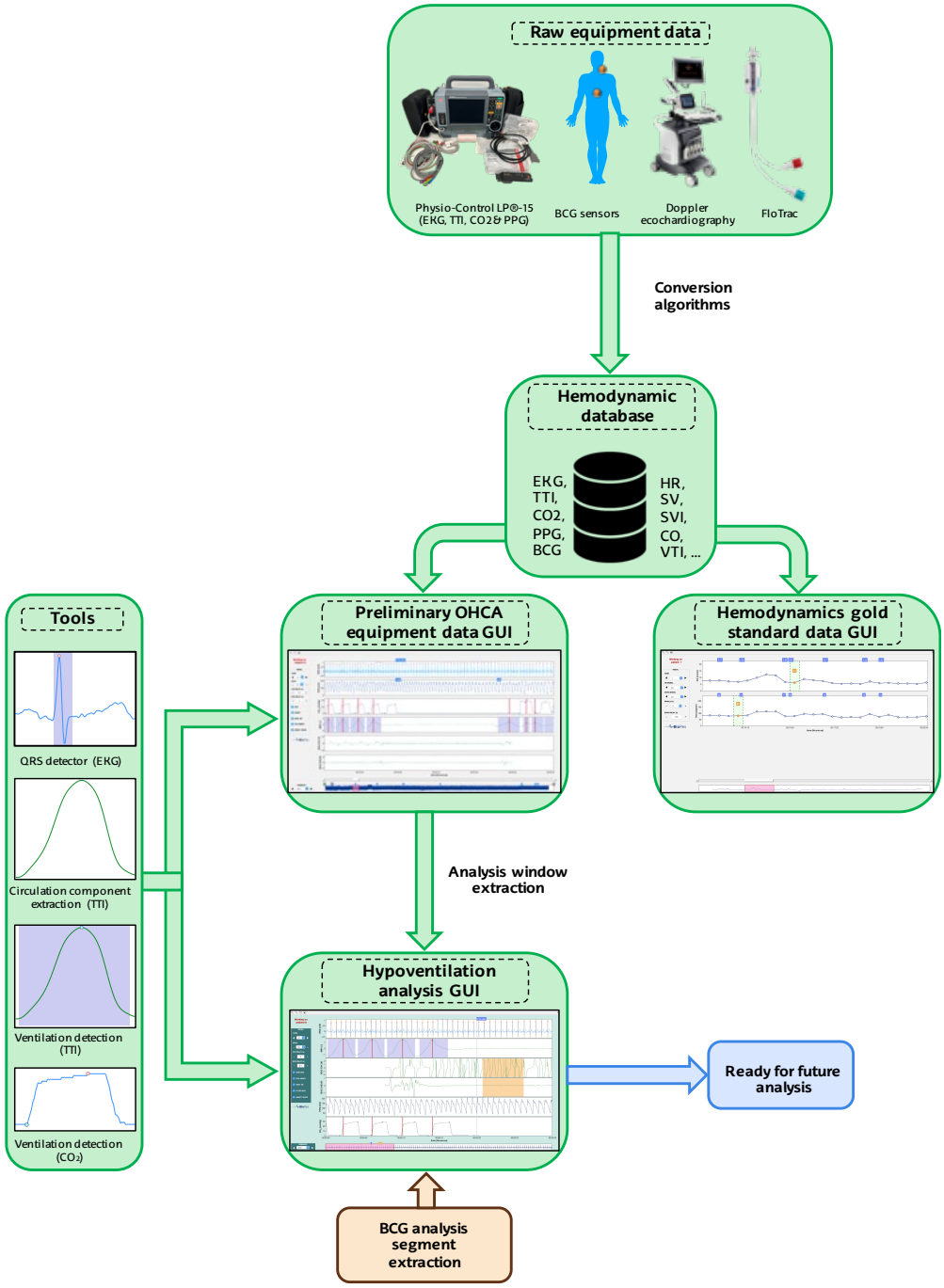

Figure 8.1: Block diagram of the main phases of the project.

8.1 Phase 1: data management and completion of the time aligned dataset

The objective of this first phase was to achieve a standardized and unified database under the common MATLAB format, giving a common format to the various and heterogeneous data sources. The summary of this phase is shown in Figure 8.2.

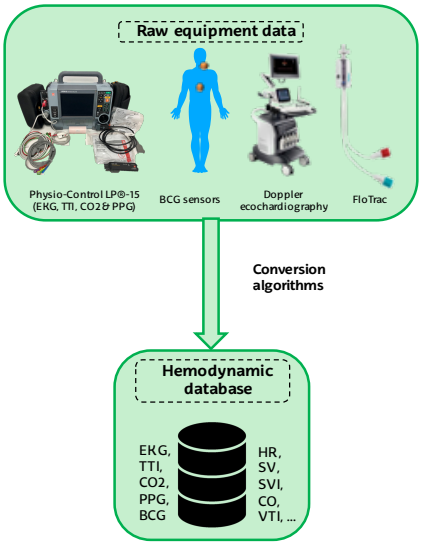

Figure 8.2: Block diagram of the Phase 1 of the project.

It should be recalled that this study was performed over a cohort of 20 patients. The same clinical drill (see section 2.8) was repeated for each of the 20 subjects, resulting in 20 sets of measurements for each type of measurement performed. The measured signals are shown in the following Figure 8.3. Table 8.1 presents the 4 types of devices/sensors used for this master thesis.

A total of 24 signals were acquired per subject (total 480), but 12 (total 240) were used in this work, as shown in Figure 8.3. These 12 signals are those already presented in the section 5.3 section and the hemodynamic parameters. Among the remaining 12 not selected so far, we find Vmax, VTI, Cardiac Input... among others.

Table 8.1: The signals used for this project.

Equipment	Signal	Sampling frequency (Hz)
Physio-Control LP®-15[1]	EKG (mV)	40
	TTI (ohm)	100
	EtCO2 (mmHg)	61
	SpO2 (mV)	125
BCG sensors	BCG in the carotid	250
	BCG in the torso	250
Doppler echocardiography[2]	CO	-
	SV	
	SVI	
	HR	
FloTrac® sensor	CO	0.05
	SV	0.05
	HR	0.05

[1] The signals from Physio-Control LP®-15 were resampled to 250 Hz.
[2] Nonuniform sampling frequency. Measurements were taken at key time points.

First, the data format of each device was studied. Subsequently, data was preprocessed and converted to a common MATLAB format using specific converters for each device/data source.

Finally, given that the clocks of the different medical devices used in this research (Physio-Control LP®-15, BCG sensors, Doppler echocardiography and FloTrac® sensor) were not synchronized, it was necessary to perform a preliminary time alignment to have the data of the 20 subjects synchronized.

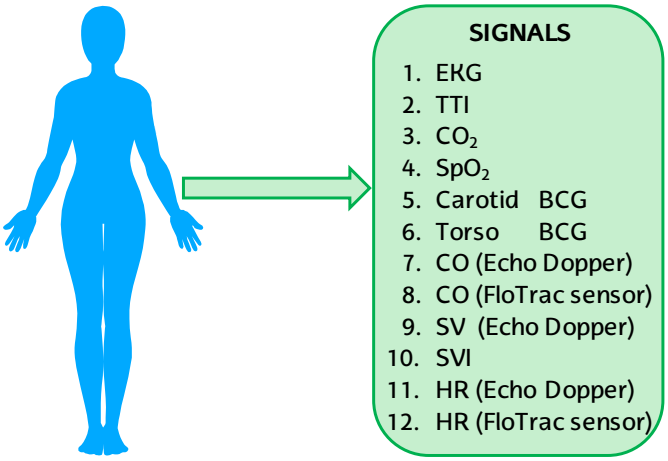

Figure 8.3: The recorded and used signals for each subject.

The measurements of each type of technology (20) for each subject (4) were also stored following a common identification format:

$$\mathrm{RANDOM\_XX.mat}$$

Where XX is the number from 01 to 20 corresponding to each subject. In total 80 measurement files where generated, 20 per technology type (one per subject). In addition, 3 metadata files were created to save data about the measurement equipment (BCG sensors metadata was included in the $\mathrm{RANDOM\_XX.mat}$ file).

By convention, the $\mathrm{s\_}$ prefix-named variables presented in the following subsections contained the values of each of the measured signals, while the $\mathrm{fs\_}$ prefix-named variables contained the sampling frequency of each of the signals. The following subsections describe the procedure to convert the data from each device to a common Matlab format.

8.1.1 Physio-Control LP®-15

Initially, the data operated under the proprietary Physio-Control software (see Table 8.2), with pco format. The first step was to convert the data to comma-separated values (CSV) format using Physio-Control's $\mathrm{CODE\text{-}STAT}$ software. Data was also resampled to 250 Hz.

Table 8.2: Example of the file names from 4 subjects. The files came raw from the Physio-control LP®-15 monitor defibrillator.

File name	Format
000_14b00faf 000_4beecbd 001_14b0220f 001_14bf0314	pco

As shown in the figure above, the pco file for each subject yielded to 3 CSV files. The file ending with $\mathrm{\_Continuous\_Waveform}$ includes metadata of the measurement and the values of each of the four signals (see Table 8.4).

For its part, the file ending with $\mathrm{\_CprEventLog}$ records the annotations taken with the compressions and ventilations applied to the subject in each case.

The third type of file, ending with $\mathrm{\_EventLog}$, includes the different annotations taken by the physicians to indicate the different phases of the clinical drill, such as the timestamp of equipment start-up, intravenous (IV) access or intubation. The different types of annotations

taken by the clinicians are summarized in the following table:

Table 8.3: Data structure created from the CSV files of Table 8.5 with the convertCodeStat data converter.

LP®-15 Annotation	Meaning	Approx. duration (min)
Power on	Device powered on	-
Generic	Normal respiration	1
Oxygen	Hyperventilation	0.5
IV Access	Hypoventilation	0.5
Nitroglycerin	Leg-end raised	1
Morphine	Tranport to ambulance	1
Intubation	In Ambulance	4
CPR	Tranport from ambulance	1
Epinephrine	IV fluid (500 ml)	4
Atropine	IV fluid stop	-
Lidocaine	Observation	1
Power off	Device powered off	-

Table 8.4: The information extracted from the _EvetLog files.

Structure	Field	Meaning
metadataLP15	reg_name	Name of each of the generated mat file
	patient_ID	Identification number of each subject
	dev_model	Name of the device which recorded the measures
	rec_date	Date of the device when each subject's measure started
	rec_time	Time of the device when each subject's measure started
	ann	Annotations shown in Table 8.3
	t_ann	Time stamps where the annotations were taken
	SpO2	SpO2 saturation
	t_LP15	Time stamps where SpO2 saturation was measured

Once we had the CSV data the next step was to convert them to common MATLAB format using a specific algorithm and the database shown below was generated.

Table 8.5: Example of the file names from 4 subjects. The files came raw from the Physio-control LP®-15 monitor defibrillator.

File name	Format
0_988906_Continuous_Waveform	csv
0_988906_CprEventLog	
0_988906_EventLog	
1_1029578_Continuous_Waveform	
1_1029578_CprEventLog	
1_1029578_EventLog	

For each subject, the convertCodeStat algorithm created a MATLAB (.mat) file containing the information presented in Table 8.6

Table 8.6: Data structure created from the CSV files of Table 8.5 with the convertCodeStat algorithm.

Structure	Field	Variable
dataLP15	channels	EKG TTI CO2 SpO2
	signals	s_ekg s_tti s_CO2 s_SpO2 fs_ekg fs_tti fs_CO2 fs_SpO2

The sampling frequency of the Physio-Control LP®-15 signals was resampled to 250 Hz in all cases. The Physio-Control LP®-15 defibrillator monitor recorded approximately 37 minutes of recording per subject. Although the EKG, SpO2 and TTI signals were synchronized, it is important to note that the CO_2 has a delay caused by gas transport in the CO_2 probe, so it was necessary to correct the offset later (both in the preliminary time-alignment and in the GUI afterwards).

8.1.2 BCG sensors

Measurements from the BCG sensors were collected using the Digillent WaveForms Discovery 2 oscilloscope. The BCG sensors (one on the torso and one on the carotid artery see Figure 5.9) produced a series of CSV files as presented in Table 8.7.

Table 8.7: Example of the CSV raw files of the BCG sensors from 2 subjects.

File name	Format
T1V_1 T1V_2 T1V_3 T1V_4 T1V_5 T1V_6 T1V_7 T2E_1 T2E_2 T2E_3 T2E_4	csv

The oscilloscope generated a variable number ([4,7]) of CSV files per subject, and their identifying nomenclature was not uniform for all

subjects as presented in Table 8.7. The files contained two types of information as shown in Table 8.8.

Table 8.8: Data types of the CSV files created by the BCG signals acquisition.

Data type	Stored
metadata	date of start of measurements sampling frequency number of collected samples serial number of the oscilloscope
data	Each BCG sensor sample values.

In this case a specific data conversion software was developed in order to:

- Unify the different files.
- Store the data and metadata information associated to each subject.

For each patient BCG measurements were taken in carotid and torso for approximately 19 minutes.

Each CSV file for each subject represents a measurement set within the same measurement session. Taking into account the start times of each measurement ($\mathrm{starttime}$ from Table 8.9) reflected in each CSV, the number of samples collected in each CSV, and the sampling frequency, the termination time of each measurement set was estimated. The measurement sets for each subject were not consecutive. For example, the first measurement set of subject 1 starts on 2020-09-28 at 09:13:31, so since each session records a total of 290,000 samples, the last set should end at approximately 09:32:31. However, it ends at 09:50:46.

Thus, it was necessary to take into account the differences between the ending time of a set of a subject's measurement and the beginning of the next set of the same subject. For this purpose, the samples of the measurement sets were interpolated with zeros to show the actual value of the session duration of each subject, so that each BCG file $\mathrm{RANDOM\_XX.mat}$ contains approximately 65 minutes of measurement.

The specific data converter created for this kind of data generated 20 $.\mathrm{mat}$ files following the structure described in Table 8.9:

Table 8.9: Data structure created from the CSV files of Table 8.7 with the written specific algorithm. The dd/mm/yyyy expression refers to day/month/year and hh:mm:ss.ms to hours:minutes:seconds.miliseconds.

Structure	Variables	Stored
dataBCG	sensor	Carotid BCG samples Torso BCG samples
	starttime	Date time in dd/mm/yyyy hh:mm:ss.ms
	fs	Sample frequency, 250 Hz

8.1.3 FloTrac® sensor

The HemoSphere® advanced hemodynamics monitor generated 20 xls files (one per subject) from the measurements taken by the FloTrac® sensor (see Table 8.10).

Table 8.10: Example of a 11 different subjects xls raw files of the FloTrac® sensor, collected by the HemoSphere® advanced hemodynamics monitor.

File name	Format
SHM_13801142_280920_095253 SHM_13801142_280920_104544 SHM_13801142_280920_115024 SHM_13801142_280920_134149	xls

The files were in excel's 2007 xls file format, so a Python script was developed to convert the data into the most recent xlsx version, which ensured the compatibility with all the computers used within this project.

The Hemosphere® files contain a lot of information. As in the previous cases it can be divided between metadata and data. The information contained in each case is shown in Table 8.11.

Table 8.11: Data types of the xlsx files from the HemoSphere® advanced hemodynamics monitor with the FloTrac® sensor.

Data type	Variable
metadata	Subject ID Age of the subject Height of the subject Weight of the subject BSA of the subject Measure start date and hour Serial number of the HemoSphere®
data	CO (l/min) SVI (ml/b/^{2}) SV (ml/b) HR (bpm) arterial systolic blood pressure (SYSART) (mmHg) arterial diastolic blood pressure (DIAART) (mmHg) mean arterial pressure (MAP) (mmHg) stroke volume variation (SVV) (%) CI (l/min/m^2) pulse preassure variation (PPV) (%) tissue muscle oxigenation (StO2) (%) tissue perfusion index (TPI) (%)

A custom data converter had to be created to extract the information from the xlsx files. The RANDOM_XX.mat file structure generated for each subject contains the following information:

Table 8.12: Data structure created from the xlsx files obtained from the xls files of Table 8.10, with the written specific data converter.

Structure	Variables	Stored
dataHS	measures	CO SVI SV HR SYSART DIAART MAP SVV CI PPV StO2 TPI
	starttime	Date time in dd/mm/yyyy hh:mm:ss.ms
	fs	Sample frequency, 0.05 Hz

Although the 12 signals captured by the FloTrac® sensor have been extracted, we have used 4: CO, SV, SVI, HR. Having all the extracted signals will make it easier to add them to the study in the future.

The custom algorithm also generates a metadata file containing the names and units of the 12 measurement channels extracted in the RANDOM_XX.mat file (see Table 8.12).

The Hemosphere® monitor samples with the FloTrac® sensor once every 20 seconds, so the sampling frequency in this case is 0.05 Hz. Approximately 190 samples were taken per subject, so the measurements lasted roughly 1 hour.

8.1.4 Doppler echocardiography

Unlike the other 3 technologies, the doppler echocardiograph generated only one file with the measurements of the 20 subjects. As in other technologies, the measurement file contains data and metadata:

Table 8.13: Data types of the xlsx file from the Doppler Echocardiograph.

Data type	Variable
metadata	Subject ID Age of the subject Height of the subject Weight of the subject
data	CO (l/min) SV (ml) VTI (cm) HR (bpm) LVOT (cm) V_{max} (m/s)

Another substantial difference in the measurements of this technology is that there is no uniform sampling frequency. Therefore the measurements are not equispaced in time and it is necessary to save the timestamp at which each sample/measurement was taken.

In order to extract the most relevant information from Table 8.13, we have again had to create a specific data converter. The algorithm generated the 20 RANDOM_XX.mat files and an additional metadata file. The RANDOM_XX.mat files follow the format described in the Table 8.14, while the metadata file contains the names and units of the 5 measurement channels extracted in the RANDOM_XX.mat file (see Table 8.14). There are about 32 doppler echocardiography measurements per patient, performed within 1 hour.

Table 8.14: Data structure created from the original doppler echocardiography results xlsx file with the written data converter.

Structure	Variables	Stored
dataEC	measures	CO SV HR VTI Vmax
	time	Measure time in hh:mm:ss

8.1.5 Time alignment

Once the work of the previous subsections was done, the full database was created. There was a total of 83 MATLAB common format files: 80 with the measurements of each technology for every subject, plus the 3 metadata files with information about the subjects and the technology.

However, the signals were still not synchronized. Each device started measuring at different times and, in addition, each device had its own clock. Thus, the next step was to perform a time alignment of the data. To do this, the starting point was a document where the physicians had written down, for each subject, the time, in hh:mm:ss format, at which they believed they had started measuring with every device. For example, for the first two subjects the time alignment was this:

Table 8.15: Time alignment of 2 out of the 20 subjets of the study.

Subject	LP®-15	BCG sensors	FloTrac® sensor	Doppler echocardiograph
1	09:12:00	09:13:31	09:04:14	09:11:00
2	10:17:00	10:22:32	10:15:26	10:16:00

The Physio-Control LP®-15 defibrillator monitor is used as a reference, because it is the only equipment that measures throughout the entire clinical drill, and has an option to add timestamps for specific events during patient monitoring. Its starting time was the start reference time. The rest of the times indicated in the table above will mark the zero of the signals from the remaining 3 pieces of equipment.

Specific code was created to translate the time difference between the start times of the different devices to a sample offset of the signals. It was essential to have the start times of each device, which we already had available thanks to the RANDOM_XX.mat files of each technology (starttime variable).

The calculated offset for the devices in each case (subject) was saved under a new file named offset.mat. In this way, by loading the signals from the $\mathrm{RANDOM\_XX.mat}$ files together with the $\mathrm{offset.mat}$offsets, a preliminary time alignment was achieved. We speak of preliminary time alignment since, as we will see below, a posterior fine tuning was possible thanks to the GUIs.

8.2 Phase 2: preliminary database visualization and annotation tool

At this point we already had a database created, with a standardized structure and in a common MATLAB format. In addition, the signals had a preliminary time alignment. Therefore, the next step of the project and objective of this phase was the development of a software tool to visualise the recordings and annotations in the database. Moreover, the GUI should allow to change the offset/delay of the signals to perform a fine tuning of the time alignmet so that the signals are truly aligned.

Given the number of signals and their different sampling rates we decided to create two GUIs to visualize the complete database. On the one hand, one with the signals from the Physio-Control LP®-15 and BCG sensors, which in turn are intended to extract the hemodynamic parameters. On the other hand, those from the equipment of the well-established technologies: FloTrac® sensor and the doppler ecochardiograph. The summary of this phase is shown in Figure 8.4.

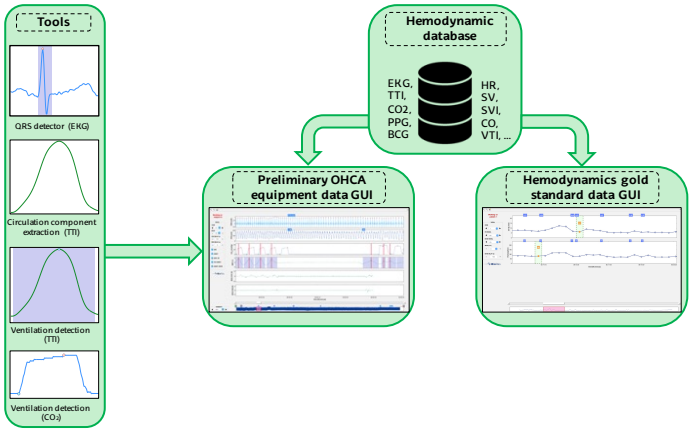

Figure 8.4: Block diagram of the Phase 2 of the project.

These have been designed using MATLAB's Guide (GUI design environment). The tools had to be user-friendly to be used by non-

technical operators such as physicians, while providing a fast and clear interface to display the measurements and their annotations.

8.2.1 GUI for Physio-Control LP®-15 and BCG sensors data

A general overview of the GUIs is shown in Figure 8.5.

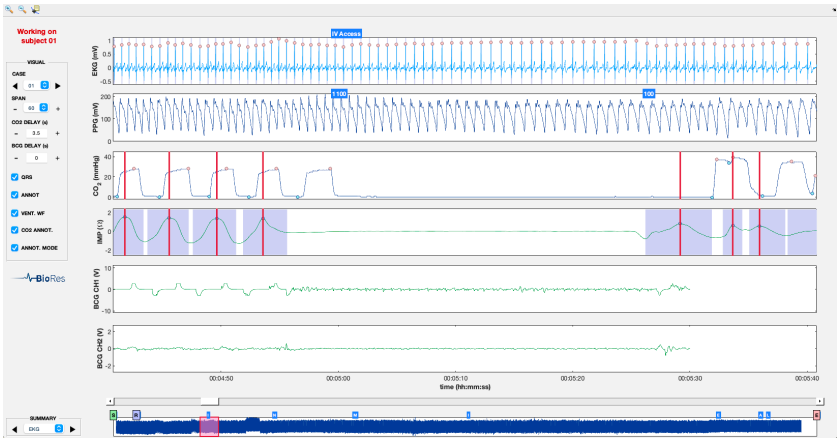

Figure 8.5: GUI for Physio-Control LP®-15 and BCG sensors data.

The interface is divided into three parts: the display, the *Visual* tools and the summary.The display area is constituted by the panels of the 6 signals. This area is shown in Figure 8.6.

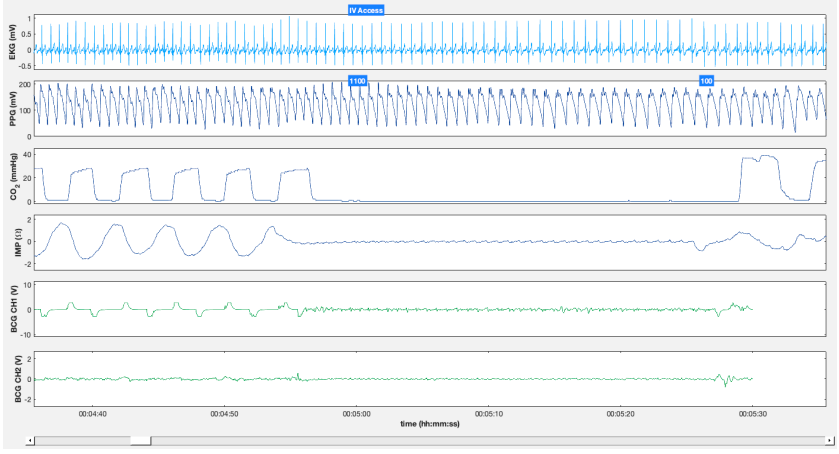

Figure 8.6: Display area of the GUI for Physio-Control LP®-15 and BCG sensors data. Just the annotations checkbox is clicked, the rest of the options are unactive.

On the display, the signals of the Physio-Control LP®-15 are painted in blue and those of the BCG sensors in green. The BCG1 signal corresponds to the measurements taken on the torso, while the BCG2 signal corresponds to the carotid artery.

The display shows the EKG signal with a different blue since it is the signal selected at this time. This is better explained in the third area. The display also integrates the annotations made by the physicians and saved as metadata in Table 8.4.

If we right click over the EKG signal panel, a context menu appears (see Figure 8.7), which permits 3 actions: add, delete or move a heartbeat.

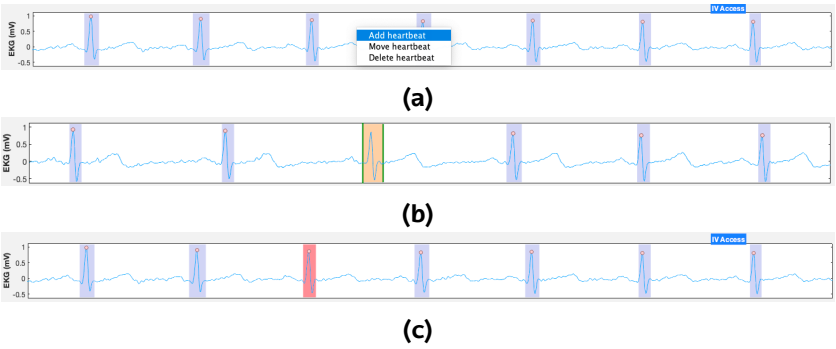

Figure 8.7: Segment of the EKG signal with **a)** the context menu,**b)** the patch resulting of adding a heartbeat, **c)** the action of deleting a heartbeat.

Same occurs if clicking over the CO_2 signal (see Figure 8.8), but this time the context menu gives the choice of adding, deleting or moving a ventilation.

Figure 8.8: Context menu of the CO_2 signal panel.

There is a third context menu, this in the panels of the BCG signals. We have added this feature to be able to superimpose the BCG signals with the EKG signal.

Once the *view EKG* option is activated, the EKG appears and looks like shown in Figure 8.9.

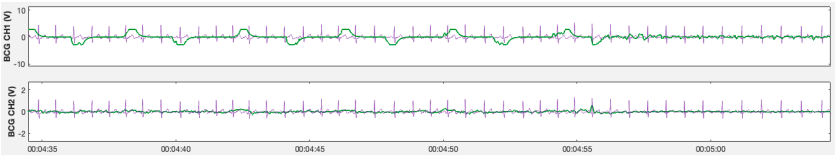

Figure 8.9: EKG superimposed to the BCG signals.

At the bottom of the display there is a slider that allows to navigate through the current case. All the signals are linked, so when we move forward or backward through one signal with the slider, we move forward or backward through all of them at the same time.

The *Visual* area shown in Figure 8.10a.

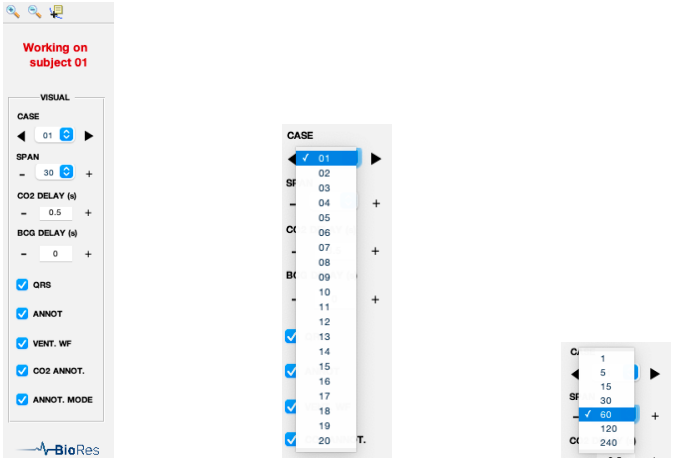

(a) **(b)** **(c)**

Figure 8.10: a) *Visual* area of the GUI for Physio-Control LP®-15 and BCG sensors data. **b)** CASE and **c)** SPAN pop-up of the GUI for Physio-Control LP®-15 and BCG sensors data.

This area permits interacting with the GUI directly and is composed by the following options:

- At the top there is a toolbar with 3 tools. The first from the left is to freely zoom in any signal. The second one zooms out. And the third one allows to put markers on the signals.
- Below, in red, appears the subject under analysis.
- **CASE**: allows to select the case (subject) among the 20 options. Clicking the central button opens a pop-up menu see Figure 8.10b. Here, we can select the desired recording of the database. To improve the user experience, we have added two arrow buttons to shift between the previous and next subjects.
- **SPAN:** allows to select the span display of the case we are working on (see Figure 8.10c). The time-interval to choose varies between 1 and 240 s. It works as in the previous case, except that this time

the minus and plus symbols have been added to zoom in or zoom out.

- **CO2 DELAY/BCG DELAY (s):** used for fine tuning the time alignment of the CO_2 and BCG signals. The indicated delay is expressed in seconds. The minus and plus symbols subtract or add 1 s to the existing delay.
- **QRS**: this checkbox activates the patches shading the QRS complex of each detected beat.
- **ANNOT:** this checkbox changes the visibility of the annotations that were made by the physicians (remind that these were saved into the Physio-Control LP®-15 $\mathrm{metadata.mat}$ file, see Table 8.4).
- **VENT WF:** the checkbox activates the results of the ICC extraction algorithms (in this case, filtering of the ICC component of the TTI signal) and detection of ventilations in TTI signal (markers on the peak of each detected ventilation and patches on the duration of the ventilation).
- **CO2 ANNOT:** activating this checkbox implies displaying two dots per detected breath. The first, in blue, indicates the start of ventilation. The red one, the EtCO2.
- **ANNOT. MODE:** activates red vertical lines in the impedance and CO_2 signal panels. The vertical lines have as value on the abscissa the time stamp where the ventilation was detected by the ventilation detector in the TTI signal.

Finally, the summary area is the one shown in the Figure 8.11a:

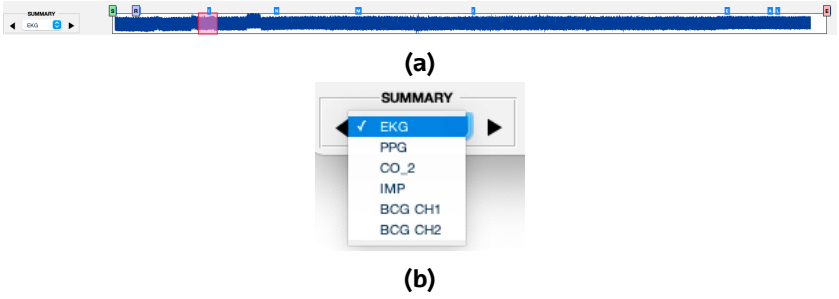

Figure 8.11: a) *Summary* area of the GUI for Physio-Control LP®-15 and BCG sensors data. The selected signal is the EKG. **b)** SPAN pop-up of the summary area.

In the bottom pannel there is a summary of the whole episode for the selected signal, which serves both as reference and navigation

tool through the episode. In addition, a red patch appears above this panel highlighting the signal segment that we are visualizing in the display area panels. The width of the patch corresponds to the span value. The annotations corresponding to the selected case also appear on the summary panel.

This summary panel is useful in the case of the BCG signal for example (see Figure 8.12). As discussed in subsection 8.1.2, the BCG measurements are not continuous throughout the entire clinical drill, but occur at certain times. The bottom pannel shows an overview where the BCG use intervals are shown.

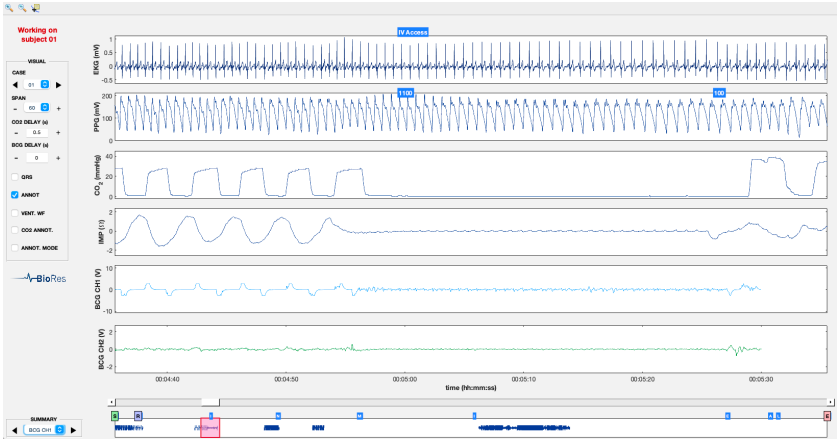

Figure 8.12: *Summary* area of the GUI for Physio-Control LP®-15 and BCG sensors data.

As shown in Figure 8.12, changing the selected signal also changes the signal highlighted in blue.

To finish with this area, it is worth mentioning that a *drag & drop* function has been added: the slider is no longer necessary. Now moving to the signal point of interest is as simple as clicking on it in the signal summary.

Also, one can drag the red patch over the summary signal to navigate through the signals of the display area.

As mentioned in the *Visual* area, several algorithms have been used to help analyzing the signals: a QRS detector (heartbeat detector plus EKG delineator), a ICC extractor from the TTI signal, and two ventilation detectors, one based on the TTI signal and the other on the CO_2 signal.

8.2.1.1 QRS detector

The HT algorithm was applied to the EKG measurements of the database to detect the R-peaks of the EKG. The HT algorithm package was provided by BioRes.

The HT algorithm returns the time stamps where the R-peaks should occur, although the heartbeat detections are not normally placed at the R-peak (see Figure 8.13) Therefore, the values had to be corrected and the detections of the algorithm had to be placed at the R-peaks by doing a local maximum search around the returned heartbeat detection.

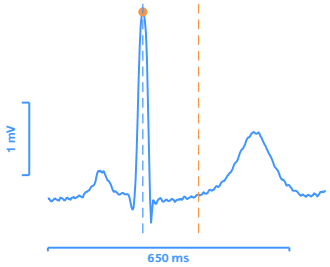

Figure 8.13: Example of heartbeat detection. The blue dashed vertical line represents the time instant of the R-peak and the orange one the detection of the HT algorithm. The orange dot indicates the R-peak of the QRS complex.

We also applied the Wavedec algorithm (BSICoS Research Group, University of Zaragoza [Gro15]). This algorithm takes as input a the EKG, its sampling frequency and the R-peak locations detected by the HT algorithm.

For each heartbeat, the software returns the time stamps where the Q, R and S signals occur, the QRS complex shown in Figure 8.14.

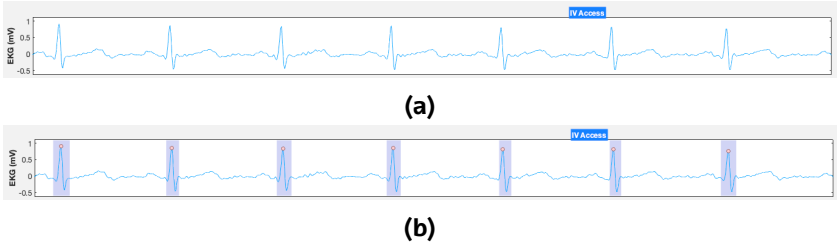

Figure 8.14: Segment of the EKG signal with the QRS checkbox deactivated **a)** and activated **b)**.

8.2.1.2 ICC extraction and ventilation detector from the TTI signal

If the VENT. WF checkbox is deactivated, the raw TTI signal appears in the TTI signal panel (see Figure 8.15a). When the checkbox is activated, the result of passing the TTI signal through two algorithms is displayed:

- The one of Alonso et al. [Alo16] for the extraction of the ICC from the TTI signal. In this case, we have filtered the ICC of the TTI signal.
- The automatic detector of ventilations in the TTI signal of Jauregui-beitia et al. [Jau20] for the automatic detection of ventilations The results can be seen in Figure 8.15b.

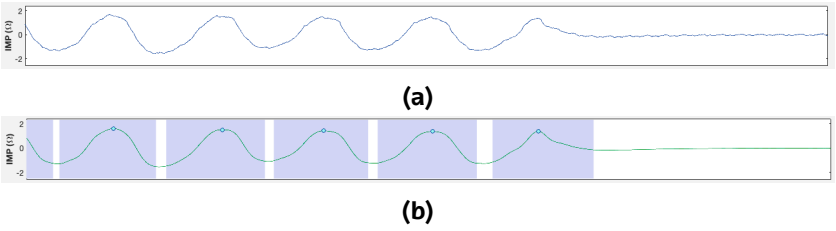

Figure 8.15: Segment of the TTI signal with the VENT. WF checkbox deactivated **a)** and activated **b)**.

8.2.1.3 Ventilation detector on the CO_2 signal

The algorithm of Aramendi et al. [Ara17] has been used for automatic detection of ventilations in the CO_2 signal. The ventilations as well as the EtCO2 value are visible in each case when the CO2 ANNOT checkbox is activated (see Figure 8.16b). The peak values of the TTI ventilations detection together with the onset of the ventilation (blue dot) will be used as a reference to fine tune the CO_2 signal with the EKG, SpO2 and TTI signals.

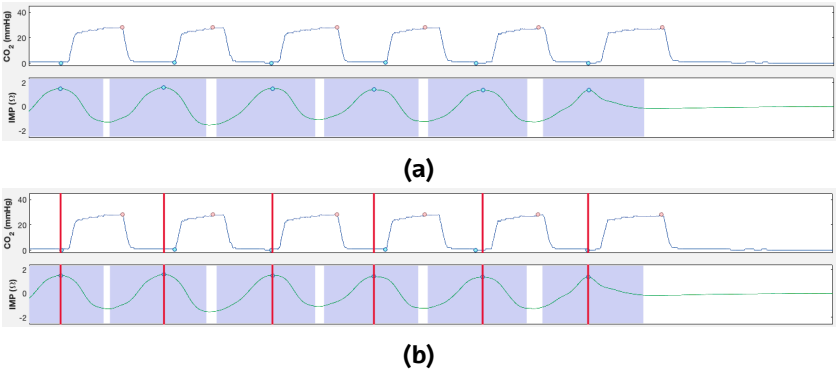

Figure 8.16: Segment of the TTI signal with the VENT. WF checkbox deactivated **a)** and activated **b)**.

8.2.2 GUI for FloTrac® and doppler echocardiography data

Following the scheme defined in Figure 8.5, the GUI presented below has been built:

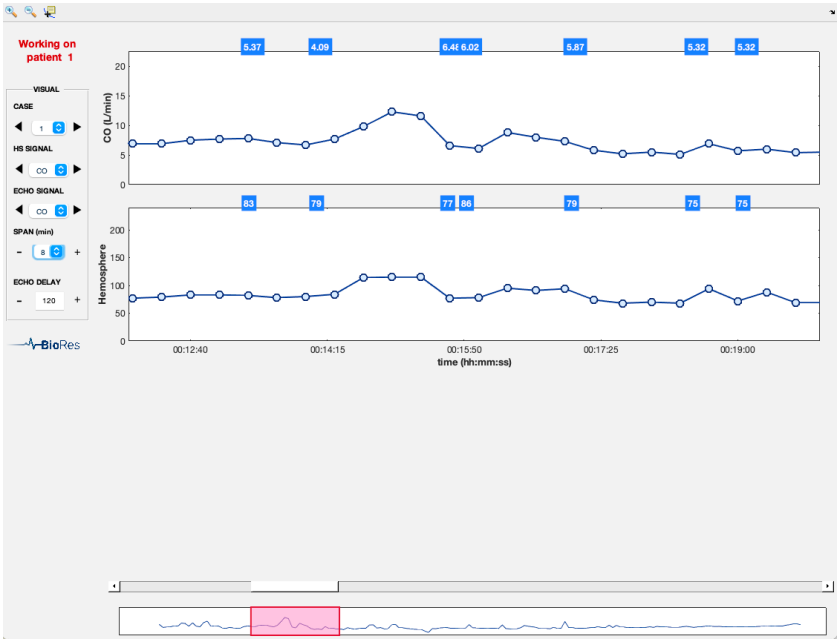

Figure 8.17: GUI for FloTrac® and doppler echocardiography data.

It is apparently very similar to the one defined in subsection 8.2.1. However, it presents some important differences due to the nature of the measurements of these two technologies.

First of all, in the display area there are only two panels, one for each type of technology. The upper panel shows the measurements acquired by the doppler echocardiograph; the lower panel shows the measurements recorded by the HemoSphere® advanced hemodynamics monitor connected to the FloTrac sensor.

Round markers have been used to represent the measurements since the number of samples in both cases was quite small. Now, on the plotted signals instead of annotations (they were from the Physio-Control LP®-15), the HemoSphere® CO value is shown in the upper panel.

In the lower panel, the HR measurements from doppler echocardiography appear above the panel.

Having the measurements of the different technologies *crossed* will make it easier to perform fine tuning of the time alignment of the measurements. However, it is not very easy to compare numerical values with markers.

To ease the comparison task, each time the cursor is hovered over a marker, the marker environment is highlighted and the numerical value of the marker is displayed (see figureMarker). In this way, you only have to compare the two numerical values.

The highlight and the marker value disappear when the cursor is no longer hovered over. To fix it, click on it. To release it, click on it again.

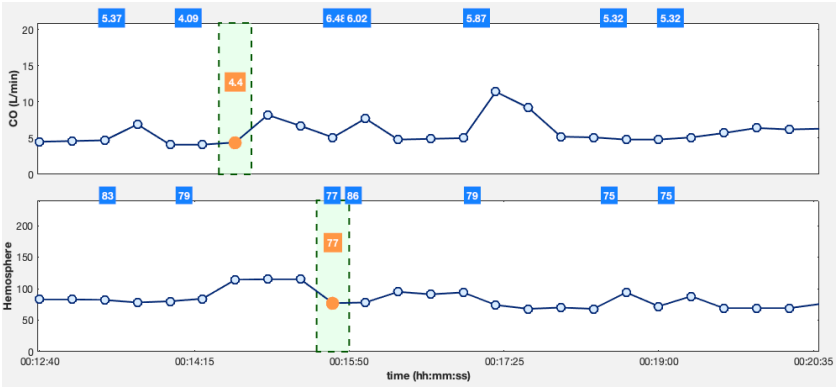

Figure 8.18: Patches funcionality within the GUI for FloTrac® and doppler echocardiography data.

As for the *Visual* area, there are also some changes as can be seen in the Figure 8.19a.

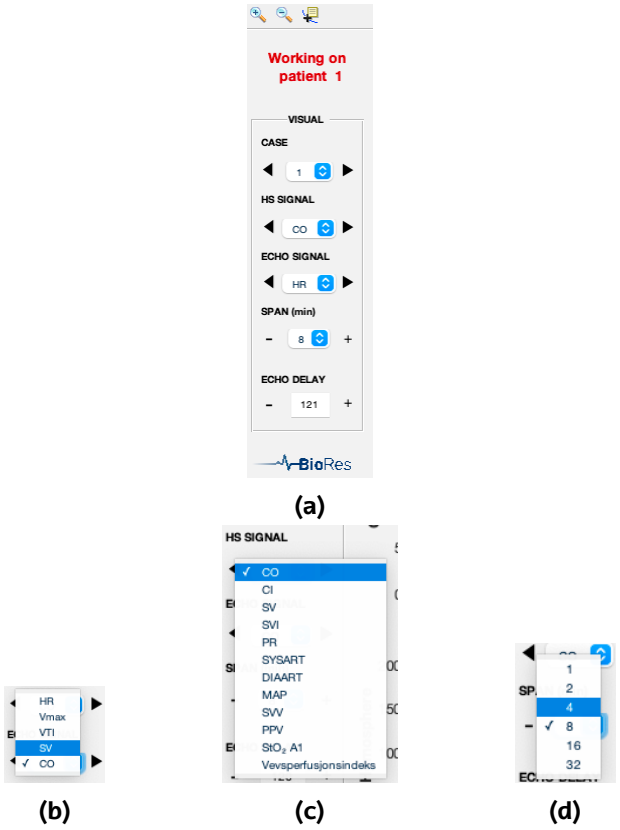

Figure 8.19: a) *Visual* area of the 2nd GUI. Pop-up menus with the values of the **b)** doppler echocardiograph **b)** HemoSphere connected to the FloTrac sensor. **c)** Possible new values of the span.

Now, there are two new popupcases, one for each technology (ver Figure 8.19b y Figure 8.19c), so that you can choose which technology signal to plot at any time. The span has also been changed (see Figure 8.19d), now it is expressed in minutes due to the low and non-uniform sampling frequency.

At the bottom of the *Visual* area (see Figure 8.19a) we find a text box where we can fine tune the time alignment with the help of what has already been explained in the display area.

Finally, looking at the summary area, the main difference with respect the previous case (see Figure 8.5) is that now the pop-up that was there at the bottom to change signal is now in the *Visual* area (see Figure 8.19a).

8.3 Phase 3: hypoventilation windows visualization and annotation tool

After both Figure 8.5 and Figure 8.17 were accepted, a meeting was held with the physicians at NAKOS and it was decided to start analyzing the hypoventilation windows of the subjects. With that meeting the third phase of the project started, which is resumed in Figure 8.20.

To identify the onset of the hypoventilation windows, the time stamp of the IV Access annotation was located (see Table 8.3). Hypoventilation windows have an approximate duration of 30 s.

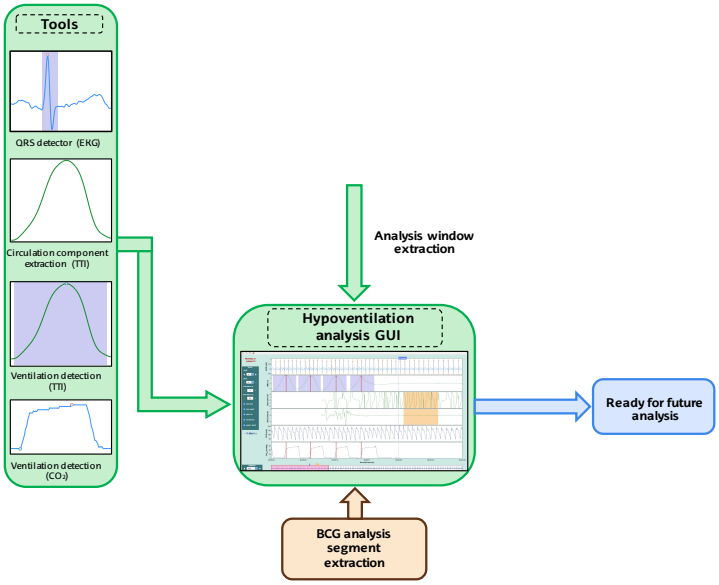

Figure 8.20: Block diagram of the Phase 3 of the project.

To check what was going on before and after the hypoventilation window, the signal values were taken from 20 s prior to the IV Access time stamp, and 80 s after the beginning of the hypoventilation window. In total 100 s were extracted for each subject and the following file was generated and added to the already created database.

Table 8.16: Structure created to store the hypoventilation windows of every subject.

Structure	Variable
hyp_db	s_ekg
	s_tti
	s_vent
	s_SpO2
	s_bcg1
	s_bcg2

Where s_vent is the signal obtained from filtering the ICC from the TTI signal with the algorithm of Jaureguibeitia et al. [Jau20].

To display these windows correctly, a new GUI was created, which is shown below:

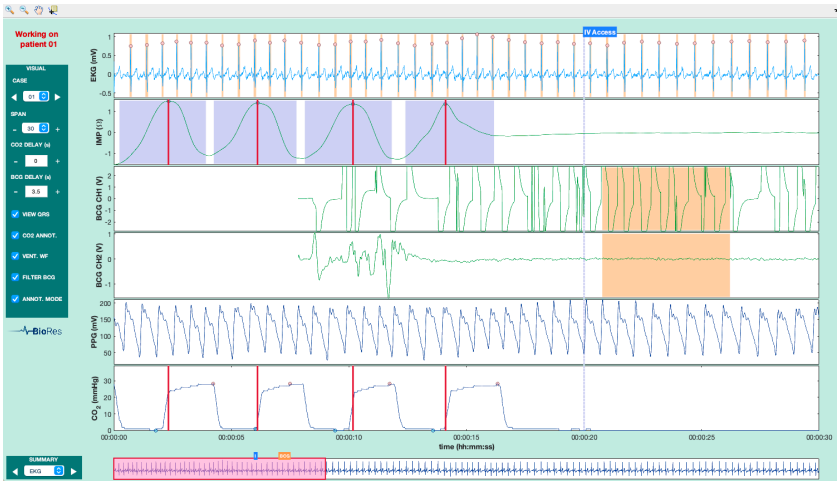

Figure 8.21: GUI for the hypoventilation windows of the Physio-Control LP®-15 and BCG sensors data.

The first thing that stands out is the color, it is no longer gray but medical green. The summary area has not changed at all between the Figure 8.5 and the new one. However, the display area has now changed a little, maintaining the functionalities it had and incorporating two new ones. On the one hand, BCG signal analysis segments can now be created and saved as soon as they are created (see Figure 8.22).

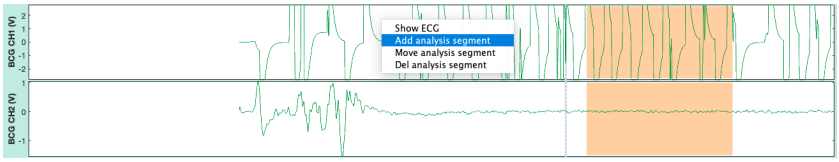

Figure 8.22: New options of the BCG context menu in the GUI for the hypoventilation windows of the Physio-Control LP®-15 and BCG sensors data.

As in Figure 8.5, the generated patches can also be deleted and moved, but now, when we make a two clock appear in the patch, see Figure 8.23. The first indicating the time stamp hh:mm:ss at which the current analysis segment has started. The second displays the instantaneous time stamp of the cursor as it moves through the BCG.

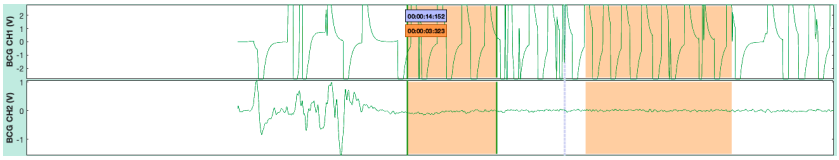

Figure 8.23: The new funcionalities added to the patches of the GUI for the hypoventilation windows of the Physio-Control LP®-15 and BCG sensors data.

Furthermore, now when the *Show EKG* option is selected in the context menu of the BCG signals, the EKG amplitude remains unchanged no matter how much we change the BCG signal amplitude (see Figure 8.24).

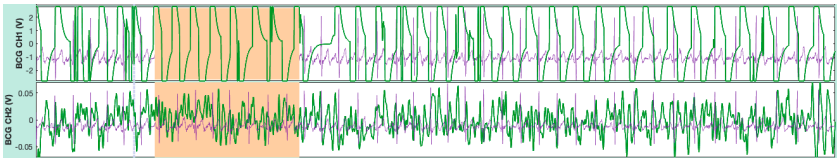

Figure 8.24: Example of the updated *Show EKG* option of the GUI for the hypoventilation windows of the Physio-Control LP®-15 and BCG sensors data.

As for the *Visual* area, an icon has been added to the toolbar at the top to drag and move the signals without any limitation.

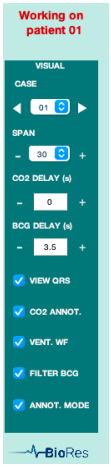

Figure 8.25: *Visual* area of the GUI for the hypoventilation windows of the Physio-Control LP®-15 and BCG sensors data.

The last change made has been the insertion of a BCG signal filtering option. This has been implemented to try to extract the signal component associated to circulation from the BCG sensor data.

8.4 Summary of results

To conclude this chapter, in this section we analyze the most relevant results achived by the project.

8.5 Results of Phase 1

After applying the various data converters to the proprietary software we have seen how we have managed to generate a database with a defined structure, whose files comply with the open Matlab format. The logical scheme presented in Figure 8.26 shows the database structure achieved in this first phase.

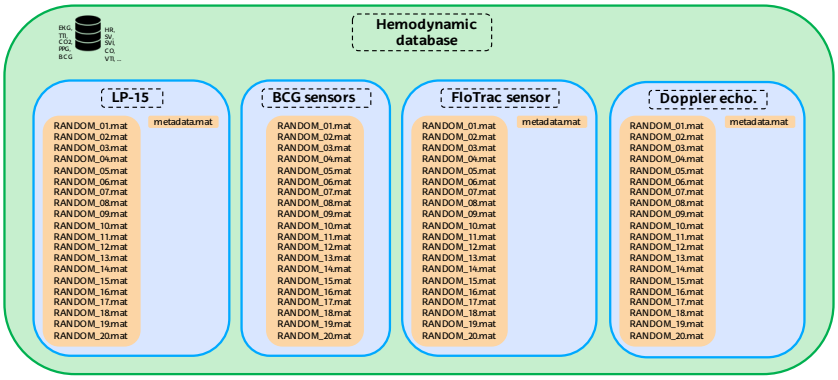

Figure 8.26: Logical scheme of the database of the project at the end of Phase 1.

As can be seen in the figure above, a hemodynamics database has been constructed from 4 different types of data sources. However, if new types of data sources are incorporated in the future, such as cerebral oximetry, adding the files from that technology to the database would be relatively simple: the conversion codes already built can be reused, applying specific modifications for every new data source. The figure below shows the generalized database, where *N* is the number of data sources used.

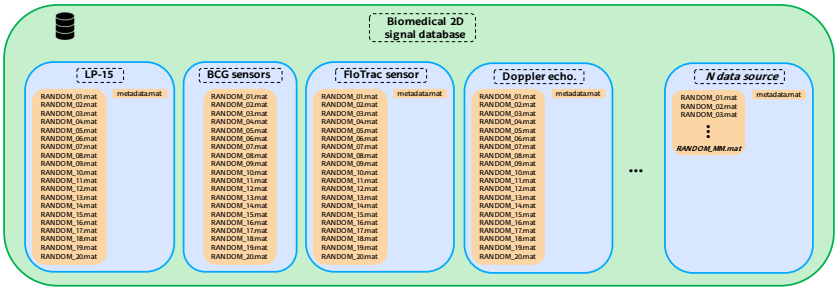

Figure 8.27: Logical scheme of the generalized database.

As the Figure 8.27 shows, the database is also flexible with respect to the number of subjects it stores. Although we have used a cohort of 20 healthy subjects for this study, it should be remembered that this study is part of a more ambitious project that is still ongoing. In fact, in May 2021 the collection of data from OHCA patients started. Integrating these new patients into the existing database will be as simple as re-running the codes on the new data as they arrive.

In addition, the database does not even have to be hemodynamic-specific, really any kind of 1D biomedical signal database could be created (2D and 3D images require more advanced processing).

We have also seen that by standardizing the structure of the file contents for all data sources, we have simplified the code needed to load the data into MATLAB. This has saved code writing time and is more computationally efficient than having a load code for each data source.

To finish with the results of Phase 1, we have also seen that the code responsible for the time alignment, although simple, is very useful for presenting the data at the beginning of phase 2 (see section 8.2).

However, it has a limitation: it depends on the physicians having correctly annotated the timestamps where each piece of equipment has been started. In the future a code could be developed that automatically aligns the data based on thresholds and/or autocorrelations between signals.

8.6 Results of phase 2

In this phase we have developed two GUIs to visualize and annotate the data from the Physio-Control LP®-15 and BCG sensors and from the well stablished technologies respectively.

The first GUI takes 3.363 s to open for the first time (Figure 8.28a), while it took only 1.112 s to change study case/subject (see Figure 8.28b). Of that 1.112 s 0.1 s is due to a forced pause to momentarily change the color of the signals to alert the operating technician that the case has changed. Regarding the navigation speed of the integrated drag & drop functionality, this is 0.249 s (see Figure 8.28c).

Profile Summary (Total time: 3.363 s)

Flame Graph

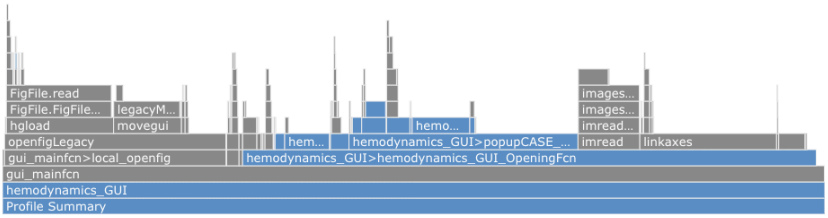

Generated 09-jun.-2021 8:42:48 using performance time.

Function Name	Calls	Total Time (s)	Self Time* (s)	Total Time Plot (dark band = self time)
gui_mainfcn	7	3.357	0.039	
hemodynamics_GUI	7	3.343	0.003	
hemodynamics_GUI>hemodynamics_GUI_OpeningFcn	1	2.346	0.038	
hemodynamics_GUI>popupCASE_Callback	1	0.937	0.417	

(a)

Profile Summary (Total time: 1.112 s)

Flame Graph

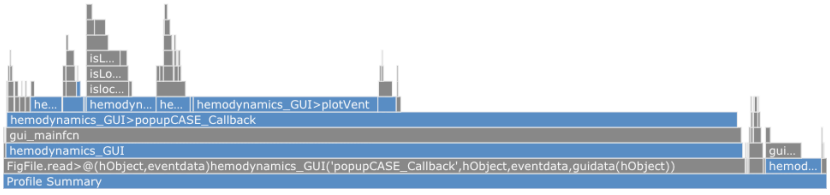

Generated 09-jun.-2021 8:50:58 using performance time.

Function Name	Calls	Total Time (s)	Self Time* (s)	Total Time Plot (dark band = self time)
...s_GUI('popupCASE_Callback',hObject,eventdata,guidata(hObject))	1	1.002	0.003	
hemodynamics_GUI	1	0.995	0.002	
gui_mainfcn	1	0.993	0.005	
hemodynamics_GUI>popupCASE_Callback	1	0.987	0.453	
hemodynamics_GUI>plotVent	1	0.249	0.249	
hemodynamics_GUI>plotEachSignal	6	0.094	0.033	
hemodynamics_GUI>mouseMove	119	0.077	0.028	

(b)

Profile Summary (Total time: 0.249 s)

Flame Graph

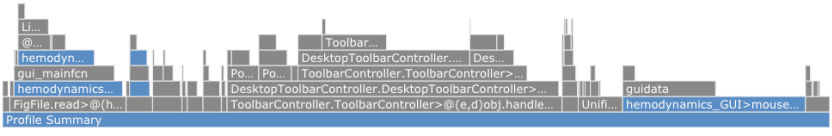

Generated 09-jun.-2021 8:53:50 using performance time.

Function Name	Calls	Total Time (s)	Self Time* (s)	Total Time Plot (dark band = self time)
...opToolbarController>DesktopToolbarController.handleMouseMotion	53	0.104	0.010	
...barController.ToolbarController>@(e,d)obj.handleMouseMotion(e,d)	51	0.101	0.001	
...rController.ToolbarController>ToolbarController.handleMouseMotion	53	0.072	0.004	
hemodynamics_GUI>mouseMove	51	0.055	0.027	
...sktopToolbarController>DesktopToolbarController.canShowToolbar	53	0.054	0.026	
hemodynamics_GUI	4	0.039	0.003	

(c)

Figure 8.28: a) Opening, **b)** case changing and **c)** patch drag& drop navigation performance measure of the GUI for Physio-Control LP®-15 and BCG sensors data.

The second GUI takes 2.188 s to open (see Figure 8.29). It need less time to open than the first one because it loads less signals and less samples per signal. The response times of the user-GUI interaction are similar to those of GUI 1. In 1968 Miller [Mil68] made 4 important contributions as far as human-machine interaction is concerned. These are still valid today and are the following:

- A response time of 100 ms or less is perceived as instantaneous by the user.
- If the response times are 1 s or less, the users will feel a smooth interactivity with the information.
- If the response times are greater than 10 s, the attention of the user is completely lost. Martin concluded that a response time of 2 s is already sufficient for the user to feel comfortable in the human-machine interaction.

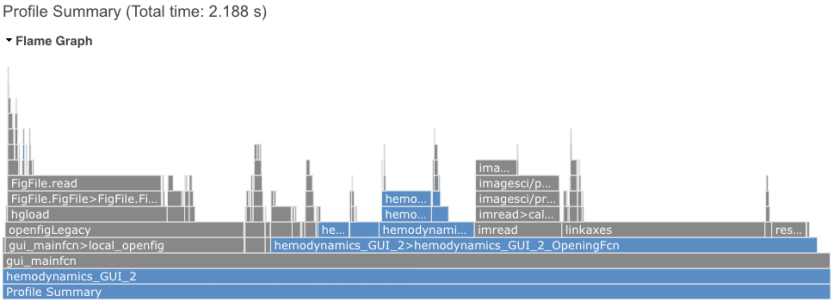

Function Name	Calls	Total Time (s)	Self Time* (s)	Total Time Plot (dark band = self time)
gui_mainfcn	7	2.183	0.038	
hemodynamics_GUI_2	7	2.171	0.003	
hemodynamics_GUI_2>hemodynamics_GUI_2_OpeningFcn	1	1.445	0.021	
gui_mainfcn>local_openfig	2	0.622	0.001	
openfigLegacy	2	0.621	0.129	
linkaxes	1	0.537	0.479	

Figure 8.29: Opening performance measure of the GUI for Physio-Control LP®-15 and BCG sensors data.

Taking into account what Miller published, we can say that the opening of the GUIs may be the bottleneck of its performance. However, since the user will not continuously opening and closing the GUI, we believe that it is not a problem.

Among the different functions integrated in the first GUI, we can say that the annotation mode was quite useful to be able to align the

CO_2 signal with the EKG, SpO2s and TTI signals (see Figure 8.30). In this project it was not too hard to align the signals of the 20 subjects, however, if instead of having 20 cases we had 1000 cases, aligning the cases would be very heavy work that would be made easier with an algorithm that automatically performs this work reliably.

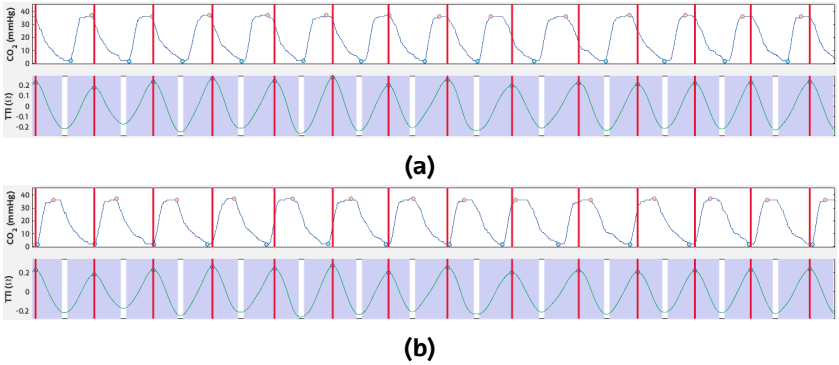

Figure 8.30: Segment of the TTI and EKG signals **a)** not time aligned and **b)** fine tuning time aligned using the **annotation mode** (vertical red lines).

Another useful tool that facilitated the alignment of the signals, in this case those of the echocardiographic doppler sensor and the FloTrac® sensor, was the scatterplot representation of the samples of one technology with the value of the samples of the other above the panel as annotations. This visualization approach, coupled with the fact that the value of the scatterplot samples is displayed when the cursor is hovered over, allows for a quick assesment of the values of both signals.

However, the fact that we have a nonuniform sampling rate in doppler echocardiography, and that the physicians were also unsure of the exact moment at which the measurements were taken, made time alignment so difficult that we are still not sure that we got it right.

To continue with the results of phase 2 (see section 8.2) we have to comment that although at most in a GUI we have displayed 9 signals in total (6 from the panels plus the 2 from the BCG context menu and the SpO2s saturation as an annotation on the SpO2s signal panel), we have realized that we can display more. By correctly using the context menus of each panel and using the annotation fields above each panel we can triple the number of signals displayed against those we would have if we only used the panels.

If used correctly, this technique allows up to 18 signals to be displayed without overwhelming the user with the amount of data (signals can be made to appear and disappear and annotations can

be made to appear and disappear at the click of a button). Having all signals in the same GUI could allow a more efficient overview and analysis.

The time alignment of the BCG signal was fine tuned using the GUI and making use of the summary area. Thanks to this lower panel it was possible to have a global view of the selected signal.

We have also seen that the algorithm used for the presentation of the signals manages to adjust them correctly to each panel, which gives a homogeneous appearance despite the fact that not all the signals are of the same magnitude.

We can comment that the *Visual* menu of GUI 1 currently consists of 9 functions, but thanks to the code flexibility of the GUI it will be easy to integrate them. Among the 9 functions were the algorithms for beat detection and delineation, ICCs extraction and ventilation detection (on TTI and CO_2 signal). However, we could not assess the performance because we did not have the ground truth annotations to compare with the results reported by the algorithms.

The manual annotation of the thousands of instants in which the R-wave peaks, the TTI waves and the onset of the ventilations occurred in the CO_2 signal is an arduous task that requires a time that is beyond the time available for this project. In spite of this and after superficialy reviewing at a glance the 20 cases, we can say that the chosen algorithms performed very well, as expected after having been selected in the analysis of alternatives (see chapter 6). In that chapter we report their performance results, which have been validated against annotated databases.

We have to say another result of Phase 2 (see section 8.2) is Phase 3 (see section 8.3). Physicians decided the analysis windows using GUI 1 of this phase.

8.7 Results of Phase 3

This phase started with the creation of a third GUI for the display of the analysis windows. We found that the development of this third GUI was considerably faster than the previous 2 GUIs thanks to having created flexible code in the previous phase. This will in turn make it easier to build new GUIs in the future.

Finally we can highlight that clinicians were able to analyze the BCG signal in more detail thanks to the zoom-in and zoom-out magnifiers that appear on the toolbar in the *Visual* area. The result of a correct use of the zoom tools is shown in Figure 8.31.

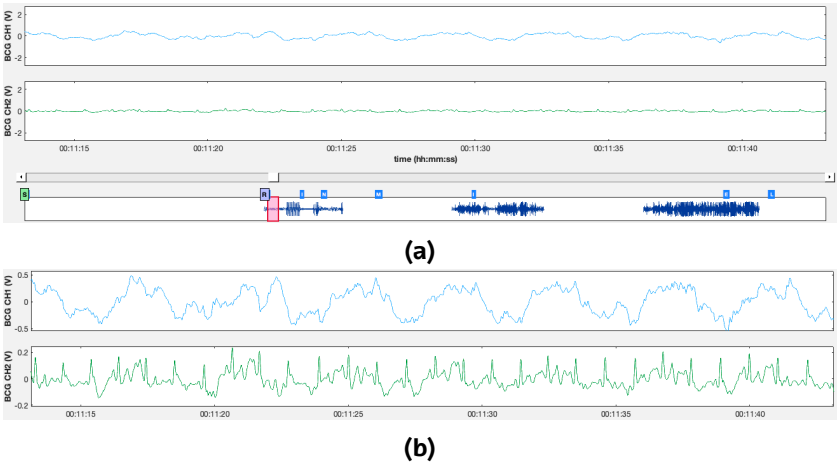

(a)

(b)

Figure 8.31: Segment of the BCG1 and BCG2 signals **a)** not proper centered for that time window, **b)** with zoom applied manually using the magnifiers from the top toolbar of the GUI.

As we can see in the summary panel of Figure 8.31a, sometimes the BCG signals are saturated, making the signal displaying algorithm to show the signals with an inappropiate ordinate axis limits. To solve that, one approach is to manually zoom-in the region of interest. In Figure 8.31 we can see the effect of using the magnifier tool, what looked like there were two noisy signals with no information, in reality were bad-scaled signals.

9. CHAPTER

Methodology

The project planning provides control techniques to manage the complexity, amount of data and deadlines of the project. This is made before starting any project, and it is essential to define the tasks and responsibilities of all those who take part in the project.

In order to carry out the project, efficiently and in controlled way, it is also fundamental to define the limits and duration of the work packages (WP) of each participant. So in this section of the master thesis, we will introduce the WG and the WPs carried out by those teams.

The WPs in which the project is divided include:

- **Tasks** to be performed and their resulting **deliverables**.
- **Milestones**, which should reflect the checkpoints or critical dates of the project.

In the following subsections, the members of the WG are listed and the different WPs are described in detail. Finally, we present the Gantt diagram of the project.

9.1 Working group

The members of the team that consitute the work group of this project are shown in Table 9.1:

Table 9.1: Working group of the project.

ID	Position	Name and surnames	Function
G1	Project manager	Unai Irusta Zarandona	Proposes the project, indicates the necessary stages to follow and takes care of the correction and supervision of the work.
G2	Junior engineer	Gorka Zubia Garea	It is in charge of the development the project and of writing the document.

9.2 Work packages

The total amount of work of the project has been divided into 5 WPs. The following tables (Table 9.2,Table 9.3,Table 9.4,Table 9.5 and Table 9.6) show the defined WPs. The table corresponding to each WP shows its description and the corresponding tasks are explained, specifying the duration and the start and end dates of each of the tasks. The duration of every WP is expressed in days.

Table 9.2: The first work package.

WP1	Starting data	Ending data	Duration
PROJECT MANAGEMENT: Monitoring and administration carried out to verify the proper development of the project.	**01/10/2020**	**02/07/2021**	**274**
T.1.1. Management, monitoring and supervision of work: Coordination and supervision work from the start to the end of the project.	01/10/2020	02/07/2021	274

Second stage of the project:

Table 9.3: The second work package.

WP2	Starting date	Ending date	Duration
BASIC TRAINING: acquiring the basic knowledge to be able to begin with the preparation of the project	**01/10/2020**	**11/11/2020**	**42**
T.2.1. Learning advanced GUI programming: learn about new ways to develop MATLAB GUIs following online courses.	01/10/2020	26/10/2020	26
T.2.2. Study the importance of hemodynamics: reading scientific papers and book sections about the hemodynamics monitoring at in-hospital and OHCA events.	07/10/2020	11/11/2020	42

Third stage of the project:

Table 9.4: The third work package.

WP3	Starting date	Ending date	Duration
PROJECT PREPARATION: acquisition of knowledge necessary before specifying the course of the project and its development	**11/11/2020**	**31/12/2020**	**51**
T.3.1. Data conversion software session: explanation about which tools does currently BioRes use to convert the data acquired by monitor-defibrillators to MATLAB common format	11/11/2020	11/11/2020	1
T.3.2. Project definition: Definition of the project guidelines and the work plan.	11/11/2020	31/12/2020	51
T.3.3. State of art: Search for relevant information and studies necessary for the development of the project.	11/11/2020	31/12/2020	51

Fourth stage of the project:

Table 9.5: The fourth work package.

WP4	Starting date	Ending date	Duration
Project development: Different sections that have been tackled for the project development	**31/12/2020**	**04/05/2021**	**125**
T.4.1. Database creation: data management and completion of the time aligned dataset	31/12/2020	04/02/2021	50
T.4.1.1 Physio-Control LP®-15 data: convert the EKG, TTI, CO2 and PPG signals of every subject to MATLAB common format. One file per subject.	*31/12/2020*	*10/01/2021*	*11*
T.4.1.2 BCG sensor data: convert the BCG data (two channels) to MATLAB common format. One file per subject.	*10/01/2021*	*15/01/2021*	*6*
T.4.1.3 FloTrac sensor data: convert the data registered by the FloTrac sensor to MATLAB common format. One file per subject.	*15/01/2021*	*19/01/20201*	*5*
T.4.1.4 Doppler ecochardiography data: convert the data registered by the echocardiograph to MATLAB common format. One file per subject.	*19/01/2021*	*25/01/2021*	*7*

T.4.1.5 Preliminary time alignment: align all data from the 4 data sources. This is tuned afterwards once the first GUIs are done.	*25/01/2021*	*04/02/2021*	*11*
T.4.2 Preliminary database visualization and annotation tool: first two GUIs to visualize the data.	04/02/2020	12/03/2021	37
T.4.2.1 GUI for Physio-Control LP®-15 and BCG sensor: design a GUI to visualize the EKG, TTI, CO2, PPG and BCG signals and their annotations.	*04/02/2020*	*12/03/2021*	*37*
T.4.2.2 GUI for FloTrac and Doppler Echocardiographys: design a GUI to visualize the hemodynamic parameters registered by the two well established technologies.	*01/03/2021*	*12/03/2021*	*12*
T.4.3 Data analysis: choice of the time windows of the clinical protocol to analyze, the hypoventilation period.	12/03/2021	16/04/2021	36
T.4.4 GUI for hypoventilations analysis: construction of a new GUI for analysing the Physio-Control LP®-15 and BCG sensor data in the hypoventilation windows.	16/04/2021	28/04/2021	13
T.4.5 Algorithms: implement in the GUIs the already existing algorithms for QRS detection, extraction of the circulation component and ventilation detection in the TTI signal, and ventilation detection in the CO_2 signal.	04/02/2021	04/05/2021	90

Fifth stage of the project:

Table 9.6: The fifth work package.

WP5	Starting date	Ending date	Duration
DOCUMENTATION AND SUBMISSION OF THE PROJECT: wording of the project and oral presentation.	**06/04/2021**	**02/07/2021**	**88**
T.5.1. Project documentation: drafting of the document that summarises the context of the project, the objectives, scope, benefits, the description of the solution, methodology and conclusions.	06/04/2021	11/06/2021	67
T.5.2. Oral presentation of the project: preparation of the presentation, rehearsal and presentation in front of the evaluation board.	11/06/2021	02/07/2021	22

The description of the working time schedule is shown in Table 9.7. Although the project was completed in 34 weeks (see Table 9.7), there was a large variation in hours per week due to other activities done by G1 and G2 during the development of the project.

Table 9.7: The working time schedule of the project.

Unit	Duration
Project	34 weeks
Week	7 days
Day	3 hours[1]

[1] This is an average, there was wide variation in hours from 0 hour to 6-hour days.

This section defines the milestones and deliverables that must be met throughout the development of the project. The milestones are shown in Table 9.8.

Table 9.8: Project milestones.

ID	Milestone	Date
M1	Beginning of the training	01/10/2020
M2	Project start-up	11/11/2020
M3	Completion of the database generation	04/02/2020
M4	Completion of the preliminar GUIs	12/03/2020
M5	Completion of the first implementation of the automatic QRS detector	12/03/2021
M6	Completion of the analysis windows identification	26/03/2021
M7	Completion of the hypoventilation analysis GUI	28/04/2021
M8	Completion of the implementation of the algorithm which extracts the circulation component extraction from the TTI signal	04/05/2021
M9	Completion of the implementation of the algorithm which detects the ventilations in the TTI signal	04/05/2021
M10	Completion of the implementation of the algorithm which detects the ventilations in the CO_2 signal	04/05/2021
M11	Completion of the project development documentation	11/06/2021
M12	End of the oral presentation	02/07/2021
M13	End of the project	02/07/2021

The defined project derivables are Table 9.9:

Table 9.9: Project deliverables.

ID	Deliverable	Date
D1	Database	04/02/2021
D2	Preliminary GUIs	12/03/2021
D3	Hypoventilation analysis GUI	28/04/2021
D4	Algorithms	04/05/2021
D5	Documentation of the report of the project	11/06/2021
D6	Presentation	02/07/2021

9.3 Gantt diagram

The following Figure 9.1 shows the tasks and milestones together with the GANTT diagram of the project planification.

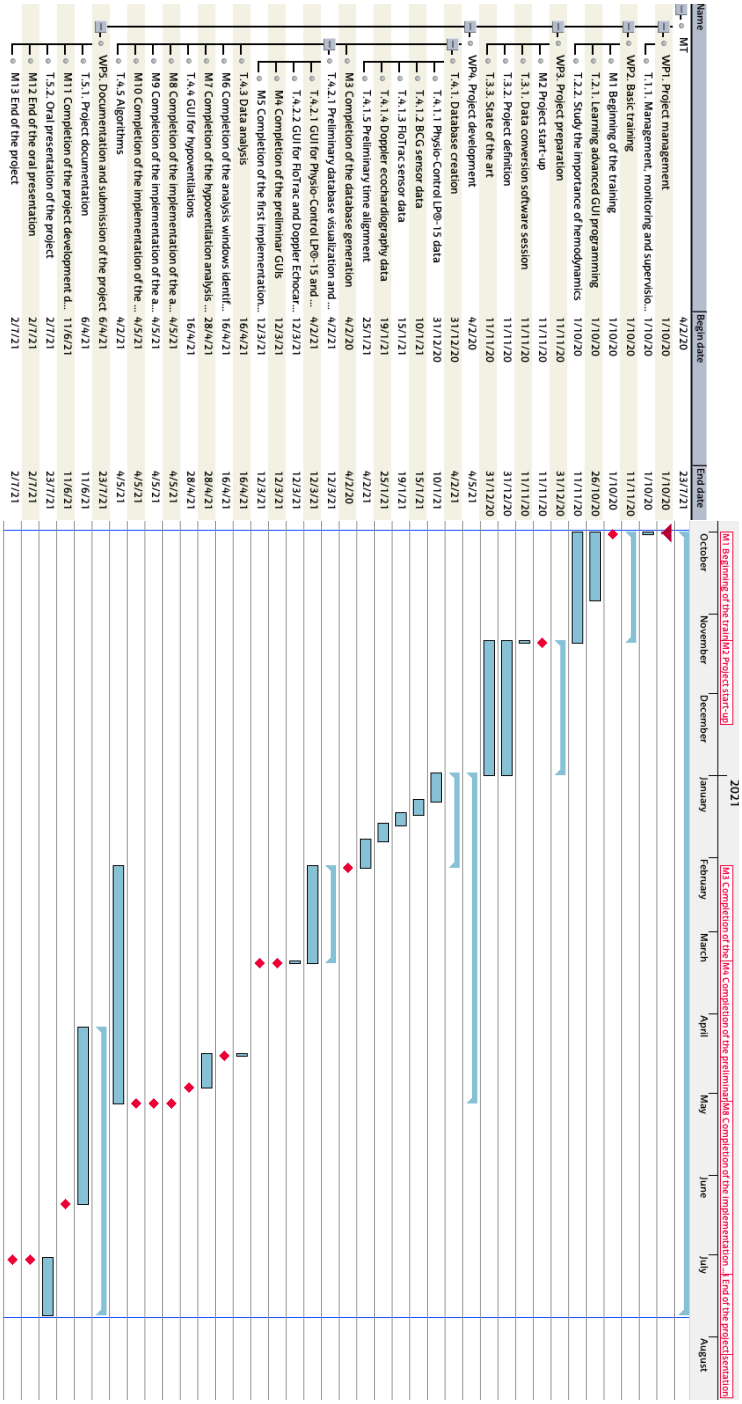

Figure 9.1: The GANTT diagram followed through the project.

10. CHAPTER

Budget of the project

This section presents the project's costs which are mainly the cost of human resources and that of the material used in the project, having in mind both depreciable material and consumables.

10.1 Human resources

This is the salary of each member of the team:

Table 10.1: Hourly wage of the WG members.

ID	Duration	Salary (€/h)
G1	Project manager	60
G2	Junior engineer	35

The Table 10.2 presents an economic balance sheet of the project's human resources (work hours), taking into account the work hours spent in the project and the unit cost of each participant.

Table 10.2: Cost of the human resources.

WP task	G2 work (h)	G2 cost (€)	G1 work (h)	G1 cost (€)	Total work (h)	Total cost (€)
T.1.1	10	300	20	1200	30	1500
T.2.1	37,5	1125	15	900	52,5	2025
T.2.2	61,5	1845	20	1200	81,5	3045
T.3.1	3	90	10	600	13	690
T.3.2	93	2790	60	3600	153	6390
T.3.3	93	2790	10	600	103	3390
T.4.1	73,5	2205	20	1200	93,5	3405
T.4.2	108	3240	25	1500	133	4740
T.4.3	35	1050	15	900	50	1950
T.4.4	36	1080	13	780	49	1860
T.4.5	30	900	15	900	45	1800
T.5.1	70	2100	20	1200	90	3300
T.5.2	30	900	15	900	45	1800
				TOTAL	**938.5**	**35,895**

10.2 Material resources

In this section we are presenting the tables of the costs of depreciable material and consumables.

10.2.1 Depreciable material

These are the costs and expenses of the depreciable material.

Table 10.3: Total cost of the depreciable material.

Material	Units	Initial cost (€)	Lifespan (months)	Use (months)	Cost (€)
MacBook Pro 15"	1	3000	72	9	375
Dell Display 27" P2719H	1	310	72	9	38.75
Dell Universal Dock Station D600	1	280	72	9	35
SDD external drive	1	125	48	9	23.44
Printer	1	50	36	0.5	1.4
				SUBTOTAL	**473.58**

10.2.2 Consumables

The next table lists the cost associated with consumables.

Table 10.4: Total cost of consumables.

ID	Material	Cost (€)
C1	Office supplies	50
C2	Energy bill	40
C3	External USB	15
	SUBTOTAL	**105**

10.3 Summary of the budget of the project

In the following table we summarise the total costs and expenses: human resources (work hours), depreciable material and consumables.

Table 10.5: Summary of the total costs and expenses.

Concept	Cost (€)
Work hours	35895
Depreciations	473.58
Consumables	105
TOTAL	**36,473.58**

Adding up all the costs, the total cost of the project development amounts to **thirty six thousand four hundred seventy three euros**. Most of the expenses correspond to work hours.

11. CHAPTER

Conclusions and future work

The aim of this master thesis has been to develop and implement the tools to help establish correlations between cardiac output (CO) and stroke volume index (SVI) values measured by well-established technologies, and the measures taken from novel noninvasive signals such as BCG sensors that could be easily used in OHCA.The project has concluded by completing all the marked objectives and tasks. These were developed according to the proposed methodology.

A database has been generated from the measurements taken by medical equipment of different nature. The database has been standardized by converting the data from proprietary software to common open MATLAB format. For this purpose, existing data converters have been applied and custom data converters have also been developed. Moreover, all signals in the database have been time aligned using an algorithm based on the temporal annotations of the physicians.

In addition, the created data converters are quite generalist and could therefore easily be adapted to new data sources or devices.

Two user-friendly, flexible, and functional graphical interfaces have been developed to enable visualization, annotation and time alignment fine tuning of the multisource standardized database. The synchronized visualization of the signals offers the clinician the possibility to study and search for possible hidden correlations between the signals. Additionally, 4 algorithms have been integrated to help in the

search for correlations. These algorithms are already validated by the literature and have been used for the automatic detection of beats in the electrocardiogram signal, the extraction of the circulation component of the transthoracic impedance signal, the detection of ventilations in the transthoracic signal and in the capnogram.

This project has reinforced the existing global partnership with the physicians of NAKOS at Oslo University Hospital and the engineers of BMDLab at the University of Stavanger from Norway (SDG goal 17). Their help has been needed to identify and extract the analysis windows. An algorithm was written to extract the analysis windows indicated by the physicians.

A more specific graphical interface has also been created to analyze the extracted windows. The development of the latter interface has been made easier thanks to the graphical interface development method created with the first two interfaces. This method is flexible enough to be able to adapt the interface to new signals with relative ease (requiring little programming time). Finally the BCG signals have been filtered in the analysis window to try extract their associated circulation component.

Although the platform has been tested for 20 subjects, the platform is scalable and can accommodate signals from an hundreds or thousands of patients, which depends only on the performance of the computers used for the application. Currently, measurements are already being taken in real OHCA cases and the signals are expected to be received and integrated into the database in the near future.

We will finish pointing out the research lines opened by this project. This platform consisting of a multisource, standardized, common MATLAB open format database and three graphical interfaces for visualization, annotation and processing has set the framework for future developments together with NAKOS physicians and BMDLab engineers.

Thus, this platform will help on the identification of the correlation between the different technologies that will save lives with real-time hemodynamic monitoring in EMS-treated OHCA (SDG goal 3).

Bibliography

[A B89] A. B. de Luna, P. Coumel, and J. F. Leclercq: *Ambulatory sudden cardiac death: mechanisms of production of fatal arrhythmia on the basis of data from 157 cases*. 117.1, 1989, pp. 151–159

[Add05] Addison, P. S.: *Wavelet transforms and the ECG: a review*. eng. Physiol Meas, 26.5, Oct. 2005, R155–199. ISSN: 0967-3334. DOI: 10.1088/0967-3334/26/5/R01

[AED12] AEDAuthorityCanada: *LUCAS Chest Compression System*. 2012. URL: https://www.youtube.com/watch?v=HvNkWpZmdHA (visited on 06/03/2021)

[Age21] Agencia Española de Medicamentos y Productos Sanitarios (AEMPS): *PROSPECTO EMLA 25 mg/g + 25 mg/g CREMA*. es. Jan. 2021. URL: https://cima.aemps.es/cima/dochtml/p/61096/Prospecto_61096.html (visited on 05/26/2021)

[Ale17] Alex: *File:Risk matrix.png - CGE Barrier Based Risk Management Knowledge base*. June 2017. URL: https://www.cgerisk.com/knowledgebase/File:Risk_matrix.png (visited on 06/04/2021)

[Alo15] Alonso, E.; Ruiz, J.; Aramendi, E.: *Reliability and accuracy of the thoracic impedance signal for measuring cardiopulmonary resuscitation quality metrics*. eng. Resuscitation,

88 Mar. 2015, pp. 28–34. ISSN: 1873-1570. DOI: 10.1016/j.resuscitation.2014.11.027

[Alo16] Alonso, E.; Aramendi, E.; Daya, M.: *Circulation detection using the electrocardiogram and the thoracic impedance acquired by defibrillation pads*. eng. Resuscitation, 99 Feb. 2016, pp. 56–62. ISSN: 1873-1570. DOI: 10.1016/j.resuscitation.2015.11.014

[Ane] Anesthesia of the Toronto General Hospita, D. of: *Cardiac Anesthesiology: Stroke Volume, Control of Blood Pressure, Cardiac Physiology, Starling's Law*. en. URL: http://pie.med.utoronto.ca/CA/CA_content/CA_cardiacPhys_strokeVolume.html (visited on 05/09/2021)

[Ara14] Aramendi, E.; Alonso, E.; Russell, J. K.: *Monitoring respiratory rate with capnography during cardiopulmonary resuscitation*. en. Resuscitation, 85 May 2014, S26–S27. ISSN: 03009572. DOI: 10.1016/j.resuscitation.2014.03.075. URL: https://linkinghub.elsevier.com/retrieve/pii/S0300957214002196 (visited on 06/08/2021)

[Ara17] Aramendi, E.; Elola, A.; Alonso, E.: *Feasibility of the capnogram to monitor ventilation rate during cardiopulmonary resuscitation*. en. Resuscitation, 110 Jan. 2017, pp. 162–168. ISSN: 03009572. DOI: 10.1016/j.resuscitation.2016.08.033. URL: https://linkinghub.elsevier.com/retrieve/pii/S0300957216304725 (visited on 06/07/2021)

[Bal16] Baldzizhar, A.; Manuylova, E.; Marchenko, R.: *Ventricular Tachycardias*. en. Critical Care Nursing Clinics of North America, 28.3, Sept. 2016, pp. 317–329. ISSN: 08995885. DOI: 10.1016/j.cnc.2016.04.004. URL: https://linkinghub.elsevier.com/retrieve/pii/S0899588516300302 (visited on 05/11/2021)

[Bar11] Barroeta Urquiza, J.; Boada Bravo, N.: *Los servicios de emergencia y urgencias médicas extrahospitalarias en España*. es. OCLC: 796225438. Alcobendas, Madrid: Mensor 2011. ISBN: 978-84-615-0990-4

[Bar13a] Barrett, K. E.; Ganong, W. F.: *Capítulo 30. El corazón como bomba*. Spanish. *Ganong fisiología médica*. OCLC: 859161951. México, D.F.: McGraw-Hill Interamericana 2013. ISBN: 978-1-4562-1319-0. URL: http://public.ebookcentral.proquest.com/choice/publicfullrecord.aspx?p=3214445 (visited on 05/09/2021)

[Bar13b] Barrett, K. E.; Ganong, W. F.: *Ganong fisiología médica*. Spanish. OCLC: 859161951. México, D.F.: McGraw-Hill Interamericana 2013. ISBN: 978-1-4562-1319-0. URL: http://public.ebookcentral.proquest.com/choice/publicfullrecord.aspx?p=3214445 (visited on 05/09/2021)

[Ber03] Bert-Uwe Köhler; Hennig, C.; Orglmeister, Reinhold: *QRS detection using zero crossing counts*. en. Progress in Biomedical Research, 8, 2003, pp. 138–145. URL: http://www.msbt.nat.fau.de/PBMR/documents/200308030138.pdf (visited on 06/17/2019)

[Blu] Bluetooth SIG, I.: *Bluetooth Radio Versions*. en-US. URL: https://www.bluetooth.com/learn-about-bluetooth/radio-versions/ (visited on 06/02/2021)

[Bra14] Brahme, A., ed.: *Comprehensive biomedical physics*. eng. Amsterdam: Elsevier 2014. ISBN: 978-0-444-53632-7

[But13] Butterworth, J. F.; Mackey, D. C.; Wasnick, J. D.: *Chapter 5. Cardiovascular Monitoring. Morgan & Mikhail's Clinical Anesthesiology*. 5th ed. New York, NY: The McGraw-Hill Companies 2013. URL: accessanesthesiology . mhmedical . com/content.aspx?aid=57230594 (visited on 05/25/2021)

[CAR20] CARREÑO, M. S.; LLADÓ, G. P.; PRADAS, M. Á. M.: *Capítulo 47. Métodos incruentos de exploración cardíaca*. Spanish. *Medicina interna*. 19th ed. OCLC: 1198612730. Barcelona: Elsevier 2020. ISBN: 978-84-9113-545-6 978-84-9113-543-2 978-84-9113-544-9

[Cha08] Chan, P. S.; Krumholz, H. M.; Nichol, G.: *Delayed Time to Defibrillation after In-Hospital Cardiac Arrest*. en. N Engl J Med, 358.1, Jan. 2008, pp. 9–17. ISSN: 0028-4793, 1533-4406. DOI: 10.1056/NEJMoa0706467. URL: http://www.nejm.org/doi/abs/10.1056/NEJMoa0706467 (visited on 05/11/2021)

[Chu08] Chugh, S. S.; Reinier, K.; Teodorescu, C.: *Epidemiology of sudden cardiac death: clinical and research implications*. eng. Prog Cardiovasc Dis, 51.3, Dec. 2008, pp. 213–228. ISSN: 1873-1740. DOI: 10.1016/j.pcad.2008.06.003

[Col13] College, O.: *ECG Tracing with Heart Contraction*. June 2013. URL: https://commons.wikimedia.org/wiki/File:2023_ECG_Tracing_with_Heart_ContractionN.jpg#filelinks

[Com21] Company, G. E.: *Vscan Air*. en-US. Jan. 2021. URL: https://handheldultrasound.gehealthcare.com/vscan-air/ (visited on 06/08/2021)

[Cor] Corazón, F. E. del: *Holter*. es-es. URL: https://fundaciondelcorazon.com/informacion-para-pacientes/metodos-diagnosticos/holter.html (visited on 06/08/2019)

[Cor19] Corporation, E. L.: *FloTrac system | Edwards Lifesciences*. en. 2019. URL: https://www.edwards.com/devices/Hemodynamic-Monitoring/FloTrac (visited on 05/29/2021)

[Cre] Creative: *Capnógrafo de Mano PC-900B*. es. URL: https://www.ribasmedicina.com/producto/capnografo-de-mano-pc-900b/ (visited on 06/02/2021)

[Cro08] Cromie, N. A.; Allen, J. D.; Turner, C.: *The impedance cardiogram recorded through two electrocardiogram/defibrillator pads as a determinant of cardiac arrest during experimental studies*. eng. Crit Care Med, 36.5, May 2008, pp. 1578–1584. ISSN: 1530-0293. DOI: 10.1097/CCM.0b013e318170a03b

[Cro10] Cromie, N. A.; Allen, J. D.; Navarro, C.: *Assessment of the impedance cardiogram recorded by an automated external defibrillator during clinical cardiac arrest*. eng. Crit Care Med, 38.2, Feb. 2010, pp. 510–517. ISSN: 1530-0293. DOI: 10.1097/CCM.0b013e3181c02ca1

[Cum91a] Cummins, R. O.; Chamberlain, D. A.; Abramson, N. S.: *Recommended guidelines for uniform reporting of data from out-of-hospital cardiac arrest: the Utstein Style. A statement for health professionals from a task force of the American Heart Association, the European Resuscitation Council, the Heart and Stroke Foundation of Canada, and the Australian Resuscitation Council*. en. Circulation, 84.2, Aug. 1991, pp. 960–975. ISSN: 0009-7322, 1524-4539. DOI: 10.1161/01.CIR.84.2.960. URL: https://www.ahajournals.org/doi/10.1161/01.CIR.84.2.960 (visited on 05/12/2021)

[Cum91b] Cummins, R and Thies, W: *Automated external defibrillators and the Advanced Cardiac Life Support Program: a new initiative from the American Heart Association*. 9 1991, pp. 91–93

[Dea10] Deakin, C. D.; Nolan, J. P.; Soar, J.: *European Resuscitation Council Guidelines for Resuscitation 2010 Section 4. Adult advanced life support*. eng. Resuscitation, 81.10, Oct. 2010, pp. 1305–1352. ISSN: 1873-1570. DOI: 10.1016/j.resuscitation.2010.08.017

[Díe09] Díez-Picazo, L. D.; Barrado-Muñoz, L.; Blanco-Hermo, P.: *La capnografía en los servicios de emergencia médica*. es. Semergen, 35.3, Mar. 2009. Publisher: Elsevier, pp. 138–143. ISSN: 1138-3593. DOI: 10.1016/S1138-3593(09)70721-X. URL: https://www.elsevier.es/es-revista-medicina-familia-semergen-40-articulo-la-capnografia-servicios-emergencia-medica-13135238 (visited on 06/02/2021)

[Dip20] Dipika J. Gopal, M.: *Current State of Point-of-Care Ultrasound Curricula*. American College of Cardiology Mar. 2020. URL: https://www.acc.org/membership/sections-and-councils/imaging-section/section-updates/2020/03/16/10/31/current-state-of-point-of-care-ultrasound-curricula (visited on 05/29/2021)

[Du 16] Du BOIS, D.: *CLINICAL CALORIMETRY: TENTH PAPER A FORMULA TO ESTIMATE THE APPROXIMATE SURFACE AREA IF HEIGHT AND WEIGHT BE KNOWN*. en. Arch Intern Med (Chic), XVII.6_2, June 1916, p. 863. ISSN: 0730-188X. DOI: 10.1001/archinte.1916.00080130010002. URL: http://archinte.jamanetwork.com/article.aspx?doi=10.1001/archinte.1916.00080130010002 (visited on 05/09/2021)

[Dub07] Dubin, D.: *Electrocardiografía práctica: lesión, trazado e interpretación*. es. 3rd ed. México, D.F. [etc.] : Interamericana, 2007. ISBN: 978-968-25-0082-4

[Eat] Eaton, J. W.: *GNU Octave: About*. en. URL: https://www.gnu.org/software/octave/about (visited on 06/04/2021)

[Ebl20] Ebli, S.: *Trendelenburg position*. en. Page Version ID: 995070477. Dec. 2020. URL: https://en.wikipedia.org/w/index.php?title=Trendelenburg_position&oldid=995070477 (visited on 05/26/2021)

[Ede08] Edelson, D. P.; Litzinger, B.; Arora, V.: *Improving in-hospital cardiac arrest process and outcomes with performance debriefing*. eng. Arch Intern Med, 168.10, May 2008, pp. 1063–1069. ISSN: 1538-3679. DOI: 10.1001/archinte.168.10.1063

[Ede10] Edelson, D. P.; Eilevstjønn, J.; Weidman, E. K.: *Capnography and chest wall impedance algorithms for ventilation detection during cardiopulmonary resuscitation*. Resuscitation, 81.3, Mar. 2010, pp. 317–322. ISSN: 0300-9572. DOI: 10.1016/j.resuscitation.2009.11.003. URL: https://www.ncbi.nlm.nih.gov/pmc/articles/PMC2823837/ (visited on 06/08/2021)

[Edu] Education, E.
bibinitperiod E.: *Principles of hemodynamics. Stroke Volume, VTI (Velocity Time Integral) & Cardiac Output*. en-US. *Clinical Echocardiography*. URL: https://ecgwaves.com/topic/stroke-volume-vti-velocity-time-integral-cardiac-output/ (visited on 05/31/2021)

[Efe18] Efendijev, I.; Folger, D.; Raj, R.: *Outcomes and healthcare-associated costs one year after intensive care-treated cardiac arrest*. eng. Resuscitation, 131 Oct. 2018, pp. 128–134. ISSN: 1873-1570. DOI: 10.1016/j.resuscitation.2018.06.028

[Ein95] Einthoven, W.: *Ueber die Form des menschlichen Electrocardiogramms*. de. Pflüger, Arch. 60.3-4, Mar. 1895, pp. 101–123. ISSN: 0031-6768, 1432-2013. DOI: 10.1007/BF01662582. URL: http://link.springer.com/10.1007/BF01662582 (visited on 06/14/2019)

[Fal88] Falk, J. L.; Rackow, E. C.; Weil, M. H.: *End-Tidal Carbon Dioxide Concentration during Cardiopulmonary Resuscitation*. en. N Engl J Med, 318.10, Mar. 1988, pp. 607–611. ISSN: 0028-4793, 1533-4406. DOI: 10.1056/NEJM198803103181005. URL: http://www.nejm.org/doi/abs/10.1056/NEJM198803103181005 (visited on 06/02/2021)

[Fun21] Fundation, P. S.: *tkinter — Interface de Python para Tcl/Tk — documentación de Python - 3.9.5*. Apr. 2021. URL: https://docs.python.org/es/3/library/tkinter.html (visited on 06/04/2021)

[Gee11] Geerts, B. F.; Aarts, L. P.; Jansen, J. R.: *Methods in pharmacology: measurement of cardiac output*. eng. Br J Clin Pharmacol, 71.3, Mar. 2011, pp. 316–330. ISSN: 1365-2125. DOI: 10.1111/j.1365-2125.2010.03798.x

[Gir16] Girbau, L. M.; Terradellas, J. B.: *Capítulo 52 - Arritmias cardíacas*. es. *Farreras Rozman. Medicina Interna.* 18th ed. Vol. 1. Barcelona: Elsevier 2016, p. 28

[God] Godruma: *Equipment for making electrocardiogram wires vector image on VectorStock*. en. URL: https://www.vectorstock.com/royalty-free-vector/equipment-for-making-electrocardiogram-wires-vector-19965594 (visited on 06/08/2019)

[Gon18] González-Otero, D. M.; Gauna, S. R. d.; Gutiérrez, J. J.: *Applications of the Transthoracic Impedance Signal during Resuscitation*. en. Publication Title: Special Topics in Resuscitation. IntechOpen Oct. 2018. ISBN: 978-1-78984-252-4. DOI: 10.5772/intechopen.79382. URL: https://www.

intechopen.com/books/special-topics-in-resuscitation/applications-of-the-transthoracic-impedance-signal-during-resuscitation (visited on 06/02/2021)

[Gor77] Gordon, J. W.: *Certain Molar Movements of the Human Body produced by the Circulation of the Blood*. eng. J Anat Physiol, 11.Pt 3, Apr. 1877, pp. 533–536

[Grä16] Gräsner, J.-T.; Lefering, R.; Koster, R. W.: *EuReCa ONE - 27 Nations, ONE Europe, ONE Registry*. en. Resuscitation, 105 Aug. 2016, pp. 188–195. ISSN: 03009572. DOI: 10.1016/j.resuscitation.2016.06.004. URL: https://linkinghub.elsevier.com/retrieve/pii/S0300957216300995 (visited on 04/22/2021)

[Grä20] Gräsner, J.-T.; Wnent, J.; Herlitz, J.: *Survival after out-of-hospital cardiac arrest in Europe - Results of the EuReCa TWO study*. eng. Resuscitation, 148 Mar. 2020, pp. 218–226. ISSN: 1873-1570. DOI: 10.1016/j.resuscitation.2019.12.042

[Grä21] Gräsner, J.-T.; Herlitz, J.; Tjelmeland, I. B.: *European Resuscitation Council Guidelines 2021: Epidemiology of cardiac arrest in Europe*. en. Resuscitation, 161 Apr. 2021, pp. 61–79. ISSN: 03009572. DOI: 10.1016/j.resuscitation.2021.02.007. URL: https://linkinghub.elsevier.com/retrieve/pii/S0300957221000605 (visited on 05/11/2021)

[GRO] GROUP, S.: *ECG 2.gif (Imagen GIF, 2304 × 1536 píxeles) - Escalado (38 %)*. URL: http://www.sosgroup.co/UserFiles/Image/ECG%202.gif (visited on 06/07/2019)

[Gro15] Group, B.: *ECG detector/delineator (Wavedet)*. es. Apr. 2015. URL: https://bsicos.unizar.es/ecg-detectordelineator-wavedet/ (visited on 06/20/2019)

[Gud88] Gudipati, C. V.; Weil, M. H.; Bisera, J.: *Expired carbon dioxide: a noninvasive monitor of cardiopulmonary resuscitation*. en. Circulation, 77.1, Jan. 1988, pp. 234–239. ISSN: 0009-7322, 1524-4539. DOI: 10.1161/01.CIR.77.1.234. URL: https://www.ahajournals.org/doi/10.1161/01.CIR.77.1.234 (visited on 06/02/2021)

[Haf21] Hafen, B. B.; Sharma, S.: *Oxygen Saturation*. eng. *StatPearls*. Treasure Island (FL): StatPearls Publishing 2021. URL: http://www.ncbi.nlm.nih.gov/books/NBK525974/ (visited on 06/02/2021)

[Hal16] Hall, J. E.: *Guyton y Hall. Tratado de fisiología médica*. English. OCLC: 953858932. 2016. ISBN: 978-84-9113-025-3

[Ham86] Hamilton, P. S.; Tompkins, W. J.: *Quantitative Investigation of QRS Detection Rules Using the MIT/BIH Arrhythmia Database*. English. IEEE Transactions on biomedical engineering, BME-33.12, Dec. 1986, p. 8

[Han] Hanno Tan, MD PhD; Marieke Blom PhD; Frank Groen: *European Sudden Cardiac Arrest network: towards Prevention, Education and NEw Treatment | ESCAPE-NET Project | H2020*. en. URL: https://cordis.europa.eu/project/id/733381 (visited on 04/15/2021)

[Hea] Healthcare, T.: *What is a pulse oximeter? - Tunstall Blog*. URL: https://blog.tunstallhealthcare.com.au/connected-health/what-is-a-pulse-oximeter/

[Iba15] Ibarguren, K.; Unanue, J. M.; Alonso, D.: *Difference in survival from pre-hospital cardiac arrest between cities and villages in the Basque Autonomous Community*. English. Resuscitation, 96 Nov. 2015. Publisher: Elsevier, p. 114. ISSN: 0300-9572, 1873-1570. DOI: 10.1016/j.resuscitation.2015.09.269. URL: https://www.resuscitationjournal.com/article/S0300-9572(15)00664-4/abstract (visited on 04/22/2021)

[Isa20] Isasi Liñero, Iraia: *Signal Processing and machine learning contributions to rhythm analysis during cardiopulmonary resuscitation*. en. PhD thesis. Bilbao: Euskal Herriko Unibertsitatea (UPV/EHU), Sept. 2020. URL: http://hdl.handle.net/10810/50398 (visited on 04/26/2021)

[Ive11] Iverson, G. L.: *Positive Predictive Power*. en. *Encyclopedia of Clinical Neuropsychology*. Ed. by Kreutzer, J. S.; DeLuca, J. New York, NY: Springer 2011, pp. 1968–1970. ISBN: 978-0-387-79948-3. DOI: 10.1007/978-0-387-79948-3_1234. URL: https://doi.org/10.1007/978-0-387-79948-3_1234 (visited on 06/11/2021)

[Jam18] Jameson, J. L., ed.: *Harrison's principles of internal medicine*. Twentieth edition. New York: McGraw-Hill Education 2018. ISBN: 978-1-259-64404-7 978-1-259-64400-9

[Jau20] Jaureguibeitia, X.; Irusta, U.; Aramendi, E.: *Automatic Detection of Ventilations During Mechanical Cardiopulmonary Resuscitation*. eng. IEEE J Biomed Health Inform, 24.9, Sept. 2020, pp. 2580–2588. ISSN: 2168-2208. DOI: 10.1109/JBHI.2020.2967643

[JGu19] JGuerra: *Get Familiar with the Ultrasound Machine Components*. Section: Ultrasound Blog. Sept. 2019. URL: https://conquestimaging.com/ultrasound-blog/get-familiar-ultrasound-machine-components/ (visited on 05/31/2021)

[Kan17] Kandala, J.; Oommen, C.; Kern, K. B.: *Sudden cardiac death*. en. British Medical Bulletin, 122.1, June 2017, pp. 5–15. ISSN: 0007-1420, 1471-8391. DOI: 10.1093/bmb/ldx011. URL: https://academic.oup.com/bmb/article-lookup/doi/10.1093/bmb/ldx011 (visited on 05/11/2021)

[Kar20] Kardias: *El cateterismo cardíaco: cuidados en casa*. es-MX. Aug. 2020. URL: https://www.kardias.org/2020/08/14/el-cateterismo-cardiaco-cuidados-en-casa/ (visited on 06/01/2021)

[Ker81] Kerber, R. E.; Grayzel, J.; Hoyt, R.: *Transthoracic resistance in human defibrillation. Influence of body weight, chest size, serial shocks, paddle size and paddle contact pressure*. eng. Circulation, 63.3, Mar. 1981, pp. 676–682. ISSN: 0009-7322. DOI: 10.1161/01.cir.63.3.676

[Ker84] Kerber, R. E.; Kouba, C.; Martins, J.: *Advance prediction of transthoracic impedance in human defibrillation and cardioversion: importance of impedance in determining the success of low-energy shocks*. eng. Circulation, 70.2, Aug. 1984, pp. 303–308. ISSN: 0009-7322. DOI: 10.1161/01.cir.70.2.303

[Kim16] Kim, C.-S.; Ober, S. L.; McMurtry, M. S.: *Ballistocardiogram: Mechanism and Potential for Unobtrusive Cardiovascular Health Monitoring*. en. Sci Rep, 6.1, Nov. 2016, p. 31297. ISSN: 2045-2322. DOI: 10.1038/srep31297. URL: http://www.nature.com/articles/srep31297 (visited on 05/10/2021)

[Koh02] Kohler, B.-U.; Hennig, C.; Orglmeister, R.: *The principles of software QRS detection*. en. IEEE Eng. Med. Biol. Mag. 21.1, Feb. 2002, pp. 42–57. ISSN: 07395175. DOI: 10.1109/51.993193. URL: http://ieeexplore.ieee.org/document/993193/ (visited on 06/15/2019)

[Kos10] Koster, R. W.; Baubin, M. A.; Bossaert, L. L.: *European Resuscitation Council Guidelines for Resuscitation 2010 Section 2. Adult basic life support and use of automated external defibrillators*. eng. Resuscitation, 81.10, Oct. 2010, pp. 1277–1292. ISSN: 1873-1570. DOI: 10.1016/j.resuscitation.2010.08.009

[Kou60] Kouwenhoven, W. B.: *CLOSED-CHEST CARDIAC MASSAGE*. en. JAMA, 173.10, July 1960, p. 1064. ISSN: 0098-7484. DOI: 10.1001/jama.1960.03020280004002. URL: http://jama.jamanetwork.com/article.aspx?doi=10.1001/jama.1960.03020280004002 (visited on 05/11/2021)

[Kra] Krafft, D. T.; Prof. Dr. Luis García-Castrillo Riesgo; Prof. Dr. med. Matthias Fischer: *European Emergency Data Project EMS Data-based Health Surveillance System*. P. 109

[Kra07] Kramer-Johansen, J.; Edelson, D. P.; Losert, H.: *Uniform reporting of measured quality of cardiopulmonary resuscitation (CPR)*. en. Resuscitation, 74.3, Sept. 2007, pp. 406–417. ISSN: 03009572. DOI: 10.1016/j.resuscitation.2007.01.024. URL: https://linkinghub.elsevier.com/retrieve/pii/S030095720700038X (visited on 05/11/2021)

[LAB13] LABORALES, G. D. T. D. P. D. R.: *IMPLANTACIÓN DE DESFIBRILADORES EXTERNOS AUTOMÁTICOS Y SEMIAUTOMÁTICOS (DESAs) EN LA UNIVERSIDAD.* es. Tech. rep. Girona: Conferencia de Rectores de las Universidades Espanolas (CRUE), Oct. 2013. URL: https://www.ehu.eus/documents/1821432/1857927/DESAs+2014+en+la+Universidad.pdf/0eec0e41-3d52-4f15-8022-db6b2dda39b3 (visited on 06/08/2019)

[Leo18] Leopold, J. A.; David P. Faxon: *Chapter 237. Diagnostic Cardiac Catheterization and Coronary Angiography. Harrison's principles of internal medicine*. Ed. by Jameson, J. L. Twentieth edition. New York: McGraw-Hill Education 2018. ISBN: 978-1-259-64404-7 978-1-259-64400-9

[Let17] Leturiondo, M.; Ruiz, J.; Ruiz de Gauna, S.: *A Simple Algorithm for Ventilation Detection in the Capnography Signal During Cardiopulmonary Resuscitation*. en. Sept. 2017. DOI: 10.22489/CinC.2017.005-072. URL: http://www.cinc.org/archives/2017/pdf/005-072.pdf (visited on 06/08/2021)

[Lu06] Lu, Z.; Mukkamala, R.: *Continuous cardiac output monitoring in humans by invasive and noninvasive peripheral blood pressure waveform analysis*. eng. J Appl Physiol (1985), 101.2, Aug. 2006, pp. 598–608. ISSN: 8750-7587. DOI: 10.1152/japplphysiol.01488.2005

[Luu89] Luu, M.; Stevenson, W. G.; Stevenson, L. W.: *Diverse mechanisms of unexpected cardiac arrest in advanced heart failure*. eng. Circulation, 80.6, Dec. 1989, pp. 1675–1680. ISSN: 0009-7322. DOI: 10.1161/01.cir.80.6.1675

[M S20] M. SABATÉ TENAS: *Capítulo 48. Cateterismo cardíaco*. es. *Farreras Rozman. Medicina Interna*. OCLC: 1232714031. 2020, p. 12. ISBN: 978-84-9113-836-5

[Mar04] Martinez, J.; Almeida, R.; Olmos, S.: *A Wavelet-Based ECG Delineator: Evaluation on Standard Databases*. en. IEEE Transactions on Biomedical Engineering, 51.4, Apr. 2004, pp. 570–581. ISSN: 0018-9294. DOI: 10.1109/TBME.2003.821031. URL: http://ieeexplore.ieee.org/document/1275572/ (visited on 04/14/2019)

[Mar11] Martin, E.: *Sensitivity and Specificity*. en. *Encyclopedia of Machine Learning*. Ed. by Sammut, C.; Webb, G. I. Boston, MA: Springer US 2011, pp. 901–902. ISBN: 978-0-387-30768-8 978-0-387-30164-8. DOI: 10.1007/978-0-387-30164-8_752. URL: http://www.springerlink.com/index/10.1007/978-0-387-30164-8_752 (visited on 06/16/2019)

[Mata] MathWorks: *Inicio de Documentación*. URL: https://es.mathworks.com/help/ (visited on 06/04/2021)

[Matb] MathWorks: *MATLAB Documentation*. URL: https://www.mathworks.com/help/matlab/ (visited on 06/04/2021)

[Matc] MathWorks: *Nueva licencia de MATLAB Student R2021a*. URL: https://es.mathworks.com/store/link/products/student/new (visited on 06/09/2021)

[Mat12] Mateu Campos, M.; Ferrándiz Sellés, A.; Gruartmoner de Vera, G.: *Techniques available for hemodynamic monitoring. Advantages and limitations*. en. Medicina Intensiva (English Edition), 36.6, Aug. 2012, pp. 434–444. ISSN: 21735727. DOI: 10.1016/j.medine.2012.09.004. URL: https://linkinghub.elsevier.com/retrieve/pii/S2173572712001105 (visited on 06/02/2021)

[Mei95] Meij, S.; Klootwijk, P.; Arends, J.: *An algorithm for automatic beat-to-beat measurement of the QT-interval. Computers in Cardiology 1994*. Bethesda, MD, USA: IEEE Comput. Soc. Press 1995, pp. 597–600. ISBN: 978-0-8186-6570-7. DOI: 10.1109/CIC.1994.470121. URL: http://ieeexplore.ieee.org/document/470121/ (visited on 06/16/2019)

[Mil68] Miller, R. B.: *Response time in man-computer conversational transactions. Proceedings of the December 9-11, 1968, fall joint computer conference, part I*. AFIPS '68 (Fall, part I). New York, NY, USA: Association for Computing Machinery Dec. 1968, pp. 267–277. ISBN: 978-1-4503-7899-4. DOI: 10.1145/1476589.1476628. URL: https://doi.org/10.1145/1476589.1476628 (visited on 06/09/2021)

[Mis14] Mistovich, J. J.: *Chapter 7. Anatomy, Physiology, and Medical Terminology. Prehospital emergency care*. Ed. by Karren, K. J. Tenth edition. Boston: Pearson 2014, pp. 118–163. ISBN: 978-0-13-336913-7

[Moh10] Mohamed, A. A.; Arifi, A. A.; Omran, A.: *The basics of echocardiography*. J Saudi Heart Assoc, 22.2, Apr. 2010, pp. 71–76. ISSN: 1016-7315. DOI: 10.1016/j.jsha.2010.02.011. URL: https://www.ncbi.nlm.nih.gov/pmc/articles/PMC3727500/ (visited on 06/08/2021)

[Nat19] Nations, U.: *English: The Sustainable Development Goals, adopted on 25 September 2015 as a part of the 2030 Agenda*. Aug. 2019. URL: https://commons.wikimedia.org/wiki/File:Sustainable_Development_Goals.svg (visited on 05/11/2021)

[Nit14] Nitzan, M.; Romem, A.; Koppel, R.: *Pulse oximetry: fundamentals and technology update*. eng. Med Devices (Auckl), 7 2014, pp. 231–239. ISSN: 1179-1470. DOI: 10.2147/MDER.S47319

[Nol06] Nolan, J.; Soar, J.; Eikeland, H.: *The chain of survival*. en. Resuscitation, 71.3, Dec. 2006, pp. 270–271. ISSN: 03009572. DOI: 10.1016/j.resuscitation.2006.09.001. URL: https://linkinghub.elsevier.com/retrieve/pii/S0300957206006022 (visited on 05/11/2021)

[Nol19] Nolan, J. P.; Berg, R. A.; Andersen, L. W.: *Cardiac Arrest and Cardiopulmonary Resuscitation Outcome Reports: Update of the Utstein Resuscitation Registry Template for In-Hospital Cardiac Arrest*. en. Resuscitation, 144 Nov. 2019, pp. 166–177. ISSN: 03009572. DOI: 10.1016/j.resuscitation.2019.08.021. URL: https://linkinghub.elsevier.com/retrieve/pii/S0300957219305829 (visited on 05/12/2021)

[Nor14] Normalización y certificación), A. (E. de: *UNE-EN ISO 10555-5:2014 Catéteres intravasculares. Catéteres e...* es. Feb. 2014. URL: https://www.en.une.org/encuentra-tu-norma/busca-tu-norma/norma?c=N0052588 (visited on 06/01/2021)

[NV] N.V., K. P.: *Sistema de Ultrasonido Portátil | Philips Healthcare*. es-es. URL: https://www.philips.es/healthcare/sites/lumify (visited on 06/08/2021)

[Ola21] Olasveengen, T. M.; Semeraro, F.; Ristagno, G.: *European Resuscitation Council Guidelines 2021: Basic Life Support*. en. Resuscitation, 161 Apr. 2021, pp. 98–114. ISSN: 03009572. DOI: 10.1016/j.resuscitation.2021.02.009. URL: https://linkinghub.elsevier.com/retrieve/pii/S0300957221000629 (visited on 05/06/2021)

[Pan20] Panchal, A. R.; Bartos, J. A.; Cabañas, J. G.: *Part 3: Adult Basic and Advanced Life Support: 2020 American Heart Association Guidelines for Cardiopulmonary Resuscitation and Emergency Cardiovascular Care*. en. Circulation, 142.16_suppl_2, Oct. 2020. ISSN: 0009-7322, 1524-4539. DOI: 10.1161/CIR.0000000000000916. URL: https://www.ahajournals.org/doi/10.1161/CIR.0000000000000916 (visited on 05/11/2021)

[Par18] Park, K. S.; Yoon, H.: *Ballistocardiography*. *Seamless Healthcare Monitoring: Advancements in Wearable, Attachable, and Invisible Devices*. Ed. by Tamura, T. Cham: Springer International Publishing 2018, pp. 127–155. ISBN: 978-3-319-69362-0. DOI: 10.1007/978-3-319-69362-0_5. URL: https://doi.org/10.1007/978-3-319-69362-0_5

[Per15a] Perkins, G. D.; Handley, A. J.; Koster, R. W.: *European Resuscitation Council Guidelines for Resuscitation 2015*. en. Resuscitation, 95 Oct. 2015, pp. 81–99. ISSN: 03009572. DOI: 10.1016/j.resuscitation.2015.07.015. URL: https://linkinghub.elsevier.com/retrieve/pii/S0300957215003275 (visited on 05/11/2021)

[Per15b] Perkins Gavin D.; Jacobs Ian G.; Chamberlain Douglas: *Cardiac Arrest and Cardiopulmonary Resuscitation Outcome Reports: Update of the Utstein Resuscitation Registry Templates for Out-of-Hospital Cardiac Arrest*. Circulation, 132.13, Sept. 2015. Publisher: American Heart Association, pp. 1286–1300. DOI: 10.1161/CIR.0000000000000144. URL: https://www.ahajournals.org/doi/10.1161/cir.0000000000000144 (visited on 05/12/2021)

[Phya] Physio-Control: *Monitor/desfibrilador LIFEPAK 15*. es. URL: https://www.physio-control.com/WCProductDetails.aspx?id=2147484478&langtype=1034 (visited on 06/03/2021)

[Phyb] Physio-Control: *Physio-Control LIFEPAK® Series 12/15/20 Pediatric Defibrillation Pads Quick Combo RTS - item #11996-000093, item #DE11996000093*. URL: https://www.danleemedical.com/Physio-Control-LIFEPAK-Series-121520-Pediatric-Defibrillation-Pads-Quick-Combo-RTS-item-11996-000093-item-DE11996000093-P1802.aspx (visited on 06/03/2021)

[Phy20] Physio-Control: *Physio-Control LIFEPAK® 12/15/20 Masimo SET SpO2 Sensor-Pediatric Reusable - AED Superstore - 11171-000010, 3201655-004*. Dec. 2020. URL: https://www.aedsuperstore.com/physio-control-lifepak-12-20-masimo-set-spo2-sensor-pediatric-reusable.html (visited on 06/02/2021)

[Ris07] Risdal, M.; Aase, S. O.; Stavland, M.: *Impedance-based ventilation detection during cardiopulmonary resuscitation*. eng. IEEE Trans Biomed Eng, 54.12, Dec. 2007, pp. 2237–2245. ISSN: 0018-9294. DOI: 10.1109/tbme.2007.908328

[Rod07] Rodríguez de Viguri, N.; López Mesa, J.; Ruano Campos M, M.: *Manual de soporte vital avanzado*. es. 4th ed. Madrid, Espana: Masson 2007. ISBN: 978-84-458-1725-4

[Rom11] Romero-Bermejo, F. J.; Ruiz-Bailén, M.; Guerrero-De-Mier, M.: *Echocardiographic Hemodynamic Monitoring in the Critically Ill Patient*. Curr Cardiol Rev, 7.3, Aug. 2011, pp. 146–156. ISSN: 1573-403X. DOI: 10.2174/157340311798220485. URL: https://www.ncbi.nlm.nih.gov/pmc/articles/PMC3263479/ (visited on 05/29/2021)

[Rui13] Ruiz, J.; Alonso, E.; Aramendi, E.: *Reliable extraction of the circulation component in the thoracic impedance measured by defibrillation pads*. eng. Resuscitation, 84.10, Oct. 2013, pp. 1345–1352. ISSN: 1873-1570. DOI: 10.1016/j.resuscitation.2013.05.020

[sal20] salud, O. S. /. D. de; Vasco, E. J. /. G.: *EUSKADI. COVID-19*. es. Mar. 2020. URL: https://www.geo.euskadi.eus/covid-19-euskadi/s69-geodir/es/ (visited on 06/04/2021)

[San] Sanz, J. J. C.; Aragonés, E. A.; Latorre, M. A.: *Servicios de urgencias y emergencias 112. Recursos y actividad 2015*. es. P. 17

[Sas10] Sasson, C.; Rogers, M. A.; Dahl, J.: *Predictors of Survival From Out-of-Hospital Cardiac Arrest: A Systematic Review and Meta-Analysis*. en. Circ Cardiovasc Qual Outcomes, 3.1, Jan. 2010, pp. 63–81. ISSN: 1941-7713, 1941-7705. DOI: 10.1161/CIRCOUTCOMES.109.889576. URL: https://www.ahajournals.org/doi/10.1161/CIRCOUTCOMES.109.889576 (visited on 05/11/2021)

[Sco21] Scott D. Solomon; Justina C. Wu; Linda Gillam: *Chapter 14. Echocardiography*. English. *BRAUNWALD'S HEART DISEASE, SINGLE VOLUME: a textbook of cardiovascular medicine*. OCLC: 1249801820. S.l.: ELSEVIER - HEALTH SCIENCE 2021, p. 70. ISBN: 978-0-323-82467-5

[Sil19] Silverthorn, D. U.; Johnson, B. R.; Ober, W. C.: *Fisiología humana: un enfoque integrado*. Spanish. OCLC: 1120653233. 2019. ISBN: 978-607-8546-23-7. URL: https://www.medicapanamericana.com/VisorEbookV2/Ebook/9786078546237 (visited on 05/09/2021)

[Soa15] Soar, J.; Nolan, J. P.; Böttiger, B. W.: *European Resuscitation Council Guidelines for Resuscitation 2015*. en. Resuscitation, 95 Oct. 2015, pp. 100–147. ISSN: 03009572. DOI: 10.1016/j.resuscitation.2015.07.016. URL: https://linkinghub.elsevier.com/retrieve/pii/S0300957215003287 (visited on 05/11/2021)

[Soa21] Soar, J.; Böttiger, B. W.; Carli, P.: *European Resuscitation Council Guidelines 2021: Adult advanced life support*. en. Resuscitation, 161 Apr. 2021, pp. 115–151. ISSN: 03009572. DOI: 10.1016/j.resuscitation.2021.02.010. URL: https://linkinghub.elsevier.com/retrieve/pii/S0300957221000630 (visited on 05/07/2021)

[Sol] Solaris: *Solaris Capnograph Airway Adapter*. en. URL: https://www.medshop.com.au/products/solaris-capnograph-airway-adapter (visited on 06/02/2021)

[Son] SonoScape: *Ecógrafo S40 SonoScape para multiespecialidad, de Intecmedics*. es. URL: https://www.catalogodelasalud.com/ficha-producto/Ecografo-SonoScape-S40+101848 (visited on 05/31/2021)

[Sta18] Stanger, D. E.; Fordyce, C. B.: *The cost of care for cardiac arrest*. Resuscitation, 131 Oct. 2018. Publisher: Elsevier, A7–A8. ISSN: 0300-9572. DOI: 10.1016/j.resuscitation.2018.08.010. URL: https://doi.org/10.1016/j.resuscitation.2018.08.010 (visited on 04/26/2021)

[Str] Stryker: *Español - LUCAS - Chest Compression System*. URL: https://www.lucas-cpr.com/es/ (visited on 06/03/2021)

[Sun07] Sunde, K.; Pytte, M.; Jacobsen, D.: *Implementation of a standardised treatment protocol for post resuscitation care after out-of-hospital cardiac arrest*. en. Resuscitation, 73.1, Apr. 2007, pp. 29–39. ISSN: 03009572. DOI: 10.1016/j.resuscitation.2006.08.016. URL: https://linkinghub.elsevier.com/retrieve/pii/S0300957206005508 (visited on 05/11/2021)

[Sun08] Sun, James Xin: *Cardiac output estimation using arterial blood pressure waveforms*. en. PhD thesis. May 2008. URL: https://dspace.mit.edu/handle/1721.1/41625?show=full (visited on 04/19/2021)

[Sys] Systems, M. M.: *Performa Multipack - Catéter de angiografía by Merit Medical Systems | MedicalExpo*. es. URL: https://www.medicalexpo.es/prod/merit-medical-systems/product-81470-690078.html (visited on 06/01/2021)

[Tog13] Toggweiler, S.; Leipsic, J.; Binder, R. K.: *Management of Vascular Access in Transcatheter Aortic Valve Replacement: Part 1: Basic Anatomy, Imaging, Sheaths, Wires, and Access Routes*. en. JACC: Cardiovascular Interventions, 6.7, July 2013, pp. 643–653. ISSN: 1936-8798. DOI: 10.1016/j.jcin.2013.04.003. URL: https://www.sciencedirect.com/science/article/pii/S1936879813008029 (visited on 06/01/2021)

[Tos17] Tosi, J.; Taffoni, F.; Santacatterina, M.: *Performance Evaluation of Bluetooth Low Energy: A Systematic Review*. Sensors (Basel), 17.12, Dec. 2017. ISSN: 1424-8220. DOI: 10.3390/s17122898. URL: https://www.ncbi.nlm.nih.gov/pmc/articles/PMC5751532/ (visited on 05/31/2020)

[Val97] Valenzuela, T. D.; Roe, D. J.; Cretin, S.: *Estimating Effectiveness of Cardiac Arrest Interventions: A Logistic Regression Survival Model*. en. Circulation, 96.10, Nov. 1997, pp. 3308–3313. ISSN: 0009-7322, 1524-4539. DOI: 10.1161/01.CIR.96.10.3308. URL: https://www.ahajournals.org/doi/10.1161/01.CIR.96.10.3308 (visited on 05/11/2021)

[Vir21] Virani, S. S.; Alonso, A.; Aparicio, H. J.: *Heart Disease and Stroke Statistics—2021 Update: A Report From the American Heart Association*. en. Circulation, 143.8, Feb. 2021. ISSN: 0009-7322, 1524-4539. DOI: 10.1161/CIR.0000000000000950. URL: https://www.ahajournals.org/doi/10.1161/CIR.0000000000000950 (visited on 05/11/2021)

[War99] Warburton, D. E.; Haykowsky, M. J.; Quinney, H. A.: *Reliability and validity of measures of cardiac output during incremental to maximal aerobic exercise. Part I: Conventional techniques*. eng. Sports Med, 27.1, Jan. 1999, pp. 23–41. ISSN: 0112-1642. DOI: 10.2165/00007256-199927010-00003

[Wei02] Weisfeldt, M. L.; Becker, L. B.: *Resuscitation After Cardiac Arrest: A 3-Phase Time-Sensitive Model*. en. JAMA, 288.23, Dec. 2002, p. 3035. ISSN: 0098-7484. DOI: 10.1001/jama.288.23.3035. URL: http://jama.jamanetwork.com/article.aspx?doi=10.1001/jama.288.23.3035 (visited on 05/11/2021)

[Wik05] Wik, L.; Kramer-Johansen, J.; Myklebust, H.: *Quality of cardiopulmonary resuscitation during out-of-hospital cardiac arrest*. eng. JAMA, 293.3, Jan. 2005, pp. 299–304. ISSN: 1538-3598. DOI: 10.1001/jama.293.3.299

[WIK21] WIKIBOOKS: *MATLAB Programming/Differences between Octave and MATLAB - Wikibooks, open books for an open world*. en. Mar. 2021. URL: https://en.wikibooks.org/wiki/

MATLAB_Programming/Differences_between_Octave_and_MATLAB (visited on 06/04/2021)

[Yan20] Yan, S.; Gan, Y.; Jiang, N.: *The global survival rate among adult out-of-hospital cardiac arrest patients who received cardiopulmonary resuscitation: a systematic review and meta-analysis*. eng. Crit Care, 24.1, Feb. 2020, p. 61. ISSN: 1466-609X. DOI: 10.1186/s13054-020-2773-2

[Zol52] Zoll, P. M.: *Resuscitation of the Heart in Ventricular Standstill by External Electric Stimulation*. en. N Engl J Med, 247.20, Nov. 1952, pp. 768–771. ISSN: 0028-4793, 1533-4406. DOI: 10.1056/NEJM195211132472005. URL: http://www.nejm.org/doi/abs/10.1056/NEJM195211132472005 (visited on 05/11/2021)

[Zon03] Zong, W.; Moody, G.: *A robust open-source algorithm to detect onset and duration of QRS complexes*. *Computers in Cardiology, 2003*. Thessaloniki Chalkidiki, Greece: IEEE 2003, pp. 737–740. ISBN: 978-0-7803-8170-4. DOI: 10.1109/CIC.2003.1291261. URL: http://ieeexplore.ieee.org/document/1291261/ (visited on 06/17/2019)